DYNAMIC THERMAL MODELLING OF POWER TRANSFORMERS
Doctoral Dissertation

Dejan Susa

Helsinki University of Technology
Department of Electrical and Communications Engineering
Power Systems and High Voltage Engineering

DYNAMIC THERMAL MODELLING OF POWER TRANSFORMERS
Doctoral Dissertation

Dejan Susa

Dissertation for the degree of Doctor of Science in Technology to be presented with due permission of the Department of Electrical and Communications Engineering for public examination and debate in Auditorium S4 at Helsinki University of Technology (Espoo, Finland) on the 26th of August, 2005, at 12 noon.

Helsinki University of Technology
Department of Electrical and Communications Engineering
Power Systems and High Voltage Engineering

Teknillinen korkeakoulu
Sähkö- ja tietoliikennetekniikan osasto
Sähköverkot ja suurjännitetekniikka

Author	Dejan Susa

Name of the dissertation

Dynamic Thermal Modelling of Power Transformers

Date of manuscript	Jun, 2005	Date of the dissertation	August 26th, 2005
✔ Monograph		☐ Article dissertation (summary + original articles)	

Department	Department of Electrical and Communications Engineering
Laboratory	Power Systems and High Voltage Engineering
Field of research	Power Systems
Opponent(s)	Professor Glenn Swift
Supervisor	Professor Matti Lehtonen
(Instructor)	PhD Hasse Nordman

Abstract

Power transformers represent the largest portion of capital investment in transmission and distribution substations. In addition, power transformer outages have a considerable economic impact on the operation of an electrical network. One of the most important parameters governing a transformer's life expectancy is the hot-spot temperature value.

The classical approach has been to consider the hot-spot temperature as the sum of the ambient temperature, the top-oil temperature rise in tank, and the hot-spot-to-top-oil (in tank) temperature gradient. When fibre optic probes were taken into use to record local hot-spots in windings and oil ducts, it was noticed that the hot-spot temperature rise over top-oil temperature due to load changes is a function depending on time as well as the transformer loading (overshoot time dependent function). It has also been noticed that the top-oil temperature time constant is shorter than the time constant suggested by the present IEC loading guide, especially in cases where the oil is guided through the windings in a zigzag pattern for the ONAN and ONAF cooling modes. This results in winding hottest spot temperatures higher than those predicted by the loading guides during transient states after the load current increases, before the corresponding steady states have been reached.

This thesis presents new and more accurate temperature calculation methods taking into account the findings mentioned above. The models are based on heat transfer theory, application of the lumped capacitance method, the thermal-electrical analogy and a new definition of nonlinear thermal resistances at different locations within a power transformer. The methods presented in this thesis take into account oil viscosity changes and loss variation with temperature. The changes in transformer time constants due to changes in the oil viscosity are also accounted for in the thermal models. In addition, the proposed equations are used to estimate the equivalent thermal capacitances of the transformer oil for different transformer designs and winding-oil circulations. The models are validated using experimental results, which have been obtained from a series of thermal tests performed on a range of power transformers. Most of the tested units were equipped with fibre optic sensors in the main windings. Some of them also had thermocouples in the core and structural parts. A significant advantage of the suggested thermal models is that they are tied to measured parameters that are readily available (i.e., data obtained from a normal heat run test performed by the transformer manufacturer).

Keywords	power transformers, hot-spot, top-oil, bottom-oil, non-linear thermal resistance, oil time constants

Abstract

Power transformers represent the largest portion of capital investment in transmission and distribution substations. In addition, power transformer outages have a considerable economic impact on the operation of an electrical network. One of the most important parameters governing a transformer's life expectancy is the hot-spot temperature value.

The classical approach has been to consider the hot-spot temperature as the sum of the ambient temperature, the top-oil temperature rise in tank, and the hot-spot-to-top-oil (in tank) temperature gradient. When fibre optic probes were taken into use to record local hot-spots in windings and oil ducts, it was noticed that the hot-spot temperature rise over top-oil temperature due to load changes is a function depending on time as well as the transformer loading (overshoot time dependent function). It has also been noticed that the top-oil temperature time constant is shorter than the time constant suggested by the present IEC loading guide, especially in cases where the oil is guided through the windings in a zigzag pattern for the *ONAN* and *ONAF* cooling modes. This results in winding hottest spot temperatures higher than those predicted by the loading guides during transient states after the load current increases, before the corresponding steady states have been reached.

This thesis presents new and more accurate temperature calculation methods taking into account the findings mentioned above. The models are based on heat transfer theory, application of the lumped capacitance method, the thermal-electrical analogy and a new definition of nonlinear thermal resistances at different locations within a power transformer. The methods presented in this thesis take into account oil viscosity changes and loss variation with temperature. The changes in transformer time constants due to changes in the oil viscosity are also accounted for in the thermal models. In addition, the proposed equations are used to estimate the equivalent thermal capacitances of the transformer oil for different transformer designs and winding-oil circulations. The models are validated using experimental results, which have been obtained from a series of thermal tests performed on a range of power transformers. Most of the tested units (i.e., 80 MVA ONAN, 250 MVA ONAF, 400 MVA ONAF, 650 MVA ONAF and a 605 MVA OFAF cooled unit) were equipped with fibre optic sensors in the main windings. Some of them also had thermocouples in the core and structural parts. In addition, a comprehensive test programme was performed on a 2500 kVA ONAN cooled transformer (without external cooling) equipped with thermocouples. Finally, to properly assess the operating conditions of a 40 MVA OFAF transformer unit suffering cooling deficiency problems, temperatures recorded from the transformer while in service are compared to the corresponding temperatures calculated with the thermal models.

A significant advantage of the suggested thermal models is that they are tied to measured parameters that are readily available (i.e., data obtained from a normal heat run test performed by the transformer manufacturer).

Keywords: power transformers, hot-spot temperature, top-oil temperature, bottom-oil temperature, non-linear thermal resistance, oil time constants

Preface

The research work related to this thesis has been carried out in the Power Systems and High Voltage Engineering Laboratory of the Helsinki University of Technology during the years 2002-2005 as a natural continuation of my master's thesis. In addition to the university, ABB Oy, the Power Systems Research Pool coordinated by Finergy, and Fortum säätiö have provided the financial basis for the project.

I would like to thank the people that have been involved in the preparation of this thesis. I am deeply grateful to Professor Matti Lehtonen for accepting me into the Power Systems and High Voltage Engineering Laboratory and giving me this wonderful research project. I would also like to thank him for being my academic advisor and showing such confidence in my abilities and encouraging me to perform to the best of my capabilities.

I want to give special thanks to Doctor Hasse Nordman. Thank you for the wisdom you shared with me and for your guidance and advice, without which this document would not have been possible.

To the members of the Power Systems and High Voltage Engineering staff, I would like to extend my sincere gratitude. I would like to specially thank my friends for support along the way, and for making my stay here such a tremendous experience.

I am grateful to John Millar for his deep understanding and skill when checking and correcting the language of this manuscript.

I am also grateful to the pre-examiners of this thesis, Doctor Michael Schäfer and Doctor Dietrich Bonmann for their valuable comments on the manuscript.

Last, and most significantly, I would like to thank my family for the patience they have shown during the course of my work. I'd like to thank my wife, Aleksandra, for coming with me on this long and rather unpredictable journey, and for giving me her deep love and support over the years. She has been extremely patient with me and my work and has always been by my side whenever I have faced difficult situations. I would like to thank my parents, as well as my brother and his family, for the encouragement and support they have provided me, and their constant blessings for my success. I also thank my daughter, Ana, for bringing so much happiness and joy to my life and making the completion of this task so much easier.

Espoo, June 2005

Dejan Susa

Table of Contents

List of symbols and abbreviations

A	Area
A_1	A constant
A_2	A constant
A_3	A constant
A_4	A constant
A_5	A constant
A_6	A constant
A_7	A constant
A_8	A constant
A_9	A constant
B_p	Overshoot factor (maximum of the function $f_2(t)$)
C	A constant
C_1	A constant
C'	A constant
C''	A constant
C'''	A constant
c_{air}	Specific heat of the air
c_{wdn}	Specific heat capacity of winding material
c_{fe}	Specific heat capacity of core
c_{mp}	Specific heat capacity of the tank and fittings
c_{oil}	Specific heat capacity of oil
C_{el}	Electrical capacitance
C_{oil}	Thermal capacitance of the oil
C_{fe}	Thermal capacitance of the core
C'_{fe}	Corrected thermal capacitance of the core
C_{mp}	Thermal capacitance of the tank and other metal parts
C'_{mp}	Corrected thermal capacitance of the tank and other metal parts
C_{wdn}	Thermal capacitance of the winding
C'_{wdn}	Corrected thermal capacitance of the winding
C_{th}	Thermal capacitance
$C_{th,rated}$	Rated thermal capacitance
$C_{th\text{-}oil}$	Equivalent thermal capacitance of the transformer oil
$C_{th\text{-}oil,rated}$	Rated equivalent thermal capacitance of the transformer oil
$C_{th\text{-}wdn}$	Thermal capacitance of the winding
$C_{th\text{-}wdn,rated}$	Rated thermal capacitance of the winding
E_{HS}	Per unit eddy loss at winding hot-spot
g	Gravitational constant
g_r	Rated average winding to average oil temperature gradient
G_r	Grashof number
$f_2(t)$	Normalized time variation of hot-spot temperature rise above top-oil
h	Heat transfer coefficient
H	Hot-spot factor
H_{HS}	Per unit winding height to hot spot
HV	High Voltage
i	Electrical current
I	Load current

I_{rated}	Rated load current
IEC	The International Electrotechnical Commission
IEEE	The Institute of Electrical and Electronics Engineers
k	Oil thermal conductivity
kg	Kilogram
K	Load factor
L	A characteristic dimension length, width or diameter
LV	Low voltage
m	A constant
m_{fe}	Weight of core in kilograms
min	Minute
m_{mp}	Weight of the tank and fittings in kilograms
m_{oil}	Weight of oil in kilograms
m_{wdn}	Weight of winding material
M_{CC}	Weight of core and coil assembly in kilograms
M_{FLUID}	Weight of the oil in kilograms
M_{TANK}	Weight of the tank and fittings in kilograms
MVA	Megavoltampere
kVA	Kilovoltampere
n	A constant
n'	A constant
N_u	Nusselt number
AN	Air natural
ON	Oil natural
ONAN	Oil natural and air natural
ONAF	Oil natural and air forced
OFAN	Oil forced and air natural
OFAF	Oil forced and air forced
O_{oil}	Correction factor of oil
p	A constant
$P_{a,pu}$	Additional loss (i.e., sum of eddy and stray loss) per unit value
$P_{dc,pu}$	DC losses per unit value
P_e	Relative winding eddy losses, per unit of DC loss
$P_{eddy,pu}$	Eddy losses, per unit value
$P_{l,pu}$	Load losses, per unit value
$P_{l,pu}(\theta_e)$	Load losses' dependence on temperature at the top level
$P_{l,pu}(\theta_{be})$	Load losses' dependence on temperature at the bottom level
P_o	No-load loss
P_r	Prandtle number
P_s	Stray losses, watts
P_w	DC losses, watts
$P_{wdn,pu}$	Winding losses, per unit value
$P_{wdn,pu}(\theta_{hs})$	Winding losses dependence on temperature
$P_{wdn,pu}(\theta_{bwdn})$	Winding losses dependence on temperature at the bottom level
P_E	Eddy losses, watts
P_{TH}	Thermal power
q	Heat generation
q_{fe}	Heat generated by no-load losses

$q_{fe,rated}$	Heat generated by rated no-load losses
q_l	Heat generated by load losses
$q_{l,rated}$	Heat generated by rated load losses
q_{st}	Heat generated by the stray losses
q_{tot}	Heat generated by total losses
$q_{tot,rated}$	Heat generated by rated total losses
q_{wdn}	Heat generated by winding losses
$q_{wdn,rated}$	Heat generated by rated winding losses
R	Ratio load losses at rated current to no-load losses
R_{el}	Electrical resistance
R_{th}	Thermal resistance
$R_{th,rated}$	Rated thermal resistance
$R_{th\text{-}boil\text{-}air}$	Non-linear bottom-oil to air thermal resistance
$R_{th\text{-}bwdn\text{-}boil}$	Non-linear bottom-winding to bottom-oil thermal resistance
$R_{th\text{-}fe\text{-}oil}$	Non-linear core to oil thermal resistance
$R_{th\text{-}hs\text{-}oil}$	Non-linear winding to oil thermal resistance
$R_{th\text{-}hs\text{-}oil,rated}$	Rated non-linear winding to oil thermal resistance
$R_{th\text{-}hs\text{-}boil}$	Non-linear winding at the top-level to oil at the bottom level thermal resistance
$R_{th\text{-}insul}$	Winding insulation thermal resistance
$R_{th\text{-}insul\text{-}oil}$	Non-linear winding insulation to oil thermal resistance
$R_{th\text{-}mp\text{-}oil}$	Non-linear tank and other metal parts to oil thermal resistance
$R_{th\text{-}oil}$	Non-linear thermal resistance of the oil
$R_{th\text{-}oil\text{-}air}$	Non-linear oil to air thermal resistance
$R_{th\text{-}oil\text{-}air,rated}$	Rated non-linear oil to air thermal resistance
$R_{th\text{-}wdn}$	Winding thermal resistance
$R_{th\text{-}wdn\text{-}oil}$	Non-linear winding to oil thermal resistance
$ȝ$	Current density at rated load
s	Second
SCADA	Supervisory control and data acquisition
u	Electrical voltage
W	Watt
Y_{fe}	Portion of the core losses in the total transformer losses
Y_{st}	Portion of the stray losses in the total transformer losses
Y_{wdn}	Portion of the winding losses in the total transformer losses
ρ_{air}	Air density
ρ_{oil}	Oil density
β	Coefficient of thermal cubic expansion of the oil
μ	Oil viscosity
μ_{pu}	Oil viscosity per unit value
μ_{rated}	Oil viscosity rated value
Ψ_{air}	Air flow (the air volume)
Ψ_{oil}	Oil flow (the oil volume)
θ	Temperature
θ_{amb}	Ambient temperature
θ_{boil}	Bottom-oil temperature,
θ_{be}	Temperature at which losses are estimated in the bottom-oil model
$\theta_{be,rated}$	Rated temperature at which losses are estimated in the bottom-oil model

θ_{bwdn}	Bottom-winding hottest temperature
$\theta_{bwdn,rated}$	Rated bottom-winding hottest temperature
$\theta_{bwdn,lv}$	Bottom-winding hottest temperature/low voltage winding
$\theta_{bwdn,hv}$	Bottom-winding hottest temperature/high voltage winding
θ_e	Temperature at which losses are estimated in the top-oil model
θ_{hs}	Hot-spot temperature
$\theta_{hs,lv}$	Low voltage winding hot-spot temperature
$\theta_{hs,hv}$	High voltage winding hot-spot temperature
θ_k	Temperature factor for the loss correction
θ_{oil}	Top-oil temperature
$\theta_{wdn,average}$	Winding average temperature
θ_{BO}	Initial bottom-oil temperature
θ_{HS}	Initial winding hottest-spot temperature
θ_{TO}	Initial top-oil temperature
θ_{TDO}	Initial top-duct-oil temperature
θ_W	Initial average winding temperature
θ_{ws}	Hottest temperature of the winding conductor surface
$\Delta\theta_{boil,\,rated}$	Rated bottom-oil temperature rise
$\Delta\theta_{bwdn,\,rated}$	Rated bottom-winding hottest temperature rise over bottom-oil
$\Delta\theta_{cooler\text{-}air\text{-}gradient}$	Measured gradient between cooler air outlet and inlet
$\Delta\theta_{cooler\text{-}oil\text{-}gradient}$	Measured gradient between cooler oil outlet and inlet
$\Delta\theta_{hs}$	Hot-spot temperature rise over top-oil
$\Delta\theta_{hs,rated}$	Rated hot-spot temperature rise over top-oil
$\Delta\theta_{hs\text{-}boil}$	Hot-spot to bottom-oil gradient
$\Delta\theta_{hs\text{-}boil,\,rated}$	Rated hot-spot to bottom-oil gradient
$\Delta\theta_{oil}$	Top-oil temperature rise over ambient
$\Delta\theta_{oil,rated}$	Rated top-oil temperature rise over ambient
$\Delta\theta_{rated}$	Rated temperature rise
$\Delta\theta_{BO,R}$	Tested or rated bottom-oil rise over ambient
$\Delta\theta_{H/A,R}$	Tested or rated hot-spot rise over ambient
$\Delta\theta_{TO,R}$	Tested or rated top-oil rise over ambient
$\Delta\theta_{W/A,R}$	Tasted or rated average winding rise over ambient
$\Delta\theta_{ws\text{-}hs}$	Temperature gradient between the inner and outer surface of the insulation wrapped around the winding conductor
$\tau_{boil,rated}$	Rated bottom-oil time constant
τ_{el}	Electrical time constant
$\tau_{oil,rated}$	Rated top-oil time constant
$\tau_{oil,rated}$	Rated top-oil time constant
τ_{th}	Thermal time constant
$\tau_{th,rated}$	Rated thermal time constant
$\tau_{wdn,rated}$	Rated winding time constant
$\tau_{wdn\text{-}b,rated}$	Rated winding time constant
°C	Degrees Celsius

1 Introduction

"A power transformer is a static piece of apparatus with two or more windings which, by electromagnetic induction, transforms a system of alternating voltage and current into another system of voltage and current usually of different values and at same frequency for the purpose of transmitting electrical power," [23].

Power transformers are one of the most expensive components in an electricity system. Knowing their condition is essential to meet the goals of maximizing return on investment and lowering the total cost associated with transformer operation. The transformer winding hot-spot temperature is one of the most critical parameters when defining the power transformer thermal conditions and overloading capability beyond the nameplate rating. Therefore, in order to increase transformer operational efficiency and minimize the probability of an unexpected outage, several on-line and off-line monitoring systems have been developed [4], [9], [17], [19], [36], [38-39], [64-65], [74], [77] and [81-82].

Direct measurement of actual transformer winding temperatures using fibre optic probes has been increasing since the mid-1980s, [13], [37], [47-49], [62], [64], [66] and [78]. By analysing measured results from tested power transformers it has been noticed that the hot-spot temperature rise over top-oil temperature following load changes is a function depending on time as well as the transformer loading (overshoot time dependent function), Fig. 1.1. Similar results were obtained for distribution transformers with external cooling, [57]. The maximum values and shapes of this function (represented in terms of the overshoot factor B_p) for different transformers with external cooling, different loadings, different oil circulation modes in the windings (zigzag and axial) and different cooling modes are given in [49].
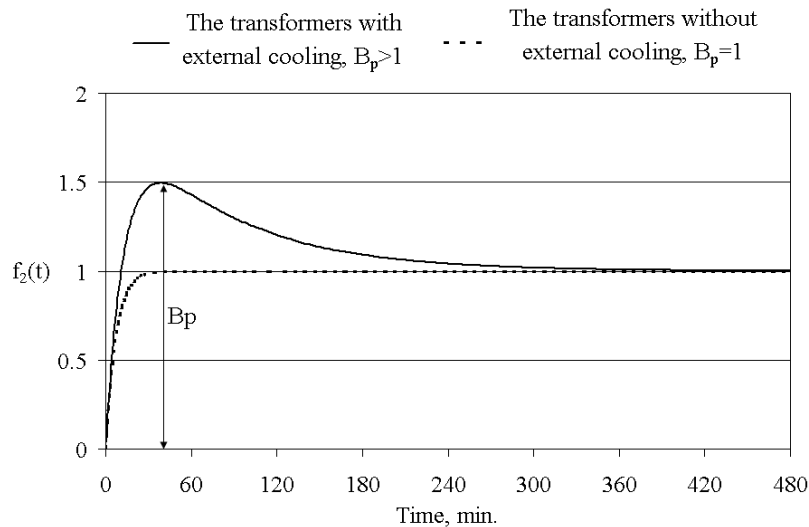

Fig. 1.1. Normalised time variation of hot-spot temperature rise above top-oil temperature, $f_2(t)$, (in tank) for a step increase in load current, [62]

15

It has also been noticed that the top-oil temperature time constant is shorter than the time constant suggested by the present loading guide, [22], especially where the oil is guided through the windings in a zigzag pattern for the *ONAN* and *ONAF* cooling modes, [49]. These values are estimated by exponential curve fitting in order to obtain the relevant numerical quantities, due to the fact that transformer time constants are functions of the transformer oil viscosity, [79], and further, they are dependent on the oil temperature, [28]. The foregoing thermal phenomena will directly cause the transient winding hottest spot temperatures to reach higher values than those predicted by both the present IEC and IEEE loading guides for oil-immersed power transformers, [22], [28] and [62].

On the other hand, a thermal test made on distribution transformers without external cooling, [69], showed that the hot-spot temperature rise over top-oil temperature for the oil temperature measured in the oil pocket due to a change in load is an exponential function, $f_2(t)$, with the time constant equal to the winding time constant, the dashed line in Fig. 1.1. It has also been observed that this top-oil time constant is longer than the time constant obtained for large power transformers with zigzag oil circulation through the windings.

Therefore, the author was strongly motivated to carry out a comprehensive transformer investigation in order to provide new solutions, in the form of transformer thermal models and their real-time application. These thermal models are based on conventional heat transfer theory, [33], [35] and [59-60], numerous transformer thermal tests and reports, [2-3], [6-7], [11-12], [15], [18], [34], [37], [40-50], [52], [57], [62], [69-70], [72] and [75-76], application of the lumped capacitance method, the thermal-electrical analogy, and the concept of nonlinear thermal resistances between different locations within a power transformer. The crucial ideas have already been published and verified in the author's work, [69-71].

The present work focuses specifically on further refinement in the definition of the nonlinear thermal resistances (by considering specific design differences between the transformer windings and vertical plates, and consequently, the fluid flow around their surfaces) and the relevant thermal models. The changes in transformer time constants with the oil viscosity are accounted for in the thermal models. In addition, the equivalent thermal capacitances of the transformer oil for different transformer designs and winding-oil circulations are estimated by the suggested equations. The methods presented in this thesis take into account oil viscosity changes and loss variation with temperature and they are validated using experimental results. Furthermore, the IEEE-Annex G method is used as a reference, [28].

The listed research methods, techniques and performed thermal tests have been successfully used to attain the following:

The scope of the research work is to develop the physical background for power transformer dynamic loading based on heat transfer theory, to allow capacity monitoring using data obtained from the normal heat run test performed by the transformer manufacturer.

2 Transformer loading capacity: basic aspects

A typical oil immersed transformer layout is shown in Fig. 2.1. During its operation a transformer is the source of energy losses, the majority of which are located in two fundamental parts, the magnetic core and the windings. In the magnetic core the losses are generated by variation of alternating flux in the magnetic circuit; therefore they are directly related to the induction and hence the applied voltage. The winding losses are primarily due to DC losses and eddy currents, however, and are related to the load. Losses are also generated in the connections, tap changers and bushings. They can be linked with the losses referred to above, and appear in the same way as in materials with good electrical conductivity. The leakage flux from the windings, terminals and connections can also create stray losses by inducing eddy currents in neighbouring non-active metallic components, such as the fastenings, tank and cover. The manufacturer must reduce these to the absolute minimum, [21], [34].
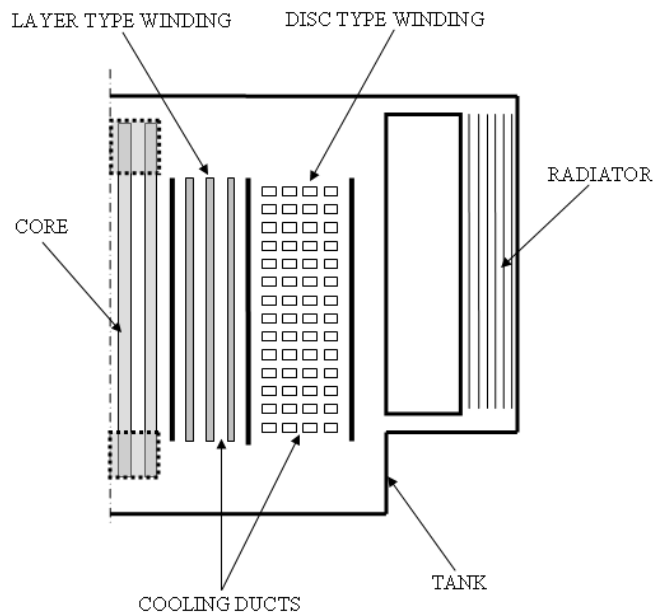

Fig. 2.1. Cross-sectional view of a typical oil-immersed transformer, [10]

All these losses cause heating in the corresponding parts of the transformer and this heat must be transferred to the transformer oil by convection and further, from the oil to the cooling medium via a heat exchanger. Although the winding copper holds its mechanical strength up to several hundred degrees Celsius and the transformer oil does not significantly degrade below about 140°C, the paper insulation deteriorates very rapidly if its temperature exceeds 90°C. In addition, the moisture content, acidity and oxygen content of the oil have a significantly detrimental effect on insulation life, [14] and [26]. Therefore, the loading capacity of a transformer is defined in terms of the thermal ageing of its insulation and the transformer hot-spot temperature. It has been reported, [7], that from 90 to 110°C the tensile strength aging rate is doubled for approximately each 8°C increase in temperature. Other authors have observed, [7], that the life of different transformer insulation materials is halved by an increase in temperature ranging from 5 to 10 degrees. Generally, the consensus is that in the

17

temperature range from 80 to 140°C, the life expectancy is halved by each 6°C increase in temperature, [22] and [34]. In IEC Publication 76, the rate of ageing of the interturn insulation of transformers under the effect of time and temperature is referred to a hot-spot temperature of 98°C (i.e., to a value that normally corresponds to a 20°C cooling air temperature under the continuous rated load), [24]. The service life of such a transformer due to ageing is about 30 years. IEC-76 defines temperature rise limits (e.g., top-oil and average winding temperature rises above ambient temperature for different cooling modes) and specifies test methods for temperature-rise measurements, [24]. The IEEE standard test code for liquid-immersed distribution, power, and regulating transformers, [29], also deals with temperature rises and related test procedures similar to IEC-76 parts 1 and 2, [23 and 24].

In addition, the IEC 354 loading guide for oil immersed power transformers, [22], and the IEEE guide for loading mineral-oil-immersed transformers, [28], indicate how oil-immersed transformers can be operated in different ambient conditions and load levels without exceeding the acceptable deterioration limit of insulation due to thermal effects. According to the loading guides, the hot-spot temperature in a transformer winding consists of three components: the ambient temperature rise, the top-oil temperature rise and the hot-spot temperature rise over the top-oil temperature, Fig. 2.2. It is assumed that during a transient period the hot-spot temperature rise over the top-oil temperature varies instantaneously with transformer loading and independently of time.
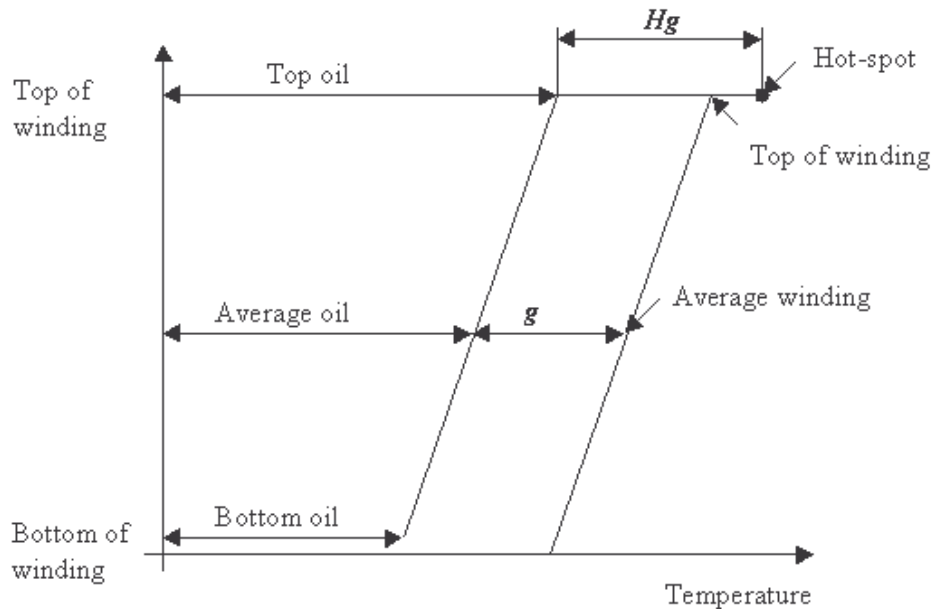

Fig. 2.2. A transformer thermal diagram that shows the main temperature distribution along the winding height as well as the oil temperature distribution inside the transformer tank

The variation of the top-oil temperature is described by an exponential equation based on a time constant (oil time constant). The top-oil time constant suggested by the IEC loading guide is 150 min for the oil natural-air natural (ONAN) and oil natural-air forced cooling modes (ONAF). In the case of the oil forced-air forced cooling mode (OFAF) it is suggested to use the oil temperature of the oil leaving the winding. This

has not been practiced in industry due to difficulties in recording the temperature of the oil leaving the winding. The suggested oil-time constant for OFAF cooled units is 90 min. The IEEE Loading Guide, [28], suggests a design specific calculation method for the top oil time constant. In this case the time constant is calculated separately for each transformer unit, depending on both the cooling mode (ONAN, ONAF or OFAF) and the masses of the various components comprising a transformer, such as the oil, tank, radiators, insulation, clamps, and windings.

At the time when the present IEC 354 loading guide for oil immersed power transformers was made, fibre optic sensor thermal investigations had just begun. During the last twenty years fibre optic probes have been used by many authors [13], [37], [47-49], [62], [64] and [78], in order to obtain as accurate values as possible for transformer temperatures. It was shown that the dynamic winding hot-spot calculation methods proposed in the loading guides, [22] and [28], yield significantly low values during transients, especially in the case of a short-term emergency loading, [62]. The same conclusion is also valid for hot-spots in the core and structural parts, if the principles proposed in [22] and [28] are applied. This is a critical limitation in the open market environment, where network planners, operators and asset managers are trying to fully exploit the capacity of existing equipment.

In order to overcome these thermal obstacles and to increase transformer loading capacity, different calculation procedures for the winding hot-spot temperature response to load changes have been proposed by many authors. Aubin and Pierce dealt with the overshoot phenomenon by avoiding its direct modelling. They obtained hot-spot temperature calculation methods that were based on the bottom-oil temperature. These methods are published in scientific papers, [2] and [52-53]. Pierce's method is also presented as a more complex dynamic hot-spot temperature calculation procedure in the IEEE Loading Guide Annex G in [28]. Similarly, Radakovic performed thermal tests on distribution transformers with external cooling, [57], where he observed the same phenomenon and suggested a calculation procedure based on the bottom-oil temperature and application of the lumped capacitance theory. On the other hand, the author of this thesis has defined two thermal models, where the variation of the winding hottest-spot temperature rise over the top-oil temperature after a load change is defined by exponential functions with constant parameters. Both models depend only on data received in a normal heat run test, (i.e., the top-oil in the tank of the transformer, the average winding-to-top-oil gradient), [49] and [67-68]. In addition, many other authors have suggested different solutions, such as Alegi, Blake, Declercq, Lesieutre, Pierce, Pradhan, Radakovic, Ryder, Tang, and Van der Veken in references [1], [5], [10], [39], [54],[55], [56,58], [61], [75-76] and [80] . It is necessary to stress the importance of the work published by Swift for further understanding of the state of the art in transformer thermal modelling, [72-73].

A permanent on-line monitoring system, which collects information from several measurable variables, should also include a real-time application of the thermal models to provide an accurate picture of the operating condition of the transformer, allowing the operator to detect early signs of faults and correct them. The scientific papers that describe the implementation of the transformer temperature monitoring systems, based either on thermal models or temperature sensor installations, and other power

transformer diagnostic methods that consider the key parameters, e.g., the gases, moisture in oil, partial discharge, load current and voltage, insulation power factor and pump-fan operation, are listed in references [4], [8], [9], [10], [16], [17], [19-20], [36], [38-39], [51], [63-66], [74], [77] and [81-82].

Finally, the Institute of Electrical and Electronics Engineers has attempted to give general guidance to power transformer manufacturers and users in evaluating the thermal performance of the transformers by printing two new publications, the IEEE Guide for Determination of Maximum Winding Temperature Rise in Liquid-Filled Transformers, [30], and the IEEE Recommended Practice for Performing Temperature Rise Tests on Oil-Immersed Power Transformers at Loads Beyond Nameplate Ratings, [31], which consider the findings referenced above.

3 Dynamic thermal modelling of power transformers

This section starts with a short review of the thermal-electrical analogy. The thermal nonlinearty of transformer parameters is desribed by defining the relevant non-linear resistances in the following subsection. Subsequently, the dynamic thermal models for power transformers are discussed and defined. These models are the top-oil temperature model, the hot-spot temperature model, the bottom-winding and bottom-oil temperature model, and the hot-spot models based on the bottom oil temperature. At the end, the top oil time constant for the thermal models is defined.

3.1 Introduction

In order to analyse the temperature conditions inside a transformer, the analogy between thermal and electrical processes is briefly reviewed below, [69-73].

A thermal process can be defined by the energy balance equation:

$$q \times dt = C_{th} \times d\theta + \frac{\theta - \theta_{amb}}{R_{th}} \times dt \qquad (3.1)$$

where:

q is the heat generation,
C_{th} is the thermal capacitance,
θ is temperature,
R_{th} is the thermal resistance,
θ_{amb} is the ambient temperature.

The equation may be rewritten as follows:

$$q = C_{th} \times \frac{d\theta}{dt} + \frac{\theta - \theta_{amb}}{R_{th}} \qquad (3.2)$$

Now, if we define a simple electrical RC circuit, as given by Fig. 3.1, we can write a similar equation based on both the first Kirchoff's law and Ohm's law:

$$i = C_{el} \times \frac{du}{dt} + \frac{u}{R_{el}} \qquad (3.3)$$

where: i is the electrical current, C_{el} is the electrical capacitance, R_{el} is the electrical resistance and u is the electrical voltage.
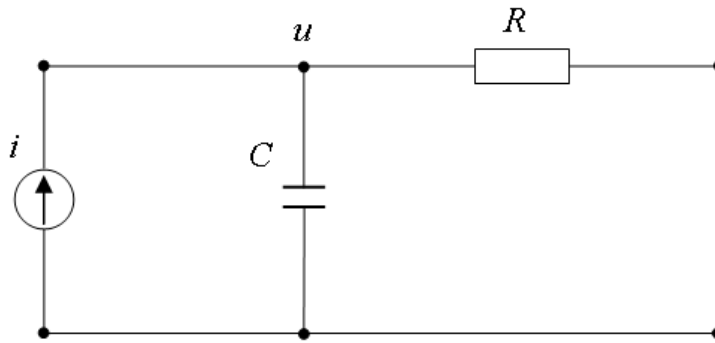
Fig. 3.1. An electrical RC circuit

Simply, by comparing equations (3.2) and (3.3) we obtain the analogy between electrical and thermal processes, Table 3.1.

Table 3.1. Thermal-electrical analogy

Thermal		Electrical	
Generated heat	q	Current	i
Temperature	θ	Voltage	u
Resistance	R_{th}	Resistance	R_{el}
Capacitance	C_{th}	Capacitance	C_{el}

The analogous thermal circuit for the electrical circuit, Fig. 3.1, is given in Fig. 3.2.
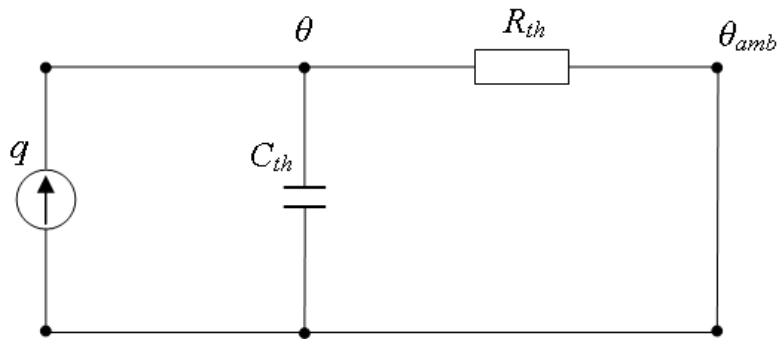

Fig. 3.2. The analogous thermal circuit

At this point the thermal resistance and capacitance can be defined as the material's ability to resist heat flow and store heat, respectively.

The foregoing analysis assumes that the thermal characteristics of the material are constant, that is, they are not changeable with temperature. In order to use this electrical-thermal analogy for transformer temperature calculations it will be necessary to further modify the lumped capacitance method by introducing a nonlinear thermal resistance, which takes changes in the transformer oil thermal parameters with temperature into account. The nonlinear thermal resistance will be clearly defined in the following sections for the top-oil, bottom-oil, bottom-winding and the hot-spot temperature models. The transformer oil has thermal characteristics strongly dependent on temperature, Table 3.2, where the oil viscosity dependence on temperature is most pronounced, [18] and [52].

Table 3.2. Thermal characteristics of transformer oil, [18]

Temperature θ, °C	Density ρ, kg/m^3	Specific heat c_{oil}, Ws/(kg°C)	Thermal conductivity k, W/(m°C)	Coefficient of thermal cubic expansion β, 1/°C	Viscosity μ, kg/(ms)
-15	896.885	1900	0.1262	8.6×10^{-4}	0.0694
-5	890.295	1940	0.1247	8.6×10^{-4}	0.0463
5	883.705	1980	0.1232	8.6×10^{-4}	0.0318
15	877.115	2020	0.1217	8.6×10^{-4}	0.0224
25	870.525	2060	0.1201	8.6×10^{-4}	0.0162
35	863.935	2100	0.1186	8.6×10^{-4}	0.0119
45	857.345	2140	0.1171	8.6×10^{-4}	0.0089
55	850.755	2180	0.1156	8.6×10^{-4}	0.0068
65	844.165	2220	0.1140	8.6×10^{-4}	0.0053
75	837.575	2260	0.1125	8.6×10^{-4}	0.0042
85	830.985	2300	0.1110	8.6×10^{-4}	0.0033
100	821.100	2360	0.1087	8.6×10^{-4}	0.0024

The validity of the lumped capacitance method application for power transformers is given in [34], [56-58], [69-73], [75] and [76].

3.2 The non-linear thermal resistance

The nonlinear oil thermal resistance, $R_{th\text{-}oil}$, $(m^2 K)/W$, according to heat transfer theory, [33-35], [59-60] and [69-73] is given in the following equation:

$$R_{th-oil} = \frac{1}{h \times A} = \frac{\Delta\theta_{oil}}{q} \tag{3.4}$$

where:

h is the heat transfer coefficient,
A is the area,
$\Delta\theta_{oil}$ is the oil temperature gradient,
q is the heat generated by the corresponding losses.

Hence, the nonlinear thermal resistance is inversely proportional to the heat transfer coefficient, whose dependence on temperature is explained in the text to follow.

Based on heat transfer theory, the natural convection oil flow around vertical, inclined and horizontal plates and cylinders can be described by the following empirical correlation, [33-35], [59-60]:

$$N_u = C \times [G_r \times P_r]^n \tag{3.5}$$

where C and n are empirical constants dependent on whether the oil circulation is laminar or turbulent. The basic values are given in Table 3.3, [33].

Table 3.3 Empirical values for constants C and n

The oil circulation	C	n
Laminar	0.59	0.25
Turbulent	0.10	0.33

The Nusselt number (N_u) Prandtle number (P_r) and Grashof number (G_r) are described in the following equations, [33-35] and [59-60]:

$$N_u = \frac{h \times L}{k} \tag{3.6}$$

$$P_r = \frac{c_{oil} \times \mu}{k} \tag{3.7}$$

$$G_r = \frac{L^3 \times \rho_{oil}^2 \times g \times \beta \times (\Delta\theta_{oil})}{\mu^2} \tag{3.8}$$

where:

L is the characteristic dimension, length, width or diameter,
g is the gravitational constant ,
k is the oil thermal conductivity, Table 3.2,
ρ_{oil} is the oil density, Table 3.2,
β is the oil thermal expansion coefficient, Table 3.2,
c_{oil} is the specific heat of oil, Table 3.2,
μ is the oil viscosity, Table 3.2,
$\Delta\theta_{oil}$ is the oil temperature gradient, (K).

By substituting (3.6), (3.7) and (3.8) in (3.5) the following expression is obtained:

$$\frac{h \times L}{k} = C \times \left[\left(\frac{c_{oil} \times \mu}{k} \right) \times \left(\frac{L^3 \times \rho_{oil}{}^2 \times g \times \beta \times (\Delta\theta_{oil})}{\mu^2} \right) \right]^n \tag{3.9}$$

The variation of viscosity with temperature is much higher than the variation of other transformer oil physical parameters, Table 3.2, [6], [7], [18], [34] and [52]. Therefore, all oil physical parameters except the viscosity in (3.9) will be replaced by a constant and (3.9) will be solved for the heat transfer coefficient, h, as follows:

$$h = C_1 \times \left(\frac{\Delta\theta_{oil}}{\mu} \right)^n \tag{3.10}$$

where C_1 is assumed to be a constant, expressed as:

$$C_1 = C \times \left[\rho_{oil}{}^2 \times g \times \beta \times k^{\left(\frac{1-n}{n} \right)} \times L^{\left(\frac{3n-1}{n} \right)} \times c_{oil} \right]^{(n)} \tag{3.11}$$

and μ is the viscosity, $kg/(ms)$. The viscosity dependence on temperature is given by the following equation, [52-53]:

$$\mu = A_1 \times e^{\left[\frac{A_2}{\theta_{oil} + 273} \right]} \tag{3.12}$$

where the viscosity is evaluated at the oil temperature that corresponds to the top-oil temperature in sections 3.2.1 and 3.2.2 and to the bottom-oil temperature in section 3.2.3. The constants A_1 and A_2 for the transformer oil are given in [28], [52-53] and Appendix A. The factor C_1 is depicted as a function of temperature in Fig. 3.3 for the transformer oil. It is considered that for the range of the constant n from 0.2 to 2, (where 2 is applicable for the transformer cold start, Appendix B), and at the normal operational temperatures of power transformers between 40 and $100°C$, the factor C_1 varies in range from 1 to 0.944, and from 1 to 0.964 per unit, corresponding to the values $n=0.2$ and $n=2$, respectively. As a result, it is assumed to be constant when compared to the oil

25

viscosity changes with temperature. In a case where it is necessary to consider the influence of all oil parameters, i.e., if the thermal behaviour of the transformer insulation oil differs significantly from the oil used in the transformers covered in this thesis, the corrections to be made are given in Appendix A.

$C_1(\theta)$; n=0.2 $\mu^n(\theta)$; n=0.2 $C_1(\theta)$; n=2 $\mu^n(\theta)$; n=2
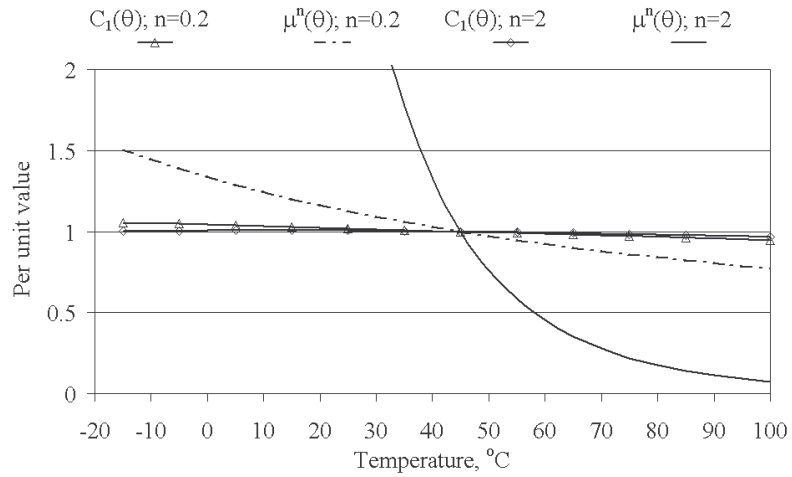

Fig. 3.3. Physical properties of transformer oil

An example of oil viscosity variation with temperature, compared with the other physical properties of transformer oil, is shown in Fig. 3.4.
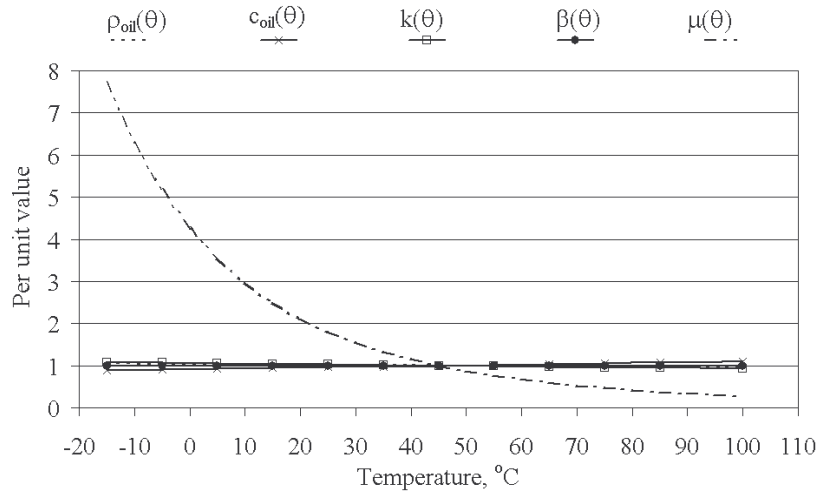
$\rho_{oil}(\theta)$ $c_{oil}(\theta)$ $k(\theta)$ $\beta(\theta)$ $\mu(\theta)$

Fig. 3.4. Oil viscosity variation with temperature

3.2.1 The top-oil temperature model

The top-oil temperature model is given as a thermal circuit, Fig. 3.5, based on the thermal-electrical analogy and heat transfer theory, [33-35], [69-73].
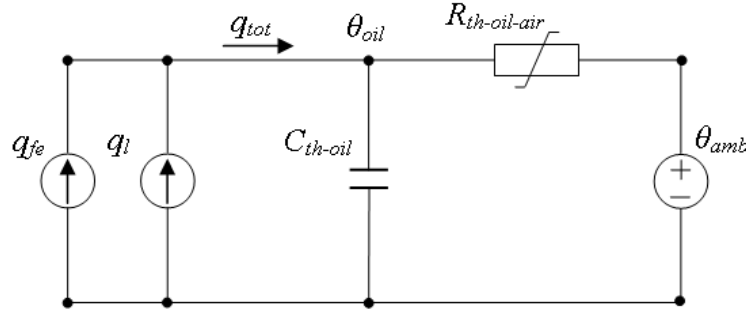

Fig. 3.5. The top-oil temperature model

where:

q_{tot} is the heat generated by total losses,
q_{fe} is the heat generated by no-load losses,
q_l is the heat generated by load losses,
$C_{th\text{-}oil}$ is the equivalent thermal capacitance of the transformer oil,
θ_{oil} is the top-oil temperature,
$R_{th\text{-}oil\text{-}air}$ is the non-linear oil to air thermal resistance,
θ_{amb} is the ambient temperature.

The heat generated by both no-load and load transformer losses is represented by two ideal heat sources and the ambient temperature is represented as an ideal temperature source, [69-73].

The differential equation for the thermal circuit shown in Fig. 3.5 is:

$$q_{fe} + q_l = C_{th-oil} \times \frac{d\theta_{oil}}{dt} + \frac{(\theta_{oil} - \theta_{amb})}{R_{th-oil-air}}$$ (3.13)

If we substitute the equation for non-linear thermal resistance, (3.4), into (3.13) the following equation is obtained:

$$q_{fe} + q_l = C_{th-oil} \times \frac{d\theta_{oil}}{dt} + \frac{(\theta_{oil} - \theta_{amb})}{\dfrac{1}{h \times A}}$$ (3.14)

Then, by substituting equation (3.10) for the heat transfer coefficient, h, the differential equation is changed to:

$$\left(q_{fe} + q_l \right) \times \left(\frac{\mu^n}{C_1 \times A} \right) = \left(\frac{\mu^n}{C_1 \times A} \right) \times C_{th-oil} \times \frac{d\theta_{oil}}{dt} + \left(\theta_{oil} - \theta_{amb} \right)^{1+n} \tag{3.15}$$

Next, we can define the variable, μ, oil viscosity, as:

$$\mu = \mu_{pu} \times \mu_{rated} \tag{3.16}$$

and the following constants:

the rated non-linear thermal resistance, $R_{th\text{-}oil\text{-}air,\ rated}$,

$$R_{th-oil-air,\ rated} = \frac{1}{C_1 \times A} \times \left(\frac{\mu_{rated}}{\Delta\theta_{oil,\ rated}} \right)^n \tag{3.17}$$

the rated top-oil temperature rise over ambient temperature, $\Delta\theta_{oil,\ rated}$,

$$\Delta\theta_{oil,\ rated} = \left(q_{fe} + q_l \right)_{rated} \times R_{th-oil-air,\ rated} \tag{3.18}$$

the rated top-oil time constant, $\tau_{oil,rated}$, section 3.3 and Appendix E,

$$\tau_{oil,\ rated} = R_{th-oil-air,\ rated} \times C_{th-oil,\ rated} \tag{3.19}$$

the ratio of load losses at rated current to no-load losses, R,

$$R = \frac{q_l}{q_{fe}} \tag{3.20}$$

and the load factor, K,

$$K = \frac{I}{I_{rated}} \tag{3.21}$$

where I is the load current and I_{rated} is the rated current. The temperature dependence of the load losses, $P_{l,pu}(\theta_e)$, is also taken into account as follows:

$$P_{l,\ pu} \left(\theta_e \right) = P_{dc,\ pu} \times \left(\frac{\theta_e + \theta_k}{\theta_{e,rated} + \theta_k} \right) + P_{a,\ pu} \times \left(\frac{\theta_{e,rated} + \theta_k}{\theta_e + \theta_k} \right) \tag{3.22}$$

where:

$P_{dc,pu}$ is the DC loss per unit value,
$P_{a,pu}$ is the additional loss (i.e., equal to the sum of eddy and stray losses) per unit value,
θ_e is the temperature at which the losses are estimated, ºC, (3.23),
θ_k is the temperature factor for the loss correction, equal to 225 for aluminium and 235 for copper.

28

Both the high and low voltage windings affect the oil, therefore the losses are estimated at a temperature equal to the mean hot-spot temperature value given below:

$$\theta_e = \frac{\theta_{hs,lv} + \theta_{hs,hv}}{2} \tag{3.23}$$

where:

$\theta_{hs,lv}$ is the low voltage winding hot-spot temperature, °C,
$\theta_{hs,hv}$ is the high voltage winding hot-spot temperature, °C.

Equation (3.15) is then reduced to its final form:

$$\frac{1 + R \times P_{l,pu}\left(\theta_e\right) \times K^2}{1 + R} \times \mu_{pu}{}^n \times \Delta\theta_{oil,rated} = \mu_{pu}{}^n \times \tau_{oil,rated} \times \frac{d\theta_{oil}}{dt} + \frac{\left(\theta_{oil} - \theta_{amb}\right)^{1+n}}{\Delta\theta_{oil,rated}{}^n} \tag{3.24}$$

which forms the basic model for top-oil temperature calculation. The importance of the oil viscosity temperature variation, μ_{pu}, is that it affects both the oil thermal resistance and top-oil time constant.

It is assumed that oil circulation inside the transformer tank is laminar and so the constant n for that particular flow type is equal to 0.25, Table 3.3. Additionally, when considering the constant n, it is necessary to take into account whether the heat is dissipated by free or forced convection, [6], [7], [18], [22], [24], [28], [34], [40-42], [46], [52-53], [69-71] and [73]. Transformers both with and without external cooling for the air natural (AN) cooling mode assume free convection heat transfer with the constant n equal to the value for laminar oil flow, i.e., $n=0.25$. This means that the oil flow is dependent on the temperature. Conversely, transformers with external cooling and forced air, i.e., the AF cooling mode, are better modelled with forced convection heat transfer and a lower value for constant n, which is corrected for improved air flow (e.g., if the velocity were to be increased to a very high value, the constant n would be dropped entirely), Table 3.4. For a transformer cold start or when the oil velocity inside the transformer tank is equal to zero (i.e., when the temperature gradient between the transformer top and bottom is approximately equal to zero), the constant n will take different empirical values for the various cooling modes and designs, Table 3.4 and Appendix B.

Table 3.4. Empirical constant n for the top-oil thermal model

Oil circulation	n		
	with external cooling		without external cooling
	ONAF/OFAF	ONAN	ONAN
initial oil circulation speed = 0 (cold start)	0.5	0	0.25
initial oil circulation speed > 0(transformer on load)	0.2	0.25	0.25

The constant n is fully empirical and its values are based on conventional heat transfer theory, [33], [35], [59-60] and on findings suggested by different authors [6], [7], [18], [22], [24], [28], [34], [40-42], [46], [52-53], [69-71] and [73]. In part, i.e., where n is more specifically related to transformer operating conditions such as a cold start, its value is obtained by fitting and extrapolation techniques performed on the results obtained during various transformer thermal tests, [48], [49], [62].

3.2.2 The hot-spot temperature model

The hot-spot temperature model, which is based on the top-oil temperature, will be defined for two different empirical correlations of the non-linear resistance between the winding insulation surface and the oil at the top of the winding. The first model is based on conventional heat transfer theory for natural convection oil flow around vertical plates, [33], [35] and [59-60]. It has already been applied and verified in the scientific papers [69-71]. The second introduces a new concept based on a thorough analysis of experimental results obtained during various thermal tests, [48-49] and [62], and partly on the theoretical approach used to define the non-linear resistance (at the beginning of section 3.2). It defines the natural convection and heat exchange phenomena by considering the specific design of the transformer windings and their influence on the oil circulation and temperature gradient at the top of the winding stack; i.e., it takes into account the fact that the winding is a complex construction consisting of alternating vertical and horizontal surfaces.

- Thermal resistance based on conventional heat transfer theory

  Similar to the conventional heat transfer theory given for the top-oil temperature model and the non-linear thermal resistance, the hot-spot temperature model is also represented as a thermal circuit, Fig. 3.6, [69-73].
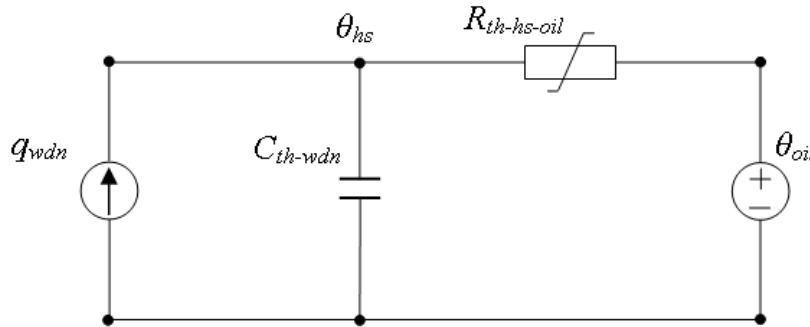

Fig. 3.6. The hot-spot temperature model

where:

q_{wdn} is the heat generated by winding losses,
$C_{th\text{-}wdn}$ is the thermal capacitance of the winding,
θ_{hs} is the hot-spot temperature,
$R_{th\text{-}hs\text{-}oil}$ is the nonlinear winding to oil thermal resistance,
θ_{oil} is the top-oil temperature.

31

The heat generated by winding losses is again represented as an ideal heat source and the oil temperature forms an ideal temperature source, [69-73]. The nonlinear thermal resistance, $R_{th\text{-}hs\text{-}oil}$, is defined by the heat transfer theory, which has already been applied to the top-oil thermal model, as explained below. The nonlinear winding to oil thermal resistance is given by the following equation:

$$R_{th-hs-oil} = R_{th-wdn} + R_{th-insul} + R_{th-insul-oil} \tag{3.25}$$

where:

$R_{th\text{-}wdn}$ is the winding thermal resistance,
$R_{th\text{-}insul}$ is the winding insulation thermal resistance,
$R_{th\text{-}insul\text{-}oil}$ is the non-linear winding insulation to oil thermal resistance.

By comparing the resistances given in (3.25), the following thermal correlations are obtained:

$$R_{th-insul-oil} \gg R_{th-wdn} \tag{3.26}$$

$$R_{th-insul-oil} \gg R_{th-insul} \tag{3.27}$$

for hot-spot temperatures measured on the outer surface of the insulation wrapped around the conductors, Appendix C, [37] and [48].
Thus, the final equation for the nonlinear winding to oil thermal resistance is:

$$R_{th-hs-oil} = \frac{1}{h \times A} \tag{3.28}$$

Equation (3.28) is similar to (3.4) for the top oil temperature model, therefore the equation for the heat transfer coefficient, h, is completely analogous to the heat transfer coefficient in (3.10):

$$h = C_1 \times \left(\frac{\Delta\theta_{hs}}{\mu} \right)^n \tag{3.29}$$

where the viscosity is again evaluated at the top-oil temperature and $\Delta\theta_{hs}$ is now the hot-spot to top-oil temperature gradient.

The differential equation for the thermal circuit shown in Fig. 3.6 is:

$$q_{wdn} = C_{th-wdn} \times \frac{d\theta_{hs}}{dt} + \frac{(\theta_{hs} - \theta_{oil})}{R_{th-hs-oil}} \tag{3.30}$$

If we substitute the equation for the non-linear thermal resistance, (3.28), into (3.30), the following equation is obtained:

32

$$q_{wdn} = C_{th-wdn} \times \frac{d\theta_{hs}}{dt} + \frac{(\theta_{hs} - \theta_{oil})}{\frac{1}{h \times A}}$$ (3.31)

Then, by substituting the equation for the heat transfer coefficient, (3.29), into (3.31), the differential equation is changed to:

$$q_{wdn} \times \left(\frac{\mu^n}{C_1 \times A}\right) = \left(\frac{\mu^n}{C_1 \times A}\right) \times C_{th-wdn} \times \frac{d\theta_{hs}}{dt} + (\theta_{hs} - \theta_{oil})^{n+1}$$ (3.32)

We again define the oil viscosity as a variable, μ, Fig. 3.4, such that:

$$\mu = \mu_{pu} \times \mu_{rated}$$ (3.33)

and the following constants:

the rated nonlinear hot-spot to top-oil thermal resistance, $R_{th\text{-}hs\text{-}oil,rated}$,

$$R_{th-hs-oil,rated} = \frac{1}{C_1 \times A} \times \left(\frac{\mu_{rated}}{\Delta\theta_{hs,rated}}\right)^n$$ (3.34)

the rated hot-spot temperature rise over top-oil temperature, $\Delta\theta_{hs,\,rated}$, as:

$$\Delta\theta_{hs,rated} = q_{wdn,rated} \times R_{th-hs-oil,rated} = H \times g_r$$ (3.35)

where H is the hot-spot factor and g_r is the rated average winding to average oil temperature gradient, [22].
The rated winding time constant, $\tau_{wdn,rated}$, Appendix D, is:

$$\tau_{wdn,rated} = R_{th-hs-oil,rated} \times C_{th-wdn,rated}$$ (3.36)

and the winding loss's dependence on temperature, $P_{wdn,pu}(\theta_{hs})$, is:

$$P_{wdn,pu}(\theta_{hs}) = P_{dc,pu} \times \left(\frac{\theta_{hs} + \theta_k}{\theta_{hs,rated} + \theta_k}\right) + P_{eddy,pu} \times \left(\frac{\theta_{hs,rated} + \theta_k}{\theta_{hs} + \theta_k}\right)$$ (3.37)

where $P_{dc,pu}(\theta_{hs})$ and $P_{eddy,pu}(\theta_{hs})$ describe the behaviour of the DC and eddy losses as a function of temperature. The DC losses vary directly with temperature, whereas the eddy losses vary inversely with temperature. θ_k is the temperature factor for the loss correction, equal to 225 for aluminium and 235 for copper.

It follows that the final equation is:

$$\left\{ K^2 \times P_{wdn,\,pu}\left(\theta_{hs}\right) \right\} \times \mu_{pu}{}^n \times \Delta\theta_{hs,\,rated}$$

$$= \mu_{pu}{}^n \times \tau_{wdn,\,rated} \times \frac{d\theta_{hs}}{dt} + \frac{\left(\theta_{hs} - \theta_{oil}\right)^{n+1}}{\Delta\theta_{hs,\,rated}{}^n} \quad\quad (3.38)$$

which is the basic model for the hot-spot temperature. In analogy to (3.24), the equation takes into account the change of thermal resistance and winding time constant due to the oil viscosity variation with temperature.

Similar to the assumption made in the top-oil thermal model that oil flow inside the transformer tank is laminar, the value for constant n where oil circulation is already formed, should be equal to 0.25. However, it is also necessary to take into account whether the heat is dissipated by free or forced convection from the winding surface. Transformers without external cooling for the oil natural, (ON), cooling mode can be modelled assuming free convention heat transfer, whose constant n is equal to the value for laminar oil flow (i.e., $n=0.25$). On the other hand, the oil circulation within transformers with external cooling and the oil natural (ON) cooling mode will be established due to both buoyancy effects and the difference between the heights of the winding and the radiator heating centres. Therefore, it is modelled as *natural forced* heat transfer, which is similar to the heat transfer in the oil forced cooling mode, (OF). Where the pumps are forcing the oil at a high rate into the bottom of the tank, some of it will be siphoned by the windings, but most of it will bypass the winding and reach the top without too much change in temperature. The constant n will have different values in the case of a transformer cold start, that is, when the oil velocity is equal to zero, Appendix B. The empirical values for constant n for different cooling modes and different oil circulation conditions are given in Table 3.5.

Table 3.5. Empirical constant n for the hot-spot thermal model

Oil circulation	n	
	with external cooling	without external cooling
	ONAF/ONAN/OFAF	ONAN
initial oil circulation speed = 0 (cold start)	2	0.25
initial oil circulation speed > 0 (transformer on load)	0.2	0.25

Similar to the constant n used in the top-oil thermal model above, the constant n for the hot-spot thermal model is fully empirical and its values are also based on conventional heat transfer theory, [33], [35] and [59-60], and on findings suggested by different authors [6], [7], [18], [22], [24], [28], [34], [40-42], [46], [52-53], [69-71] and [73]. In part, i.e., where it is more specifically related to

particular transformer operating conditions such as a transformer cold start, they are obtained by fitting and extrapolation techniques performed on the results obtained during various transformer thermal tests, [48], [49] and [62].

- Thermal resistance based on thermal tests obtained by Nordman, [48-49]

It has been already shown and verified in the author's publications, [69-71], that conventional heat transfer theory for natural convection oil flow around vertical plates can be successfully used in order to create an accurate and robust hot-spot temperature model, for which the final formulation is given above. Nevertheless, it has also been observed that this modelling can be improved by further considering the specific design of the transformer windings and their influence on the oil circulation and the temperature gradient at the top of the winding stack. This is achieved by defining a general equation for the convection and heat exchange phenomena between the winding insulation surface and the oil at the top of the winding, which is derived from equations (3.4) and (3.9) in section 3.2:

$$\Delta\theta_{hs} = C' \times \mu^p \times q_{wdn}{}^m \tag{3.39}$$

where C' is a function of the fluid properties and winding characteristic dimensions and is considered to be a constant. p and m are constants that directly affect the shape of the thermal curve, Fig. 1.1. These constants are estimated by taking into account both the steady-state and the transient hot-spot temperature rises over top-oil temperature, and using extrapolation techniques.

The non-linear thermal resistance between the winding insulation surface and the oil at the top of the transformer can now be derived from equation (3.39) as follows:

$$R_{th-hs-oil} = \frac{\Delta\theta_{hs}}{q_{wdn}} = \left(\frac{C' \times \mu^p}{\Delta\theta_{hs}{}^{(1-m)}} \right)^{1/m} \tag{3.40}$$

By following the thermal-electrical analogy and mathematical procedure used to obtain (3.38) from the thermal circuit in Fig. 3.6, the hot-spot model based on the thermal resistance in (3.40) is:

$$\left\{ K^2 \times P_{wdn,pu}(\theta_{hs}) \right\} \times \mu_{pu}{}^n \times \Delta\theta_{hs,rated}$$
$$= \mu_{pu}{}^n \times \tau_{wdn,rated} \times \frac{d\theta_{hs}}{dt} + \frac{(\theta_{hs} - \theta_{oil})^{n'+1}}{\Delta\theta_{hs,rated}{}^{n'}} \tag{3.41}$$

The new parameters, compared to (3.38), are the constants n and n', for which values are defined and given below in Table 3.6 for different cooling modes.

Table 3.6. Empirical constants n and n' for the hot-spot thermal model

Oil circulation	Constant	Cooling modes	
		with external cooling	without external cooling
		ONAF/ONAN/OFAF	ONAN
cold start	$n = n'$	2	0.25
transformer on load	$n = p/m$	0.5	0.25
	$n'=(1-m)/m$	0.1	

The cold start condition is clarified in Appendix B.

Finally, the overall thermal circuit for the transformer top level or a transformer thermal top level cascade connection is shown below.
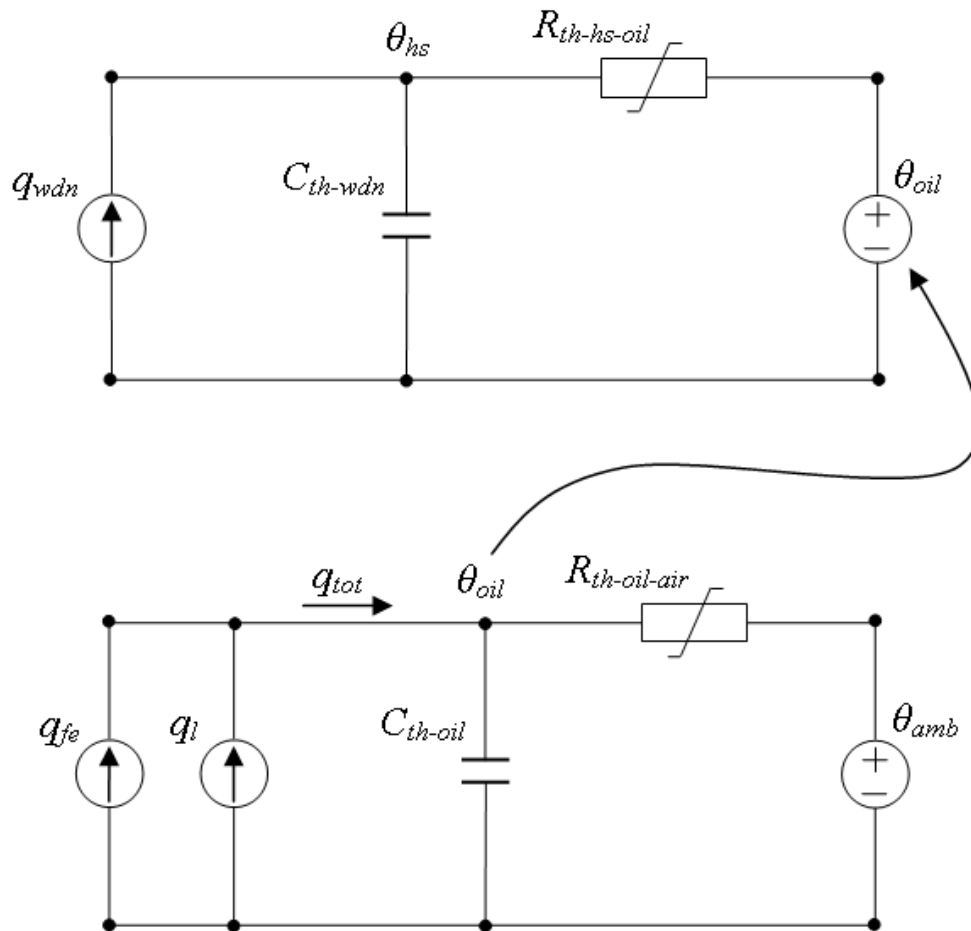
Fig. 3.7. The transformer overall top thermal model

where the nomenclature is the same as in Figs. 3.5 and 3.6.

3.2.3 The bottom-winding and bottom-oil temperature model

The information given in factory reports is usually limited to the data obtained in a heat-run test, i.e., the top-oil in the tank of the transformer and the average winding-to-average oil gradient. If the bottom-oil temperature measurements are also available, it is possible, based on the theory given for the thermal models in the preceding chapters, to generate bottom-winding and bottom-oil temperature models, Fig. 3.8, [69-73].
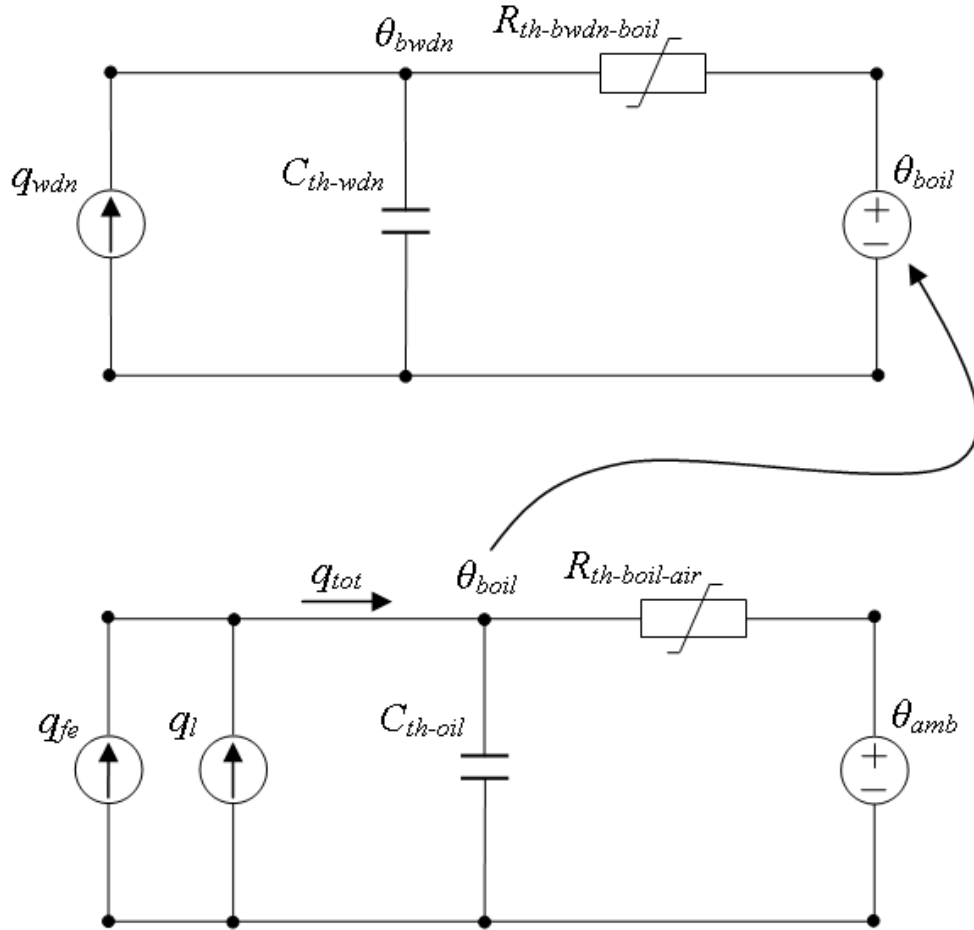

Fig 3.8. The transformer overall bottom thermal model

where:

q_{tot} is the heat generated by the total losses,
q_{fe} is the heat generated by the iron losses,
q_{wdn} is the heat generated by the winding losses,
q_l is the heat generated by the load losses,

$C_{th\text{-}oil}$ is the equivalent thermal capacitance of the transformer oil,
$C_{th\text{-}wdn}$ is the thermal capacitance of the winding,
θ_{boil} is the bottom-oil temperature,
θ_{bwdn} is the bottom-winding hottest temperature,
$R_{th\text{-}boil\text{-}air}$ is the non-linear bottom-oil to air thermal resistance,
$R_{th\text{-}bwdn\text{-}boil}$ is the nonlinear bottom-winding to bottom-oil thermal resistance,
θ_{amb} is the ambient temperature.

The differential equations for the thermal circuits in Fig. 3.8, which model the transformer bottom level, are given as follows:

- The bottom-winding temperature

$$\left\{ K^2 \times P_{wdn,pu}(\theta_{bwdn}) \right\} \times \mu_{pu}{}^n \times \Delta\theta_{bwdn,rated}$$
$$= \mu_{pu}{}^n \times \tau_{wdn,rated} \times \frac{d\theta_{bwdn}}{dt} + \frac{(\theta_{bwdn} - \theta_{boil})^{n+1}}{\Delta\theta_{bwdn,rated}{}^n} \qquad (3.42)$$

- The bottom-oil temperature

$$\frac{1 + R \times P_{l,pu}(\theta_{be}) \times K^2}{1 + R} \times \mu_{pu}{}^n \times \Delta\theta_{boil,rated}$$
$$= \mu_{pu}{}^n \times \tau_{boil,rated} \times \frac{d\theta_{boil}}{dt} + \frac{(\theta_{boil} - \theta_{amb})^{1+n}}{\Delta\theta_{boil,rated}{}^n} \qquad (3.43)$$

where:

R is the ratio of rated load losses to no-load losses, (per unit value), [22],
K is the load factor, (per unit value), [22],
θ_{bwdn} is the bottom-winding hottest temperature, ºC,
$P_{wdn,pu}(\theta_{bwdn})$ is the dependence of the load losses on temperature, (3.44),
θ_{be} is the temperature at which losses are estimated, ºC, (3.45),
$P_{1,pu}(\theta_{be})$ is the dependence of the load losses on the temperature at the bottom, (3.46),
μ_{pu} is the oil viscosity (per unit value),
θ_{amb} is the ambient temperature, ºC,
θ_{boil} is the bottom-oil temperature, ºC,
$\Delta\theta_{bwdn,\,rated}$ is the rated bottom-winding hottest temperature rise over bottom-oil, K,
$\Delta\theta_{boil,\,rated}$ is the rated bottom-oil temperature rise, K,
$\tau_{wdn,rated}$ is the rated winding time constant, min, Appendix D,
$\tau_{boil,rated}$ is the rated bottom-oil time constant, min, section 3.3,
n is an empirical constant, Tables 3.4 and 3.5, Appendix B.

The variation of the winding losses with temperature, $P_{wdn,pu}(\theta_{bwdn})$, is also included in the bottom winding thermal model as follows:

$$P_{wdn,pu}(\theta_{bwdn}) = P_{dc,pu} \times \left(\frac{\theta_{bwdn} + \theta_k}{\theta_{bwdn,rated} + \theta_k} \right) + P_{eddy,pu} \times \left(\frac{\theta_{bwdn,rated} + \theta_k}{\theta_{bwdn} + \theta_k} \right) \qquad (3.44)$$

where:

$P_{dc,pu}$ is the DC losses per unit value,
$P_{eddy,pu}$ is the eddy losses per unit value,
θ_k is the temperature factor for the loss correction, equal
        to 225 for aluminium and 235 for copper.

The high and low voltage winding effects on the oil are taken into account by estimating the losses at a temperature equal to the mean bottom winding hot-spot value given as follows:

$$\theta_{be} = \frac{\theta_{bwdn,lv} + \theta_{bwdn,hv}}{2} \qquad (3.45)$$

where:

θ_{be} is the temperature at which losses are estimated, ºC,
$\theta_{bwdn,lv}$ is the bottom-winding hottest temperature for the low voltage winding, ºC
$\theta_{bwdn,hv}$ is the bottom-winding hottest temperature for the high voltage winding, ºC.

Thus, the dependence of the load losses on temperature, $P_{l,pu}(\theta_{be})$, is defined in the following equation:

$$P_{l,pu}(\theta_{be}) = P_{dc,pu} \times \left(\frac{\theta_{be} + \theta_k}{\theta_{be,rated} + \theta_k} \right) + P_{a,pu} \times \left(\frac{\theta_{be,rated} + \theta_k}{\theta_{be} + \theta_k} \right) \qquad (3.46)$$

where:

$P_{dc,pu}$ is the DC losses per unit value,
$P_{a,pu}$ is the additional losses per unit value,
θ_k is the temperature factor for the loss correction, equal to 225 for aluminium and 235 for copper.

3.2.4 Hot-spot models based on the bottom oil temperature

The hot-spot temperature model based on the bottom oil is shown below, Fig. 3.9. It is partly defined by the theory presented above, [69-73], and partly according to the theory suggested in [3] and [52-53]. The main difference from the previous modelling is in the definition of the transformer nonlinear thermal resistance, $R_{th\text{-}hs\text{-}boil}$, between the winding insulation surface at the top level and the oil at the bottom level.
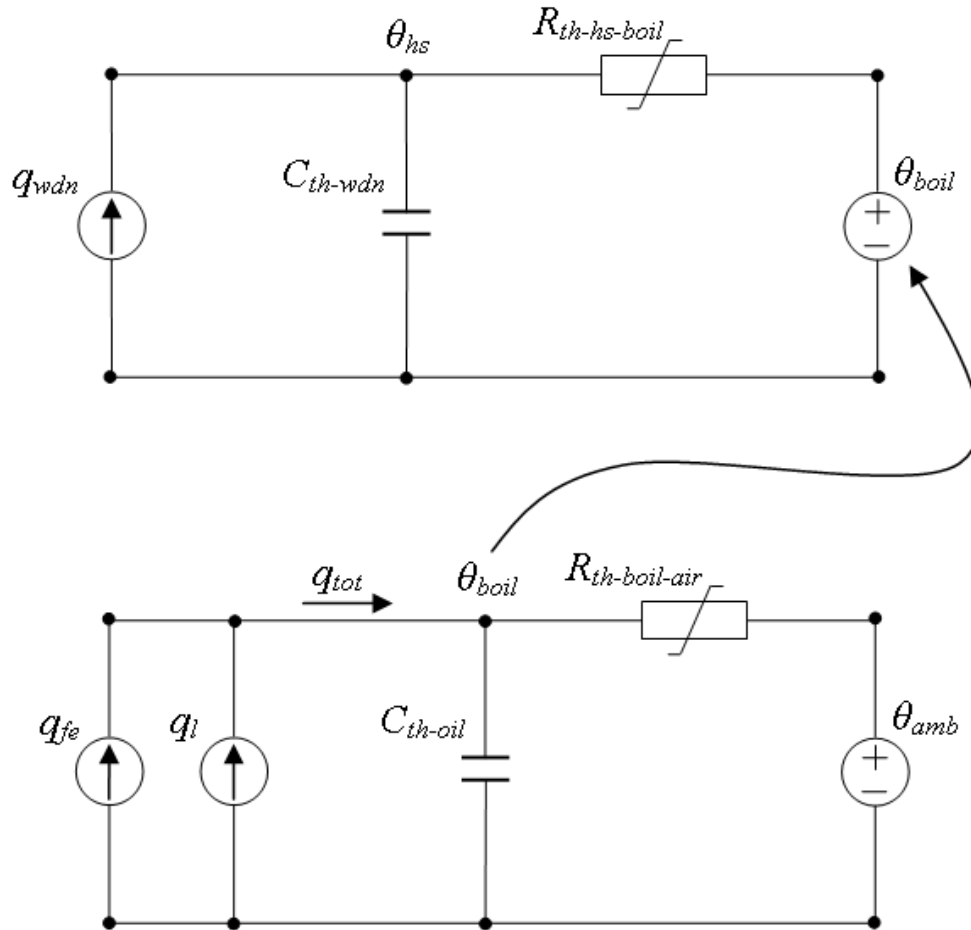
Fig 3.9. The transformer overall thermal model based on the bottom-oil

The symbols, which appear on Fig. 3.9, are the same as those used earlier for Figs. 3.6, 3.7 and 3.8.

– Thermal resistance based on Aubin experiment, [3]

The equation (3.47) for the natural convection and heat exchange phenomena between the winding insulation surface at the top level and the oil at the bottom level is given as follows:

$$\Delta\theta_{hs-boil} = C'' \times \mu^{p} \times q_{wdn}{}^{m} \tag{3.47}$$

where C'' is a function of the fluid properties evaluated at the average hot-spot to bottom-oil temperature and is considered to be a constant. p and m are constants that are partly based on experimental results obtained from thermal tests, [48-49] and [62], and partly based on the experimental results published in [3] and [18].

The thermal resistance between the winding insulation surface at the top-level and the oil at the bottom level of the transformer is characterised by equation (3.48), which is derived from (3.47):

$$R_{th-hs-boil} = \frac{\Delta\theta_{hs-boil}}{q_{wdn}} = \left(\frac{C'' \times \mu^{p}}{\Delta\theta_{hs-boil}{}^{(1-m)}} \right)^{1/m} \tag{3.48}$$

Similar to the procedure applied in the hot-spot temperature modelling in section 3.2.2, the new hot-spot model is defined by taking into account the derived thermal resistance, (3.48), as follows:

$$\left\{ K^{2} \times P_{wdn,\,pu}\left(\theta_{hs}\right) \right\} \times \mu_{pu}{}^{n} \times \Delta\theta_{hs-boil,\,rated}$$
$$= \mu_{pu}{}^{n} \times \tau_{wdn-b,rated} \times \frac{d\theta_{hs}}{dt} + \frac{\left(\theta_{hs} - \theta_{boil}\right)^{1+n'}}{\Delta\theta_{hs-boil,\,rated}{}^{n'}} \tag{3.49}$$

where the only new parameter, compared to (3.38) and (3.43), is the rated hot-spot to bottom-oil gradient, $\Delta\theta_{hs-boil,\,rated}$ in K, and the winding time constant, $\tau_{wdn-b,rated}$ in minutes, Appendix D.

The empirical values for constants n and n', for different cooling modes and transformer designs, are given in Table 3.7. The viscosity is evaluated at a temperature equal to the average of the relevant hot-spot and bottom-oil temperatures.

Table 3.7. Empirical constants n and n' for the hot-spot thermal model based on the bottom oil

Constant	with external cooling	without external cooling
	ONAF / ONAN / OFAF	ONAN
$n = p/m$	0.2	0.25
$n' = (1-m)/m$	0.75	0.25

− Thermal resistance based on the Pierce experiment, [52-53]

Similar to the experimental results shown above, Pierce obtained an empirical equation (3.50) for the natural convection and heat exchange phenomena between the winding insulation surface at the top level and the oil at the bottom level. This equation was found to fit the data obtained during a wide variety of thermal tests with different cooling modes, [52]. Thus, it implicitly takes into account the effect of viscosity as well.

$$\Delta\theta_{hs-boil} = C''' \times q_{wdn}{}^{m}$$ (3.50)

where C''' is a constant. The exponent m is a constant, its value taken from the IEEE Lading Guide-Annex G, [28] and [52-53].

The thermal resistance between the winding insulation surface at the top level and the oil at the bottom level of the transformer is characterised by (3.51), which is derived from (3.50):

$$R_{th-hs-boil} = \frac{\Delta\theta_{hs-boil}}{q_{wdn}} = \left(\frac{C'''}{\Delta\theta_{hs-boil}{}^{(1-m)}} \right)^{1/m}$$ (3.51)

Again applying the procedure used for the hot-spot temperature modelling in section 3.2.2, the new hot-spot model is now defined by taking into account the derived thermal resistance, (3.51), as follows:

$$\left\{ K^{2} \times P_{wdn,\,pu}\left(\theta_{hs}\right) \right\} \times \Delta\theta_{hs-boil,\,rated} = \tau_{wdn-b,rated} \times \frac{d\theta_{hs}}{dt} + \frac{\left(\theta_{hs} - \theta_{boil}\right)^{1+n'}}{\Delta\theta_{hs-boil,\,rated}{}^{n'}}$$ (3.52)

Empirical values for the constant n' are given in Table 3.8, for different cooling modes and transformer designs.

Table 3.8. Empirical constant n' for the hot-spot thermal model based on the bottom oil

Constant	with external cooling	without external cooling
	ONAF/ONAN/OFAF	ONAN
$n'=(1-m)/m$	1	0.5

The bottom oil model, Fig. 3.9, has already been defined in (3.43).

3.2.5 Symbol summary

The symbols used in (3.24), (3.38), (3.41), (3.42), (3.43), (3.49) and (3.52) are summarised in Table 3.9, below.

Table 3.9. Calcification of elements of thermal models

Equation	Independent Variable	Constant	Input Variables	Output Variables
(3.24)	t	n, $\tau_{\text{oil,rated}}$, $\Delta\theta_{\text{oil,rated}}$, R	$\theta_{\text{amb}}, K, \mu_{\text{pu}},$ $P_{\text{l,pu}}(\theta_e)$	$*\theta_{\text{oil}}$
(3.38)	t	n, $\tau_{\text{wdn,rated}}$, $\Delta\theta_{\text{hs,rated}}(=H\cdot g_r)$	$*\theta_{\text{oil}}, K,$ $\mu_{\text{pu}}, P_{\text{wdn,pu}}(\theta_{\text{hs}})$	θ_{hs}
(3.41)	t	n, n', $\tau_{\text{wdn,rated}}$, $\Delta\theta_{\text{hs,rated}}(=H\cdot g_r)$	$*\theta_{\text{oil}}, K,$ $\mu_{\text{pu}}, P_{\text{wdn,pu}}(\theta_{\text{hs}})$	θ_{hs}
(3.42)	t	n, $\tau_{\text{bwdn,rated}}$, $\Delta\theta_{\text{bwdn,rated}}(=H\cdot g_r)$	$**\theta_{\text{boil}}, K,$ $\mu_{\text{pu}}, P_{\text{wdn,pu}}(\theta_{\text{bwdn}})$	θ_{bwdn}
(3.43)	t	n, $\tau_{\text{boil,rated}}$, $\Delta\theta_{\text{boil,rated}}$, R	$\theta_{\text{amb}}, K, \mu_{\text{pu}},$ $P_{\text{l,pu}}(\theta_{\text{be}})$	$**\theta_{\text{boil}}$
(3.49)	t	n, n', $\tau_{\text{wdn-b,rated}}$, $\Delta\theta_{\text{hs-boil,rated}}$	$**\theta_{\text{boil}}, K,$ $\mu_{\text{pu}}, P_{\text{wdn,pu}}(\theta_{\text{hs}})$	θ_{hs}
(3.52)	t	n', $\tau_{\text{wdn-b,rated}}$, $\Delta\theta_{\text{hs-boil,rated}}$	$**\theta_{\text{boil}}, K,$ $\mu_{\text{pu}}, P_{\text{wdn,pu}}(\theta_{\text{hs}})$	θ_{hs}

$*\theta_{oil}$- represents the "output variable" in (3.24) and "input variable" in (3.38) and (3.41), so that these models form a cascaded connection.

$**\theta_{boil}$- represents the "output variable" in (3.43), and "input variable" in (3.42), (3.49), and (3.52), also forming a cascaded connection.

3.3 Top-oil time constant for the thermal models

The electrical circuit theory for an RC circuit gives the time constant as the time required to charge a capacitor, Fig. 3.1, to 63.2 percent of full charge or to discharge it to 36.8 percent of its initial value. The value of the time constant is equal to the product of the circuit resistance, R_{el}, and the circuit capacitance, C_{el}. The value of one time constant is expressed mathematically as follows:

$$\tau_{el} = R_{el} \cdot C_{el} \tag{3.53}$$

The thermal time constant has also been defined by Montsinger, [6], as the length of time required for the temperature to change from the initial value to the ultimate value if the initial rate of change is continued until the ultimate temperature is reached. The time constant is usually measured by determining the length of time required for a specific fraction of the change in temperature from initial value to ultimate value to take place. Generally, 63 percent of the temperature change occurs in a length of the time equal to the time constant, regardless of the relationship between the initial and final temperatures.

Based on the electrical-thermal analogy presented in section 3.1, a thermal time constant for a thermal circuit as shown in Fig. 3.2, can be defined as follows:

$$\tau_{th} = R_{th} \cdot C_{th} \tag{3.54}$$

where:
τ_{th} is the thermal time constant in minutes,
R_{th} is the thermal resistance in *K/W*,
C_{th} is the thermal capacitance in *(Wmin) /°C*.

Furthermore, for the rated conditions, i.e., when ultimate conditions are reached, the thermal resistance, R_{th}, is:

$$R_{th,rated} = \frac{\Delta\theta_{rated}}{q_{rated}} \tag{3.55}$$

where:

$\Delta\theta_{rated}$ is the rated temperature rise,
q_{rated} are the losses at rated load.

If we substitute (3.55) into (3.54), the general equation for the thermal time constant is:

$$\tau_{th,rated} = C_{th,rated} \frac{\Delta\theta_{rated}}{q_{rated}} \tag{3.56}$$

In order to use (3.56) to calculate the transformer top-oil time constant it is necessary to define the equivalent thermal capacitance of the transformer oil. Therefore, a more complete transformer thermal circuit is shown in Fig. 3.10. This thermal circuit is also simplified by realising that the direct heat transfer between the winding and other transformer parts, e.g., the core and the tank, can be neglected due to the insulating cylinders placed between them, [34]. Similarly, the direct heat transfer between the tank and the core is also neglected, [34].
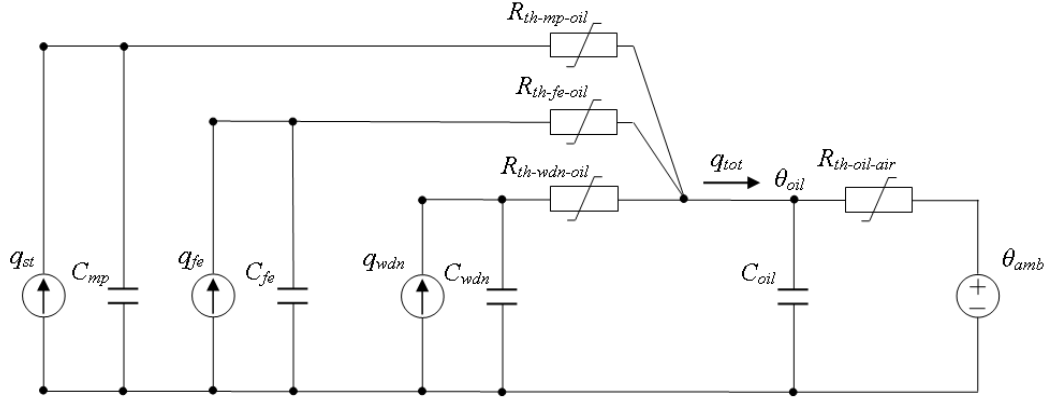
3.10. A complex top-oil thermal circuit

where:

q_{st} is the heat generated by the stray losses,
q_{fe} is the heat generated by the core losses,
q_{wdn} is the heat generated by the winding losses,
C_{wdn} is the thermal capacitance of the copper,
C_{fe} is the thermal capacitance of the core,
C_{oil} is the thermal capacitance of the oil,
C_{mp} is the thermal capacitance of the tank and other metal parts,
$R_{th-oil-air}$ is the non-linear oil to air thermal resistance,
$R_{th-wnd-oil}$ is the nonlinear winding to oil thermal resistance,
$R_{th-fe-oil}$ is the nonlinear core to oil thermal resistance,
$R_{th-mp-oil}$ is the nonlinear tank and other metal parts to oil thermal resistance,
θ_{oil} is the oil temperature,
θ_{amb} is the ambient temperature.

Furthermore, the load losses in the transformer are equal to the sum of the winding DC and eddy losses and stray losses in the metal parts. Thus the transformer total losses are:

$$q_{tot} = q_{fe} + q_{wdn} + q_{st} \tag{3.57}$$

Equation (3.57) can be rearranged as follows:

45

$$q_{tot} = \frac{q_{fe}}{q_{tot}} \times q_{tot} + \frac{q_{wdn}}{q_{tot}} \times q_{tot} + \frac{q_{st}}{q_{tot}} \times q_{tot} \qquad (3.58)$$

Additionally, the fractions from (3.58) are given the following symbols:

$$\frac{q_{fe}}{q_{tot}} = Y_{fe} \qquad (3.59)$$

$$\frac{q_{wdn}}{q_{tot}} = Y_{wdn} \qquad (3.60)$$

$$\frac{q_{st}}{q_{tot}} = Y_{st} \qquad (3.61)$$

where Y_{fe}, Y_{wdn}, and Y_{st} are the portions of the core, stray and winding losses in the total transformer losses, respectively. By comparing the loss portions given in (3.59), (3.60) and (3.61), and considering the data obtained in the thermal tests, [48-49] and [62], the following correlations are obtained:

$$Y_{st} << Y_{wdn}, \text{ and } Y_{st} << 1 \qquad (3.62)$$

$$Y_{fe} << Y_{wdn}, \text{ and } Y_{fe} << 1 \qquad (3.63)$$

By substituting (3.59), (3.60), and (3.61) into (3.58), the total loss equation becomes:

$$q_{tot} = Y_{fe} \times q_{tot} + Y_{wdn} \times q_{tot} + Y_{st} \times q_{tot}. \qquad (3.64)$$

Then the top-oil thermal circuit, Fig. 3.10, can be further modified, as shown in Fig. 3.11, below.
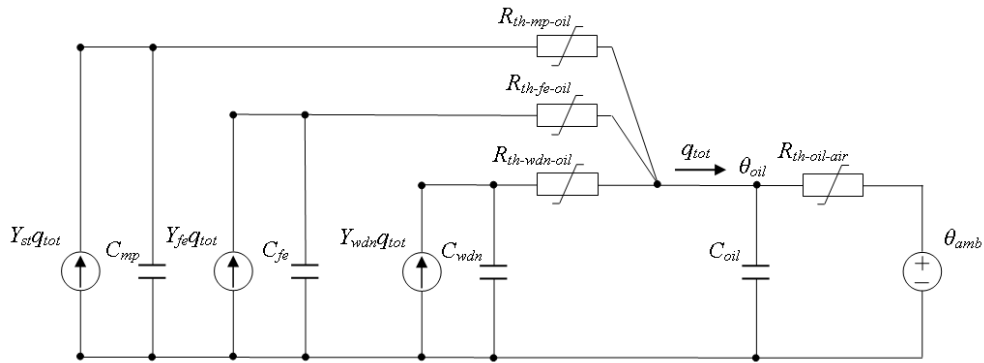
3.11. Further modified top-oil thermal circuit

where:

q_{tot} is the heat generated by the total losses,
Y_{st} is the portion of the stray losses in the total losses,
Y_{fe} is the portion of the core losses in the total losses,
Y_{wdn} is the portion of the winding losses in the total losses,
C_{wdn} is the thermal capacitance of the copper,
C_{fe} is the thermal capacitance of the core,
C_{mp} is the thermal capacitance of the tank and other metal parts,
C_{oil} is the thermal capacitance of the oil,
$R_{th\text{-}oil\text{-}air}$ is the non-linear oil to air thermal resistance,
$R_{th\text{-}wdn\text{-}oil}$ is the nonlinear winding to oil thermal resistance,
$R_{th\text{-}fe\text{-}oil}$ is the nonlinear core to oil thermal resistance,
$R_{th\text{-}mp\text{-}oil}$ is the nonlinear tank and other metal parts to oil thermal resistance,
θ_{oil} is the oil temperature,
θ_{amb} is the ambient temperature.

Based on the measured temperature rises and corresponding losses for different transformer units the thermal circuit can be further simplified by noting that the thermal resistances, $R_{th\text{-}wdn\text{-}oil}$, $R_{th\text{-}fe\text{-}oil}$, and $R_{th\text{-}mp\text{-}oil}$, yield very low values, [75-76], e.g., of the order of 5×10^{-5} K/W, so that for the purpose of this study they can be neglected. Consequently, the thermal circuit, Fig. 3.11, can be further transformed into the circuit shown in Fig. 3.12, by the conversion of the heat sources and correction of the thermal capacitances accordingly.
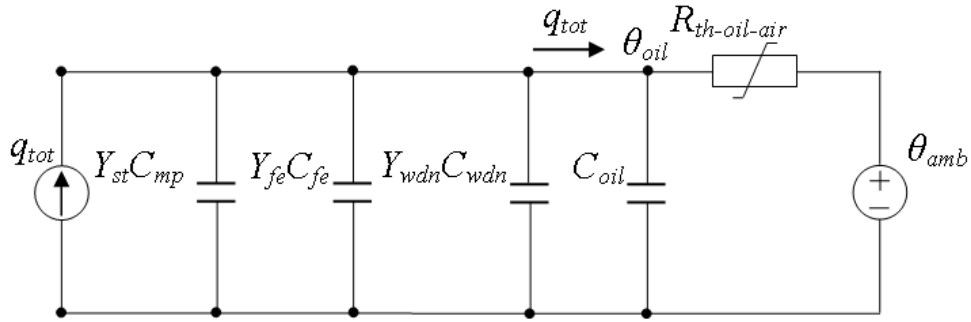
Fig. 3.12. Transformed top-oil thermal circuit

The thermal capacitances for the different branches in Fig. 3.12 can be denoted as follows:

$$C'_{wdn} = Y_{wdn} C_{wdn} \tag{3.65}$$

$$C'_{fe} = Y_{fe} C_{fe} \tag{3.66}$$

$$C'_{mp} = Y_{st} C_{mp} \tag{3.67}$$

and Fig. 3.12 can be changed into Fig. 3.13 below.
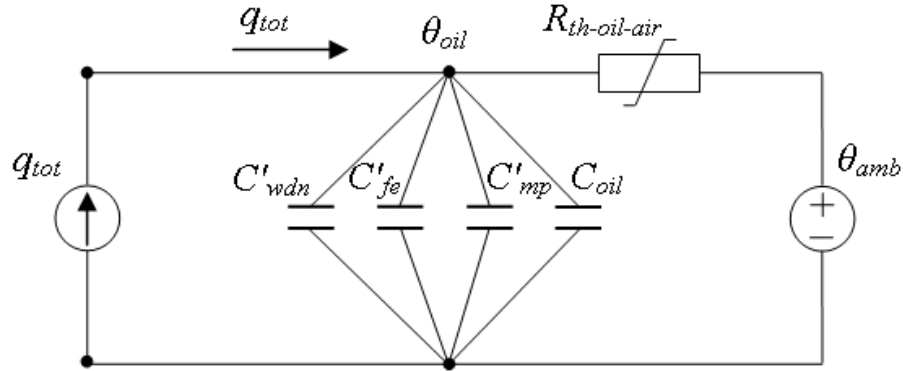

Fig. 3.13. Thermal capacitance circuit

where the four parallel thermal capacitances, C'_{wdn}, C'_{fe}, C'_{mp}, and C_{oil}, are replaced by a single equivalent thermal capacitance of the transformer oil, $C_{th\text{-}oil}$, as follows:

$$C_{th-oil} = C'_{wdn} + C'_{fe} + C'_{mp} + C_{oil} \tag{3.68}$$

and the thermal circuit, Fig. 3.13, is finally transformed into the circuit shown in Fig. 3.5.

Based on the foregoing, the equivalent thermal capacitance of the transformer oil for transformers with external cooling and a zigzag oil flow through the windings, is given by:

$$C_{th-oil} = Y_{wdn} \times m_{wdn} \times c_{wdn} + Y_{fe} \times m_{fe} \times c_{fe} + Y_{st} \times m_{mp} \times c_{mp} + O_{oil} \times m_{oil} \times c_{oil}$$

$$(3.69)$$

where:

m_{wdn} is the weight of the winding material (use only the excited parts) in kilograms,
m_{fe} is the weight of the core in kilograms,
m_{mp} is the weight of the tank and fittings in kilograms,
m_{oil} is the weight of the oil in kilograms.

c_{wdn} is the specific heat capacity of the winding material (c_{cu}=0.11 and c_{al}=0.25) in Wh/kg°C, [32],
c_{fe} is the specific heat capacity of the core (=0.13) in Wh/kg°C, [32],
c_{mp} is the specific heat capacity of the tank and fittings (=0.13) in Wh/kg°C, [32],
c_{oil} is the specific heat capacity of the oil (=0.51) in Wh/kg°C, [32].

O_{oil}=0.86   is the correction factor for the oil in the ONAF, ONAN and OFAF cooling modes,
O_{oil}=1.0   is the correction factor for the oil in the ODAF cooling mode.

48

The values for the correction factor, O_{oil}, are based on the modelling performed in this thesis and on observations made during a number of thermal tests, [48-49] and [62]. In a similar way, a correction factor of oil has been suggested in the literature, [6-7], where it was found that the best calculation results were obtained when basing the heat storage on two-thirds of the tank weight and 85 per cent of the oil. The reason for this was that the lower portion of the transformer remained comparatively cool. This has been implemented in the present IEEE loading guide for power transformers, [28].

It is necessary to scale the portion of the winding, Y_{wdn}, and stray, Y_{st}, losses based on the average winding temperature to the mean hot-spot temperature, equation (3.23), to account for the additional heat generated at the hot-spot temperature.

The equivalent thermal capacitance of the transformer oil for transformers without either external cooling or guided horizontal oil flow through the windings (where the lack of radiators and the lack of the horizontal oil flow through the winding directly affects the oil flow inside the transformer tank, thus slowing down the cooling process) is calculated according to the IEEE Loading Guide-Annex G, [28] and [52-53]:

$$C_{th-oil} = c_{wdn} \times m_{wdn} + c_{fe} \times m_{fe} + c_{mp} \times m_{mp} + c_{oil} \times m_{oil} \tag{3.70}$$

The top-oil time constant at the load considered for the thermal circuit, Fig. 3.3, can now be given by the following:

$$\tau_{oil,rated} = C_{th-oil,rated} \frac{\Delta\theta_{oil,rated}}{q_{tot,rated}} \times 60 \tag{3.71}$$

where:

$\tau_{oil,rated}$ is the rated top-oil time constant,
$q_{tot,rated}$ are the total losses at rated load, corrected for the additional heat generated at the rated mean hot-spot temperature, $\theta_{e,rated}$,
$C_{th-oil,rated}$ is the equivalent thermal capacitance of the transformer oil evaluated at the rated mean hot-spot temperature, $\theta_{e,rated}$,
$\Delta\theta_{oil,\ rated}$ is the rated top-oil temperature rise.

When the bottom oil time constant is calculated, the rated top-oil temperature rise in (3.71) should be substituted with the average oil temperature rise. The reason for using the average oil rise instead of the top-oil temperature rise is as follows:

It has been standard practice in industry to use the tank-inlet oil for the "official" bottom oil. In old designs the tank inlet pipes were taken to the bottom of the tank, which meant a well mixed, homogenous bottom oil flowed into the windings. Therefore, it was reasonable to assume that the time constant for the "bottom oil" was approximately equal to the top-oil time constant. On the other hand, in power transformers made today, the radiator inlet pipes are normally located somewhat below the mid-height of the tank. Measurements have shown that there is a gradient of 10…20 K between the "official"

bottom oil, i.e., the measured tank inlet oil, which circulates into the winding, and the oil under the winding at approximately the middle level of the bottom yoke, which is stagnant. Therefore, the bottom time constant for this design is shorter than the top oil time constant, essentially much closer to the average oil time constant.

The time constant correction for an initial temperature rise not equal to zero, a change in value of the constant n (depending on oil flow) and oil viscosity, dependent on temperature, is instantaneously made in the equations for top-oil, hot-spot, bottom-oil, and bottom-winding temperatures.
In practice, the data needed to calculate the top-oil time constant according to the procedure given above is not always available. Therefore, an empirical equation is developed and suggested in Appendix E.

3.4 Discussion

The key contribution in the research results presented above is the definition of the non-linear thermal resistances between the following transformer components:

- The winding insulation surface to oil, at the top level,
- The winding insulation surface to oil, at the bottom level,
- The winding insulation surface at the top level to the oil at the bottom level,
- The oil to air at the top level,
- The oil to air at the bottom level.

The definition is based on the heat transfer theory for the natural flow of oil around vertical, inclined and horizontal plates and cylinders, [33], as well experimental results obtained by various authors, [6], [7], [18], [40-42], [46], [52-53], [59-60], [62], [69-71] and [73]. Furthermore, the non-linear thermal resistances are introduced into the lumped capacitance method using the electrical-thermal analogy. The application of the lumped capacitance method for the evaluation of power transformer thermal behaviour has been verified by many authors and so it was also used to obtain the thermal models in this research work, section 3.2. Two basic groups of hot-spot temperature models have been presented. The first is based on the top-oil temperature and related non-linear resistances while the second is based on the bottom-oil temperature and the relevant non-linear thermal resistances. In addition, top- and bottom-oil thermal models have been established. The models take account of variations in oil viscosity and winding resistance. As a reference temperature for the oil viscosity evaluation, the top- and bottom-oil temperatures in the tank are used in each respective model. Additionally, the oil viscosity is evaluated at an average temperature (the average of the relevant hot-spot and bottom-oil temperatures) for the hot-spot temperature models based on the bottom-oil.

The constant n, which defines the shape of the thermal curve for the thermal models defined by (3.24), (3.38), (3.42) and (3.43), has been given for the various cooling modes and different transformer designs. It was also pointed out that the constant n should be corrected for both forced oil circulation (i.e., "natural forced" and "pump forced") within the transformer tank and forced air circulation within the heat exchanger (i.e., "fan forced"). Basically, the oil circulation is independent of temperature only in the cooling mode where the oil flow is directed through the windings, (ODAF), and in such a case the constant n will be equal to zero. The constants n and n' that define the shape of the thermal curve for the thermal model given in (3.41) in section 3.2.2 and for the thermal models in sections 3.2.4 are based on experimental results obtained by several authors [3], [18], [48-49], [62] and [52-53] and partly on the procedure given in [15]. The empirical constant given in Table 3.4, however, can be defined in a regular heat run test made on a transformer with installed thermocouples by using fitting and extrapolation techniques. The values given in Tables 3.5, 3.6, 3.7 and 3.8 can be defined in a similar way, but only if the transformer is equipped with fibre optic sensors in a prolonged heat run test. Note that these techniques should be applied in a manner consistent with the modelling presented in this thesis.

The equivalent thermal capacitance of the transformer oil was defined and suggested in a new solution based on uneven loss distribution within a transformer with external cooling and guided zigzag oil flow through the windings.

It is also recommended that other transformer designs, i.e., where there is no external radiator cooling or horizontal oil flow through the windings, should be accounted for. Therefore, based on observations reported in [49], [52-53] and [69], the modified equation for the equivalent thermal capacitance of the transformer oil is given.

Results from the application of the models on a comprehensive range of transformer units will be shown and discussed in the following section.

4 Application examples

The measured temperature results, which are recorded for six different transformer units and two different tank types (i.e., tanks with and without external cooling) during different load tests are compared to results obtained by both the calculation methods presented in this thesis and the IEEE-Annex G method, [28]. In addition, the real-time application of the thermal models is also shown. The input data used for the two calculation methods are given in Tables G.1 and G.2, Appendix G.

The calculation methods are named as follows in the graphs below:

- − "TM1" refers to the hot spot temperature model, equation (3.38), section 3.2.2
- − "TM2" refers to the hot spot temperature model, equation (3.41), section 3.2.2
- − "TM3" refers to the hot spot temperature model, equation (3.49), section 3.2.4
- − "TM4" refers to the hot spot temperature model, equation (3.52), section 3.2.4
- − "TM" refers to both the top- and bottom-oil temperature models, equation (3.24) in section 3.2.1, and equation (3.43) in section 3.2.3, respectively.

4.1 Transformers with external cooling

A short description of some large power transformers, all of which have been equipped with fibre optic sensors in the main windings, some also with thermocouples in the core and structural parts, and to which additional, non-standardised load tests have been made, is given below, [48-49].

4.1.1 Single-phase 80 MVA ONAN – cooled transformer

The windings were seen from the limb side, the regulating winding, the 26.25 kV main winding and the 400 kV main winding. The sketch of the core window and winding arrangement of the transformer is given in Appendix H. The short circuit impedance was 17%. The oil flow through the windings was guided by the oil guiding rings in a zigzag pattern. The transformer was equipped with a total of 7 fibre optic sensors, three in the 26.25 kV winding and 4 in the 400 kV winding. In addition to the normal delivery test the following load test was performed on the unit in the ONAN cooling mode:

- − constant load current: 1.1 p.u., duration: 11.75 h; the transformer was run from a cold start, Appendix B

The measured hot-spot temperature results, which were recorded during constant current tests, are compared with results obtained from the thermal models in Figs. 4.1, 4.2 and 4.3 below.
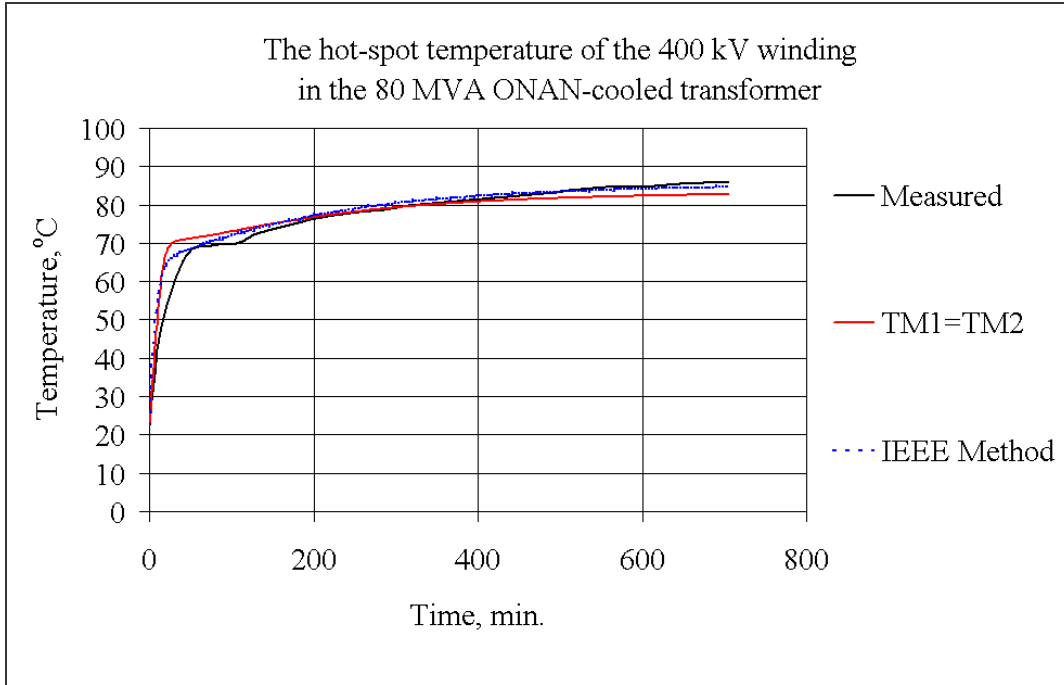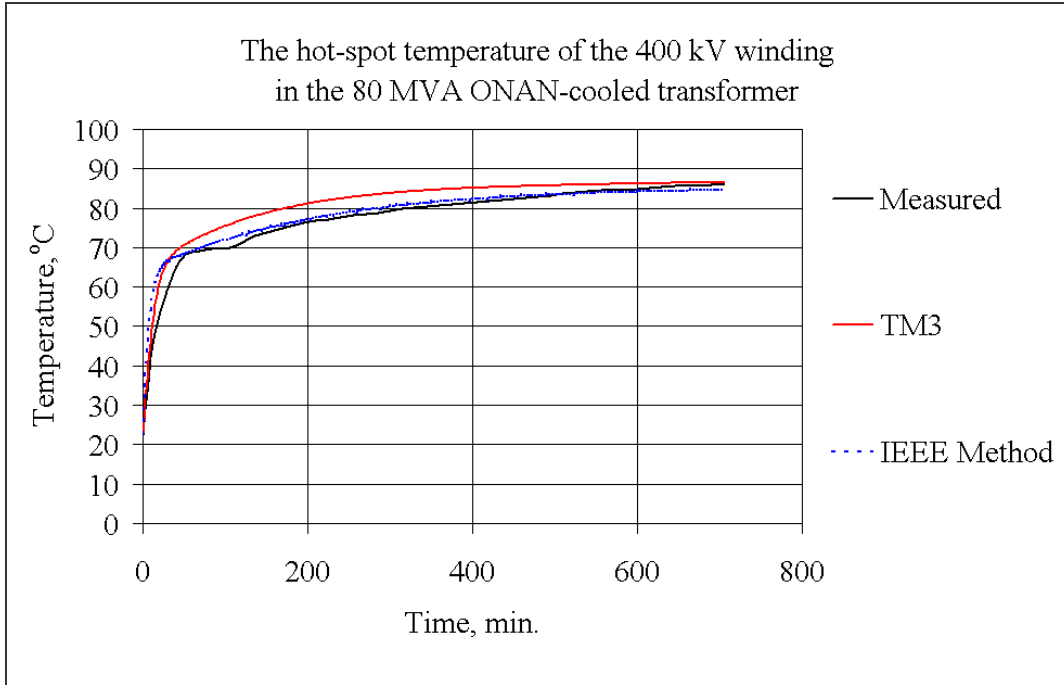
Fig. 4.1. The hot-spot temperature of the 400 kV winding in the 80 MVA ONAN-cooled transformer

Fig. 4.1 shows the comparison between the measured hot-spot temperature of the 400 kV winding in the 80 MVA ONAN-cooled transformer and the hot-spot temperatures obtained by the following calculation methods:

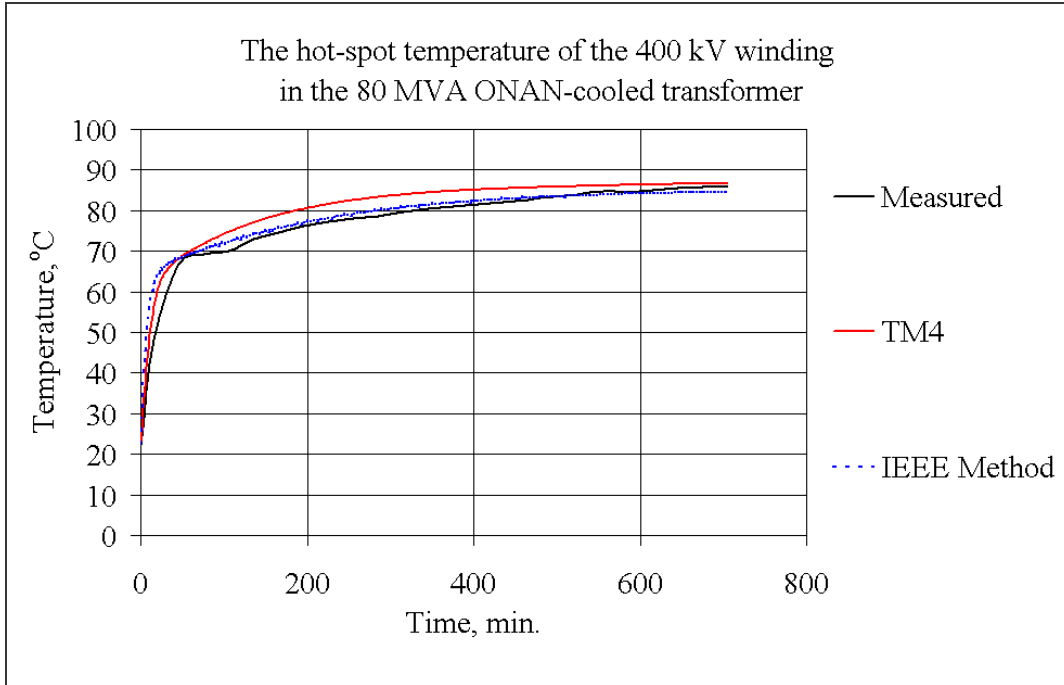- "TM1" refers to the hot spot temperature model, equation (3.38), section 3.2.2,

- "TM2" refers to the hot spot temperature model, equation (3.41), section 3.2.2,

- the IEEE-Annex G method, [28].

When the transformer is run from the cold start the thermal models TM1 and TM2 will yield the same results. Once the transformer is energised, the "cold start" exponents, which are given in Tables 3.4, 3.5 and 3.6, should be substituted for the transformer "on load" exponents at the first load change, Appendix B. Therefore, the temperature results obtained by these models can be represented with the single red line in Fig. 4.1.

Fig. 4.2. The hot-spot temperature of the 400 kV winding in the 80 MVA ONAN-cooled transformer

Fig. 4.2 shows the comparison between the measured hot-spot temperature of the 400 kV winding in the 80 MVA ONAN-cooled transformer and the hot-spot temperatures obtained by the following calculation methods:

- "TM3" refers to the hot spot temperature model, equation (3.49), section 3.2.4,

- the IEEE-Annex G method, [28].

55

Fig. 4.3. The hot-spot temperature of the 400 kV winding in the 80 MVA ONAN-cooled transformer

Fig. 4.3 compares the measured hot-spot temperature of the 400 kV winding in the 80 MVA ONAN-cooled transformer with the hot-spot temperatures obtained by the following calculation methods:

- "TM4" refers to the hot spot temperature model, equation (3.52), section 3.2.4

- the IEEE-Annex G method, [28]

Additionally, both the measured bottom- and top-oil temperature results, which were recorded during a constant current test, are compared with results obtained from the thermal models in Figs. 4.4 and 4.5 below.
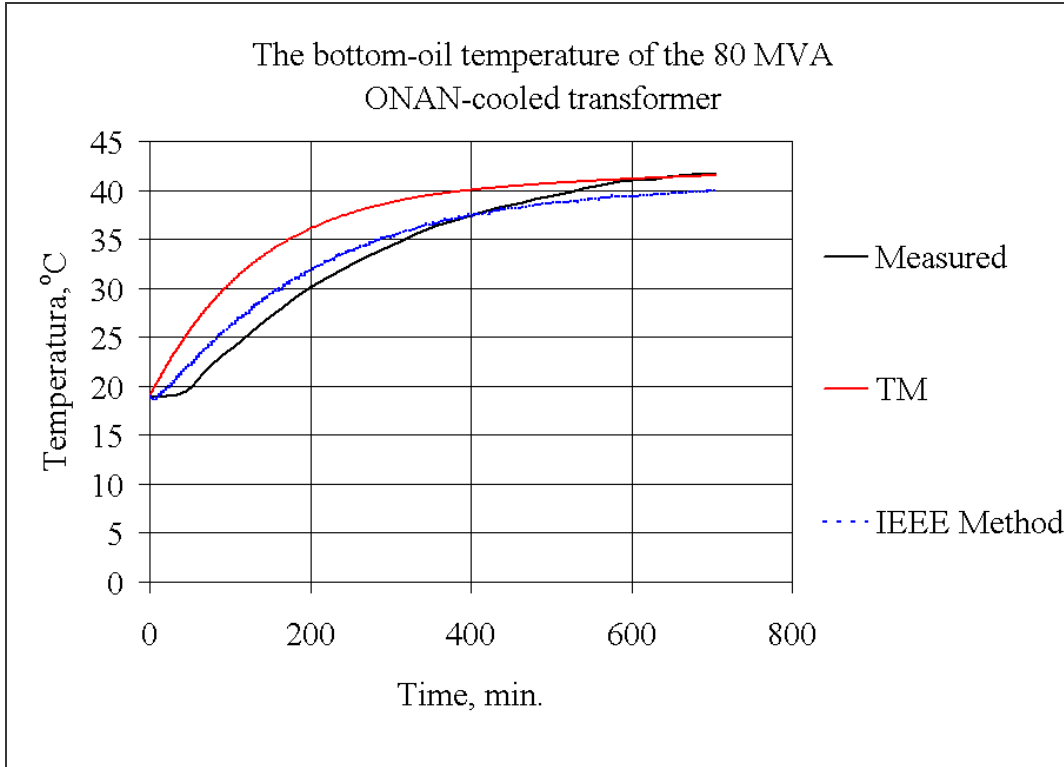
Fig. 4.4. The bottom-oil temperature of the 80 MVA ONAN-cooled transformer

Fig. 4.4 compares the measured bottom-oil temperature of the 80 MVA ONAN-cooled transformer to the bottom-oil temperatures obtained by the following calculation methods:

- "TM" refers to the bottom-oil temperature model, equation (3.43) in section 3.2.3.

- the IEEE-Annex G method, [28]
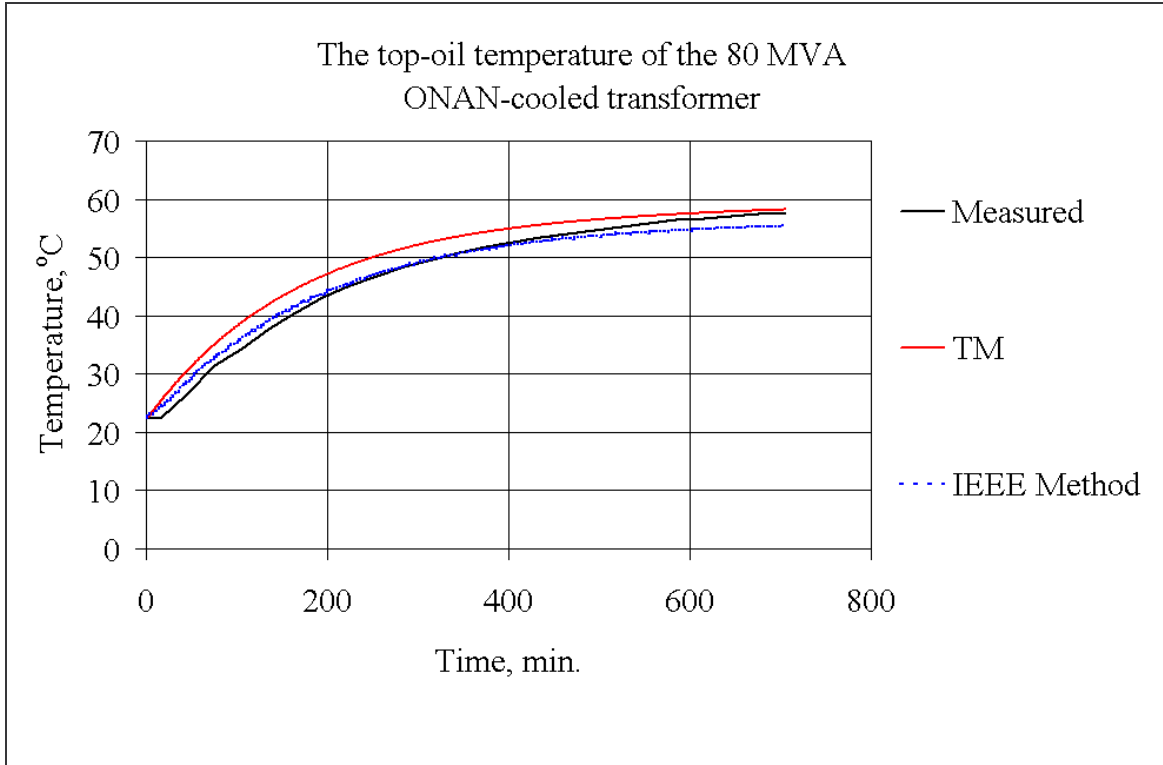
Fig. 4.5. The top-oil temperature of the 80 MVA ONAN-cooled transformer

Fig. 4.5 compares the measured top-oil temperature of the 80 MVA ONAN-cooled transformer to the top-oil temperatures obtained by the following calculation methods:

–   "TM" refers to the top-oil temperature model, equation (3.24) in section 3.2.1

–   the IEEE-Annex G method, [28]

It should be pointed out that the winding chosen for the comparison was the hottest of the two main windings in the tested transformer unit. The results are shown graphically, to enable easy visual verification. These results are further discussed in section 4.4.

4.1.2 Three-phase 250/250/75-MVA ONAF -cooled transformer

The rated voltages of the 250 MVA transformer were 230±8 x 1.5%/118/21 kV. The windings were seen from the limb side, the 118 kV and 230 kV main windings, the regulating winding and the 21-kV tertiary winding. A sketch of the core window and winding arrangement of the transformer is given in Appendix H. The connection was YNyn0d11, and the short circuit impedance in the 250/250 MVA main direction was 12%. The oil flow through the windings was guided by oil guiding rings in a zigzag pattern. The transformer was equipped with a total of 16 fibre optic sensors, eight in the 118 kV winding and eight in the 230 kV winding, according to the principles explained in [48]. In total, 14 thermocouples were located in the tie plates and outer core packets at the top level of the main windings of phase B.

In addition to the normal delivery tests, including the ONAN and ONAF heat run tests, the following load tests were performed on the unit operating in the ONAF cooling mode:

- − constant load current; 1.28 p.u.; duration 13.5 h,
- − constant load current; 1.49p.u.; duration 15 h,
- − varying load current, Table 4.1.

Table 4.1 – The load steps for the 250 MVA transformer

Time period (minutes)	Load factor
0.0 −187.4	1.0
187.4 −364.9	0.6
364.9−503.4	1.5
503.4−710.0	0.3
710.0−735.0	2.1
735.0−750.0	0.0

The measured hot-spot temperature results, recorded during a varying load current test, are compared with results obtained from the thermal models in Figs. 4.6, 4.7, 4.8 and 4.9 below.
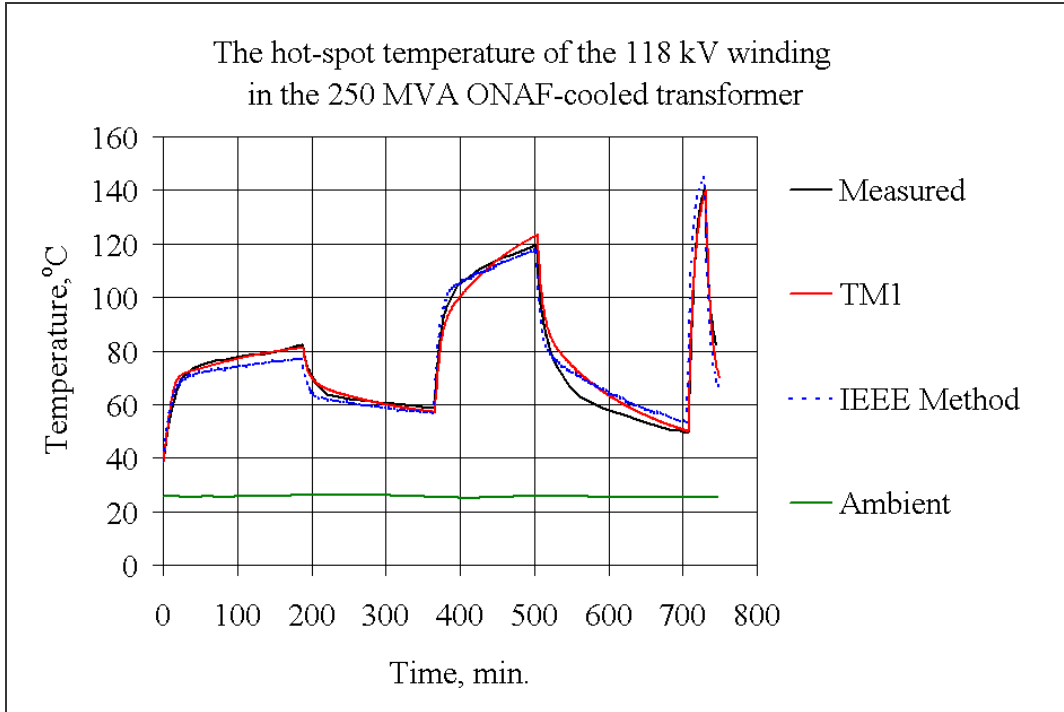
Fig. 4.6. The hot-spot temperature of the 118 kV winding in the 250 MVA ONAF-cooled transformer

Fig. 4.6 shows the measured hot-spot temperature of the 118 kV winding in the 250 MVA ONAF-cooled transformer along with the hot-spot temperatures obtained by the following calculation methods:

- "TM1" refers to the hot spot temperature model, equation (3.38), section 3.2.2
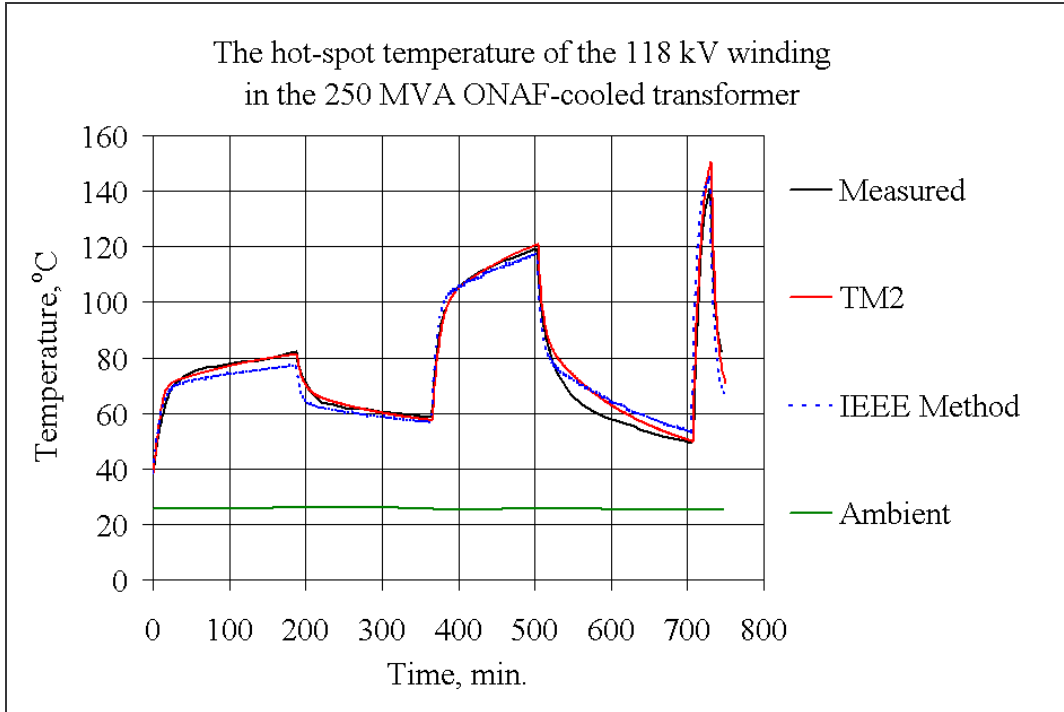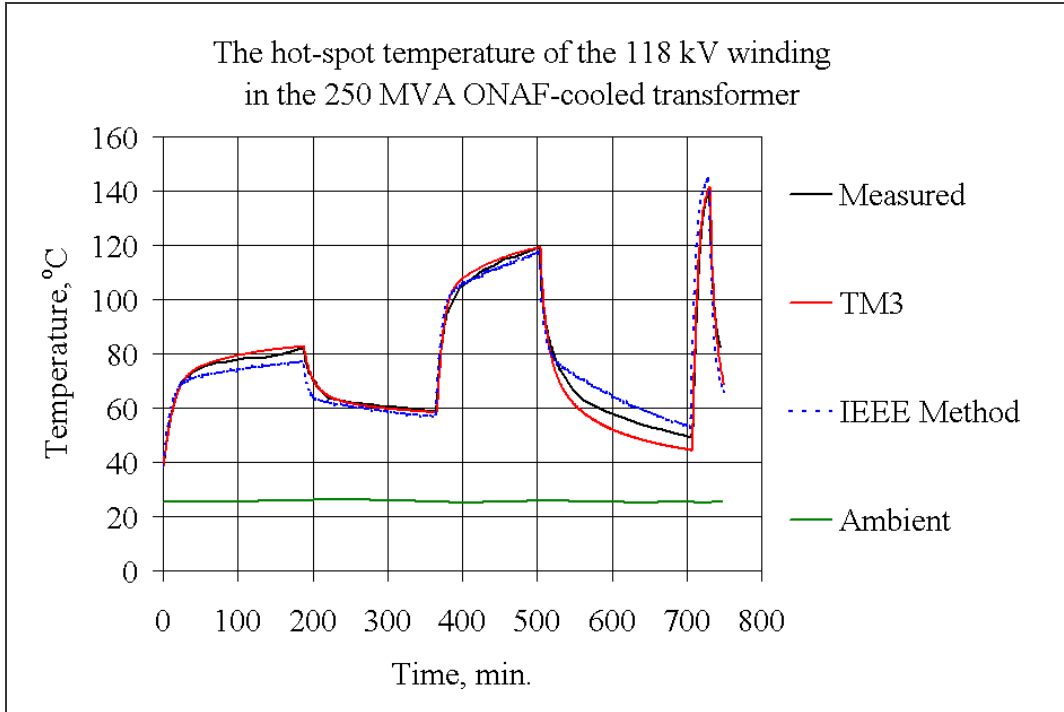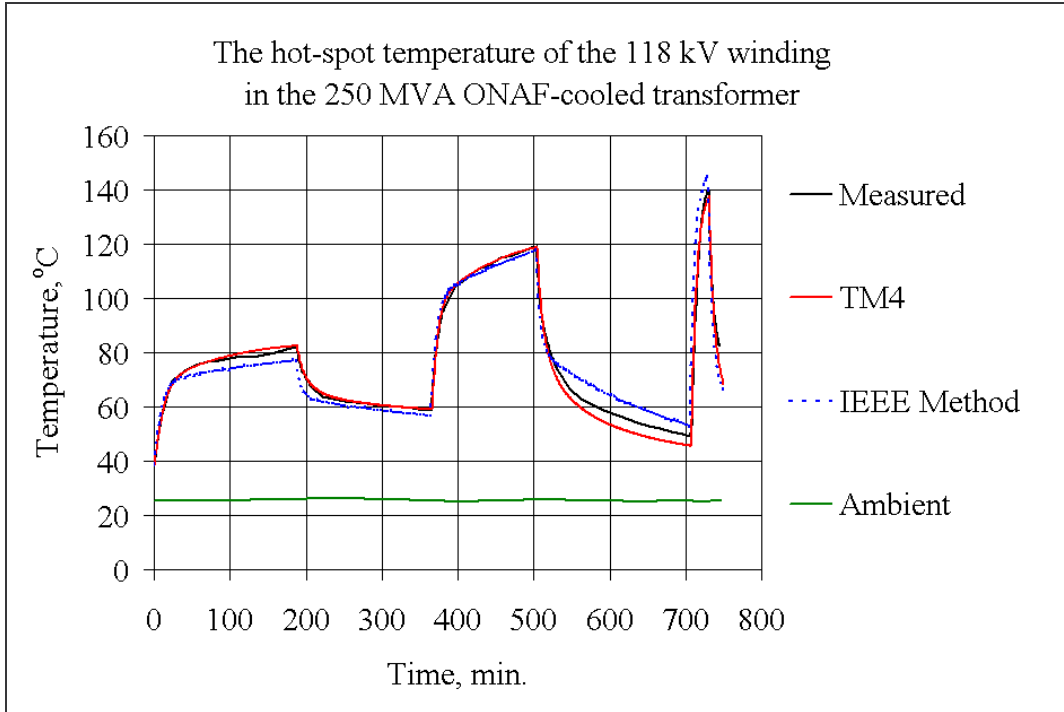
- the IEEE-Annex G method, [28]

Fig. 4.7. The hot-spot temperature of the 118 kV winding in the 250 MVA ONAF-cooled transformer

Fig. 4.7 shows the comparison between the measured hot-spot temperature of the 118 kV winding in the 250 MVA ONAF-cooled transformer and the hot-spot temperatures obtained by the following calculation methods:

- "TM2" refers to the hot spot temperature model, equation (3.41), section 3.2.2
- the IEEE-Annex G method, [28]

Fig. 4.8. The hot-spot temperature of the 118 kV winding in the 250 MVA ONAF-cooled transformer

Fig. 4.8 shows the comparison between the measured hot-spot temperature of the 118 kV winding in the 250 MVA ONAF-cooled transformer and the hot-spot temperatures obtained by the following calculation methods methods:

- "TM3" refers to the hot spot temperature model, equation (3.49), section 3.2.4

- the IEEE-Annex G method, [28]

Fig. 4.9. The hot-spot temperature of the 118 kV winding in the 250 MVA ONAF-cooled transformer

Fig. 4.9 shows compares the measured hot-spot temperature of the 118 kV winding in the 250 MVA ONAF-cooled transformer to the hot-spot temperatures calculated using the following methods:

- "TM4" refers to the hot spot temperature model, equation (3.52), section 3.2.4

- the IEEE-Annex G method, [28]

Additionally, both the measured bottom- and top-oil temperature results, which were recorded during a varying current test, are compared with results obtained from the thermal models shown in Figs. 4.10 and 4.11 below.
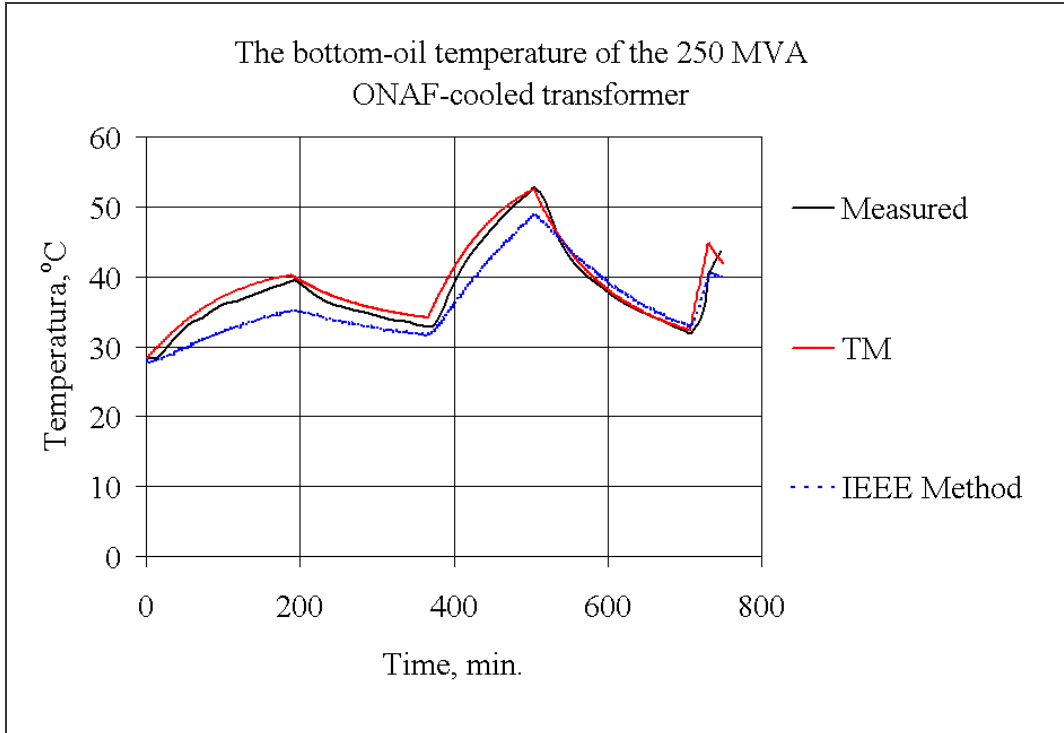
Fig. 4.10. The bottom-oil temperature of the 250 MVA ONAF-cooled transformer

Fig. 4.10 compares the measured bottom-oil temperature in the 250 MVA ONAF-cooled transformer with the bottom-oil temperatures obtained by the following calculation methods:

- "TM" refers to the bottom-oil temperature model, equation (3.43) in section 3.2.3.

- the IEEE-Annex G method, [28]
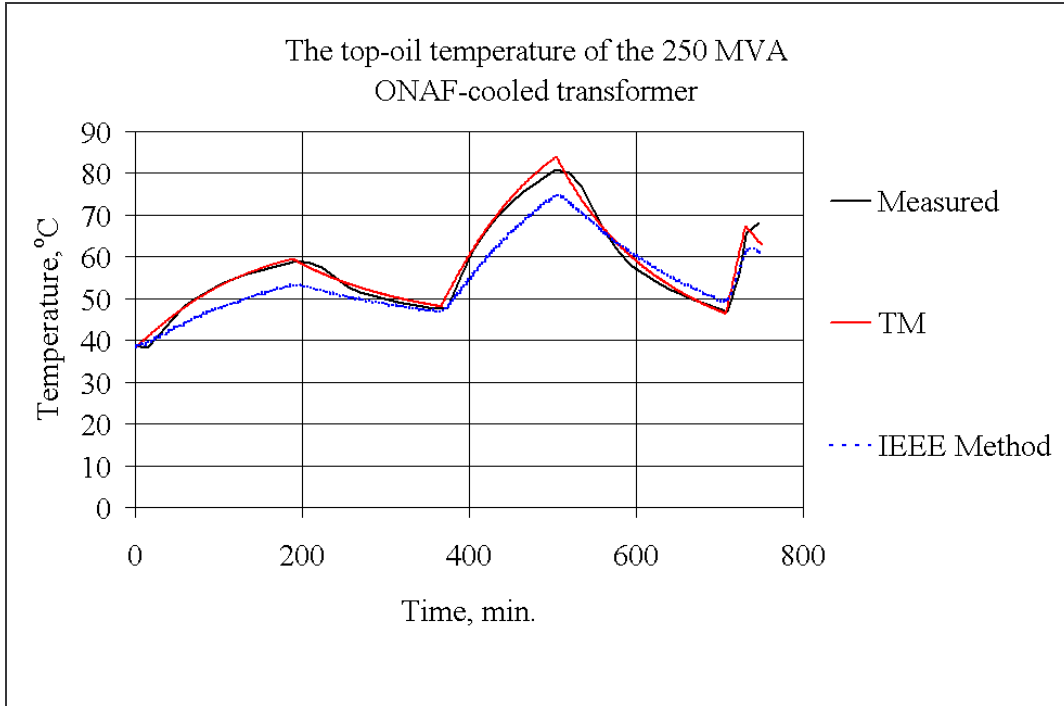
Fig. 4.11. The top-oil temperature of the 250 MVA ONAF-cooled transformer

Fig. 4.11 shows the measured top-oil temperature of the 250 MVA ONAF-cooled transformer and the top-oil temperatures obtained by the following calculation methods:

- "TM" refers to the top-oil temperature model, equation (3.24) in section 3.2.1

- the IEEE-Annex G method, [28]

It should be pointed out that the winding chosen for the comparison is the hottest one of the two main windings in the tested transformer unit. Also, the results are shown graphically, to allow visual verification. Further discussion of these results appears in section 4.4.

4.1.3 Three-phase 400/400/125 MVA ONAF -cooled transformer

The rated voltages of the transformer were 410±6x1.33%/120/21 kV. The windings were, seen from the limb side: 120 kV and 410 kV main windings, a regulating winding and a 21 kV tertiary winding. A sketch of the core window and winding arrangement of the transformer is given in Appendix H. The connection was YNynd, and the short circuit impedance in the 400/400 MVA main direction was 20%. The oil flow through the windings was guided by the oil guiding rings in a zigzag pattern. The main windings in this transformer are representative of two basic cases: "restricted oil flow" (≤ 2 mm radial spacers in the 120 kV winding) and "unrestricted oil flow" (≥ 3mm radial spacers in the 410kV winding). The main windings were equipped with a total of 16 fibre optic probes (eight in each winding) and the tie plates, outer core packets and yoke clamps had a total of 37 thermocouples. Additional load tests with ONAF cooling were as follows:

- Constant load current: 1.0 p.u.; duration 12h,
- Constant load current: 1.29 p.u.; duration 10h,
- Constant load current: 1.60 p.u.; duration 15h,
- Varying load current, Table 4.2.

Table 4.2. – The load steps for the 400 MVA transformer

Time period (minutes)	Load factor
0.0 −300.0	1.0
300.0 −600.0	0.65
600.0−780.0	1.6

The measured hot-spot temperature results, which were recorded during a varying load current test, are compared with results obtained from the thermal models in Figs. 4.12, 4.13, 4.14 and 4.15 below.
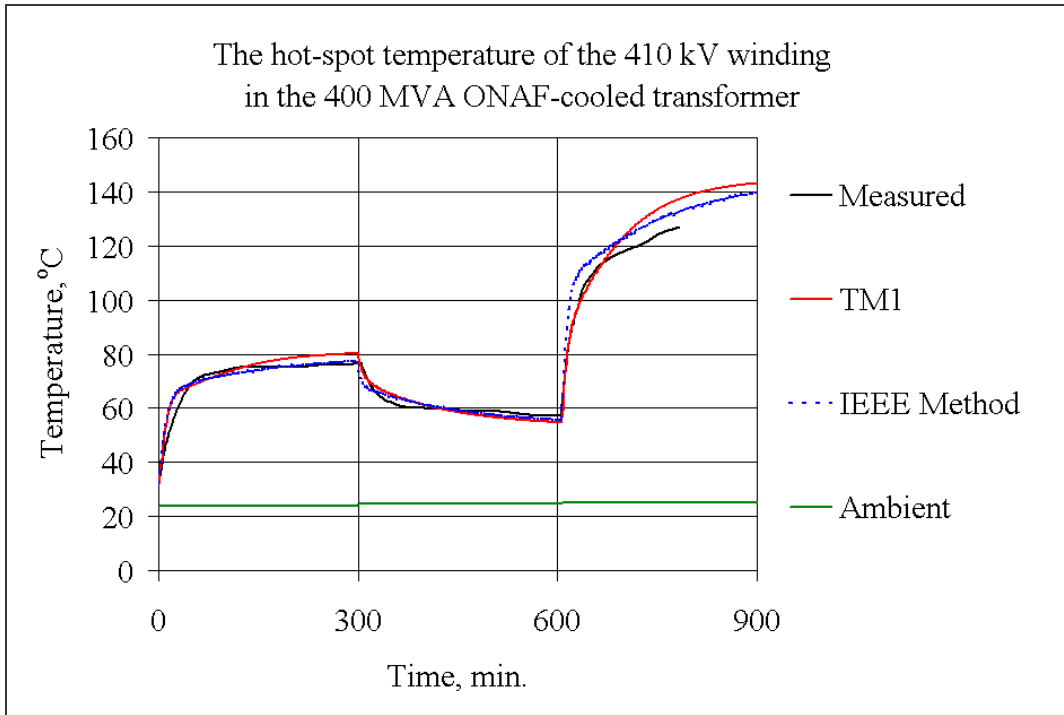
Fig. 4.12. The hot-spot temperature of the 410 kV winding in the 400 MVA ONAF-cooled transformer

Fig. 4.12 shows the measured hot-spot temperature of the 410 kV winding in the 400 MVA ONAF-cooled transformer and the hot-spot temperatures obtained by the following methods:

– "TM1" refers to the hot spot temperature model, equation (3.38), section 3.2.2
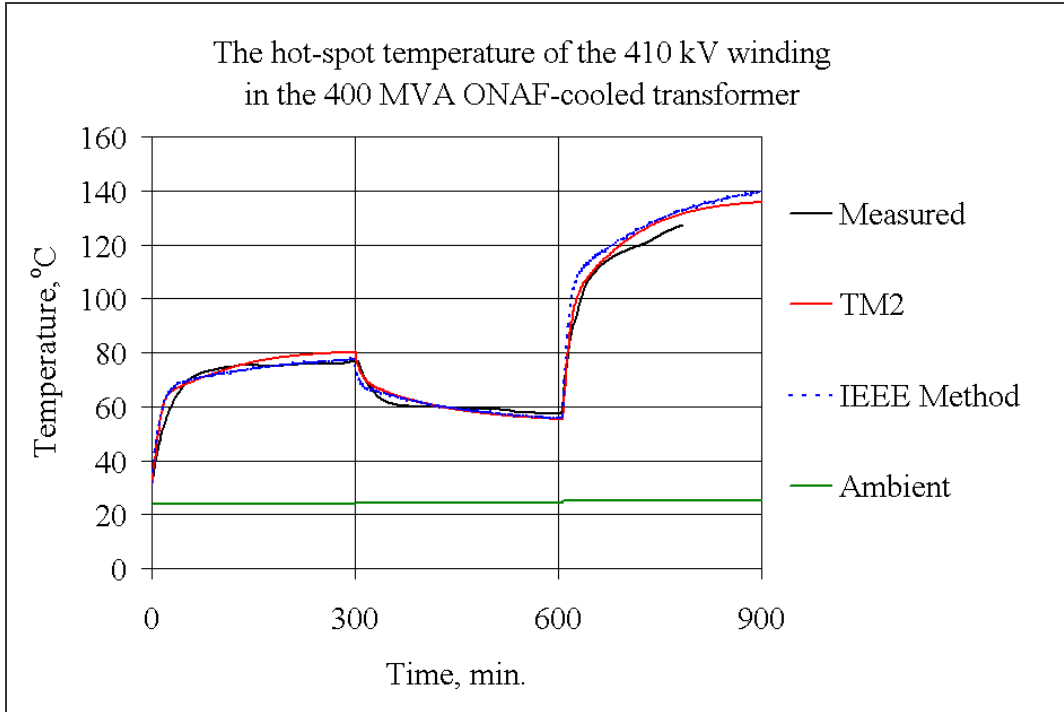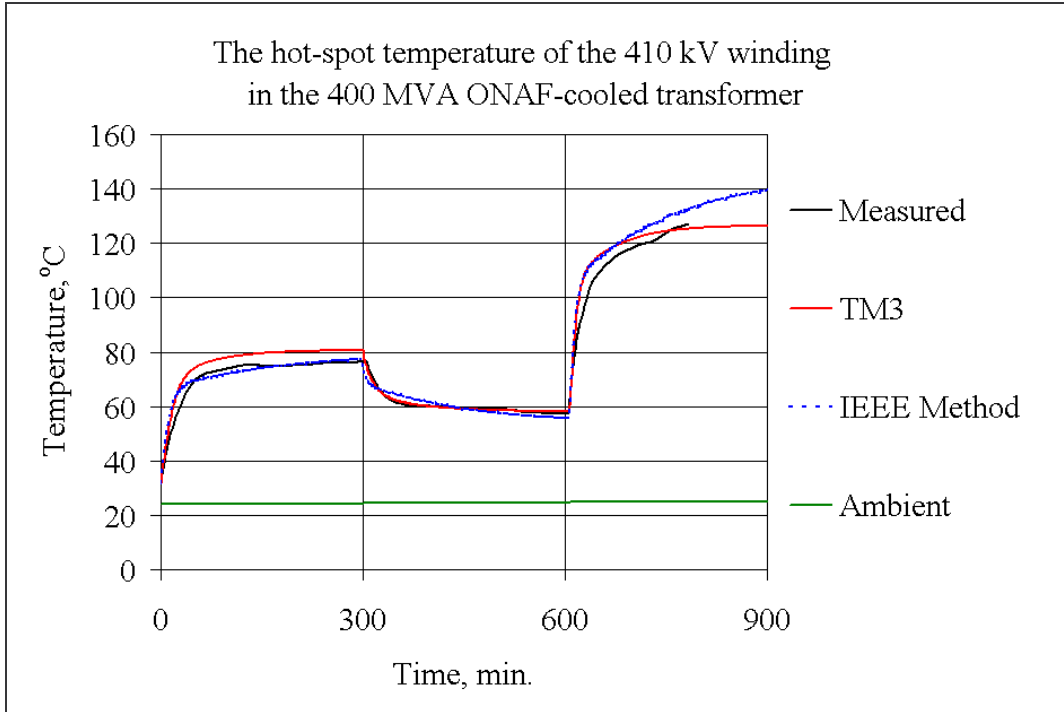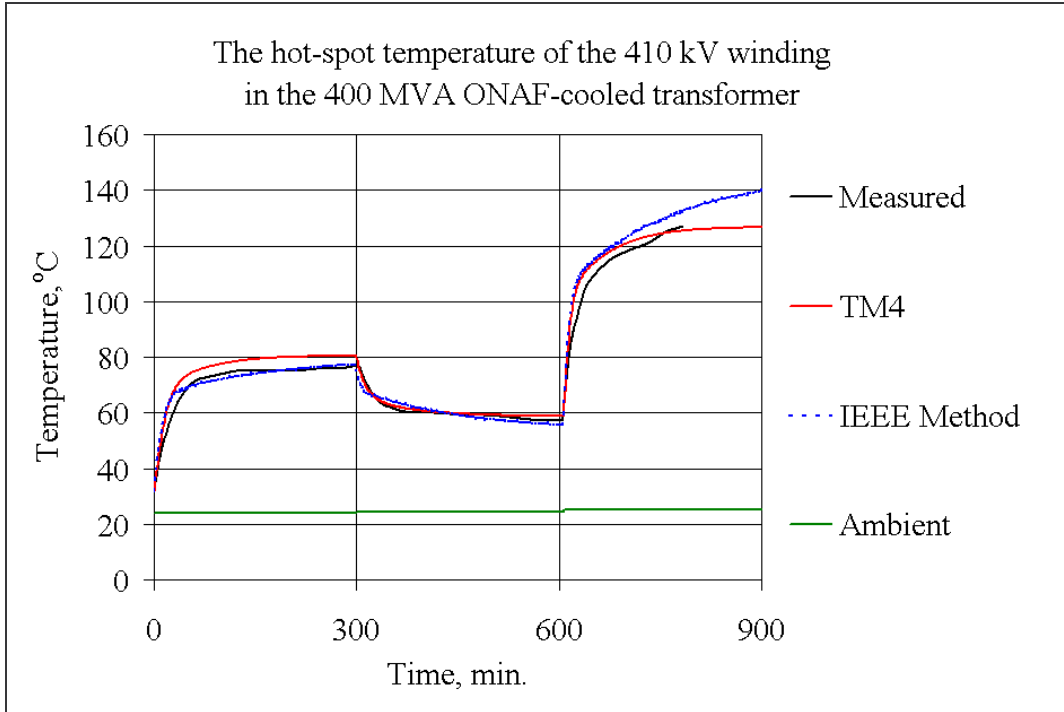
– the IEEE-Annex G method, [28]

Fig. 4.13. The hot-spot temperature of the 410 kV winding in the 400 MVA ONAF-cooled transformer

Fig. 4.13 compares the measured hot-spot temperature of the 410 kV winding in the 400 MVA ONAF-cooled transformer with the hot-spot temperatures obtained by the following calculation methods:

- "TM2" refers to the hot spot temperature model, equation (3.41), section 3.2.2

- the IEEE-Annex G method, [28]

Fig. 4.14. The hot-spot temperature of the 410 kV winding in the 400 MVA ONAF-cooled transformer

Fig. 4.14 shows the measured hot-spot temperature of the 410 kV winding in the 400 MVA ONAF-cooled transformer and the hot-spot temperatures obtained by the following calculation methods:

– "TM3" refers to the hot spot temperature model, equation (3.49), section 3.2.4

– the IEEE-Annex G method, [28]

Fig. 4.15. The hot-spot temperature of the 410 kV winding in the 400 MVA ONAF-cooled transformer

Fig. 4.15 compares the measured hot-spot temperature of the 410 kV winding in the 400 MVA ONAF-cooled transformer with the hot-spot temperatures obtained by the following calculation methods:

– "TM4" refers to the hot spot temperature model, equation (3.52), section 3.2.4

– the IEEE-Annex G method, [28]

Additionally, the measured bottom- and top-oil temperature results, which were recorded during varying current tests, are compared with results obtained from the thermal models in Figs. 4.16 and 4.17 below.
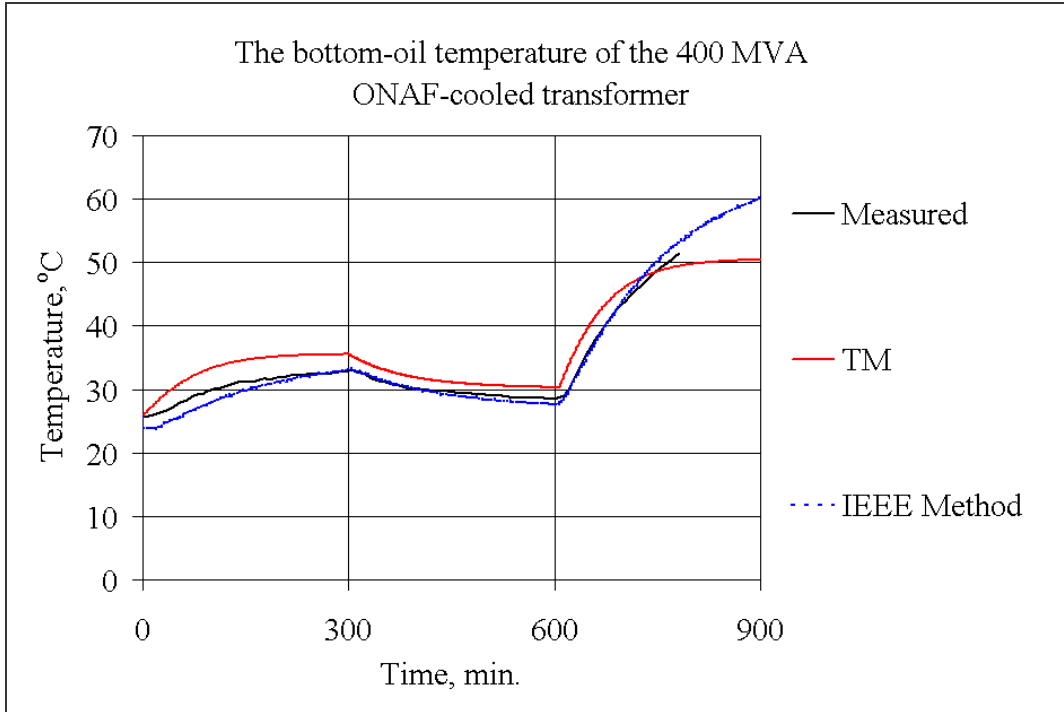
Fig. 4.16. The bottom-oil temperature of the 400 MVA ONAF-cooled transformer

Fig. 4.16 shows the comparison between the measured bottom-oil temperature of the 400 MVA ONAF-cooled transformer and the bottom-oil temperatures obtained by the following calculation methods:

- "TM" refers to the bottom-oil temperature model, equation (3.43) in section 3.2.3,
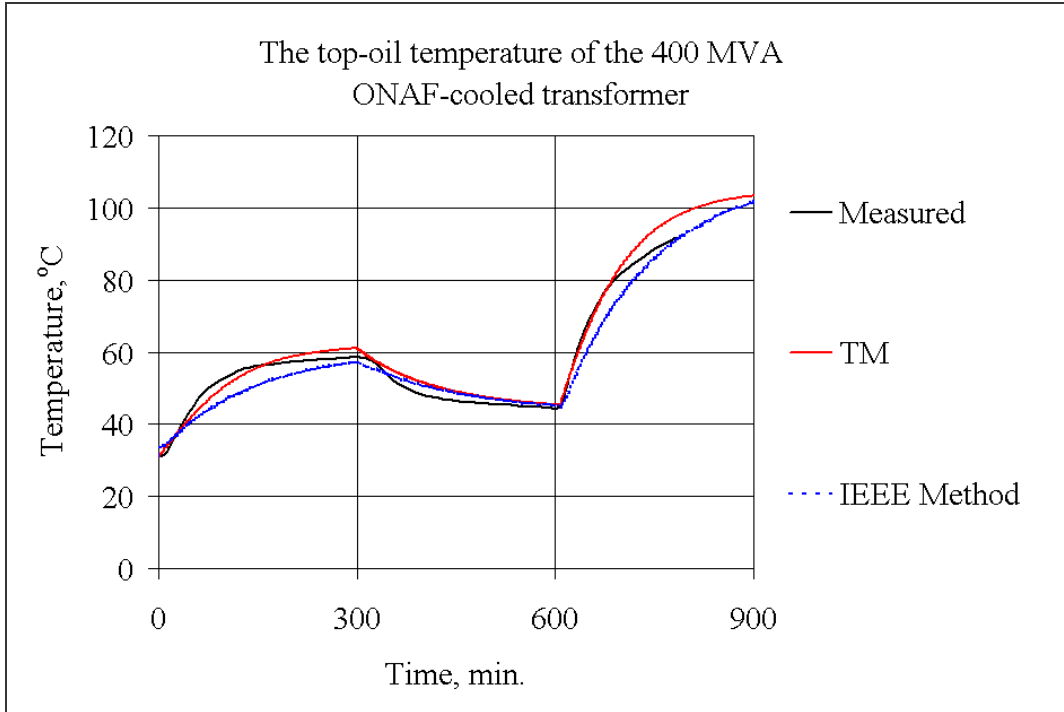
- the IEEE-Annex G method, [28]

Fig. 4.17. The top-oil temperature of the 400 MVA ONAF-cooled transformer

Fig. 4.17 shows the measured top-oil temperature of the 400 MVA ONAF-cooled transformer along with the top-oil temperatures obtained by the following calculation methods:

- "TM" refers to the top-oil temperature model, equation (3.24) in section 3.2.1

- the IEEE-Annex G method, [28]

It should be pointed out that the winding chosen for the comparison is the hottest of the two main windings in the tested transformer unit. The results are shown graphically, which facilitates a visual check. The presented results are further discussed in section 4.4.

4.1.4 Three-phase 605 MVA OFAF -cooled transformer

The 605 MVA transformer was a generator step up (GSU) unit with the windings seen from the limb side: part of the HV winding (i.e., 362 kV-winding), the double shell LV winding (i.e., 22 kV-winding) and the main part of the HV winding. A sketch of the core window and winding arrangement of the transformer is given in Appendix H. The oil circulation through the windings was guided by the oil guiding rings in a zigzag pattern in such a way that the oil flow through the LV winding was restricted ($\leq$2mm radial spacer) and through the HV winding unrestricted ($\geq$3mm radial spacer). The transformer was not a sealed OD (i.e., the oil circulation was not forced through the winding block). In total, 24 fibre optic sensors were installed in the top disc/turns of the outer shell of the LV winding and the outer part of the HV winding. In addition to the normal heat run tests, the following load tests were made with OFAF cooling:

- Constant load current: 1.00 p.u.; duration 12h,
- Constant load current: 1.30 p.u.; duration 1.2h,
- Varying load current, Table 4.3.

Table 4.3. – The load steps for the 605 MVA transformer

Time period (minutes)	Load factor
0.0 −300.0	1.0
300.0 −600.0	0.65
600.0−649.8	1.3

The measured hot-spot temperature results, which were recorded during a varying load current test, are compared with results obtained from the thermal models and are shown in Figs. 4.18, 4.19, 4.20 and 4.21 below.
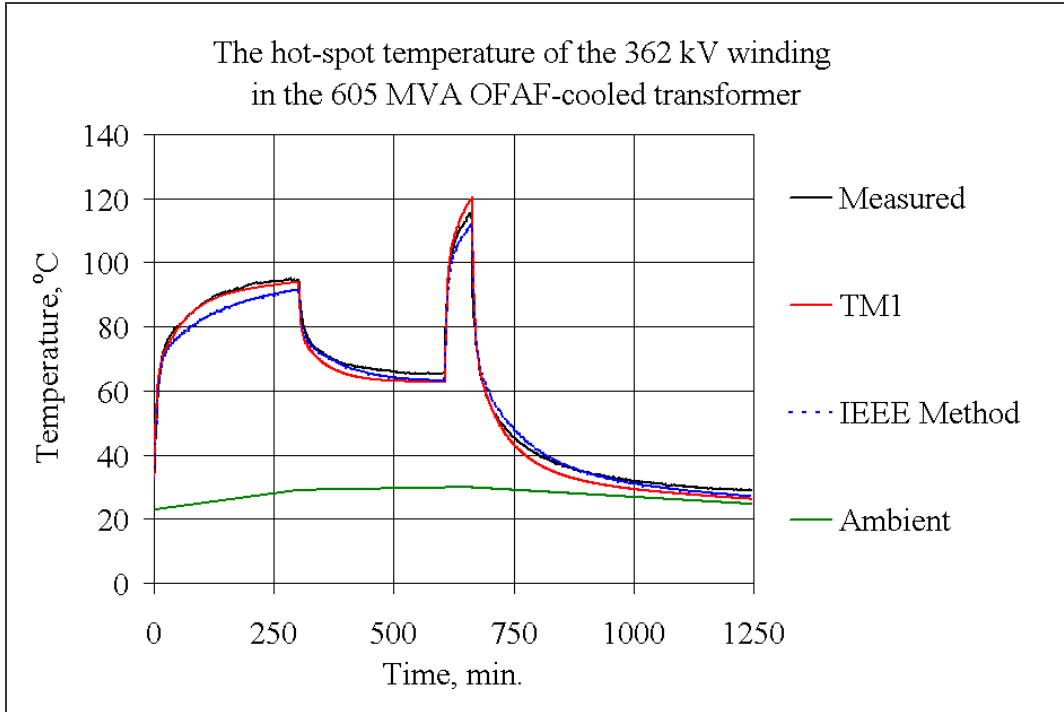
Fig. 4.18. The hot-spot temperature of the 362 kV winding in the 605 MVA OFAF-cooled transformer

Fig. 4.18 compares the measured hot-spot temperature of the 362 kV winding in the 605 MVA OFAF-cooled transformer with the hot-spot temperatures obtained by the following calculation methods:

- "TM1" refers to the hot spot temperature model, equation (3.38), section 3.2.2
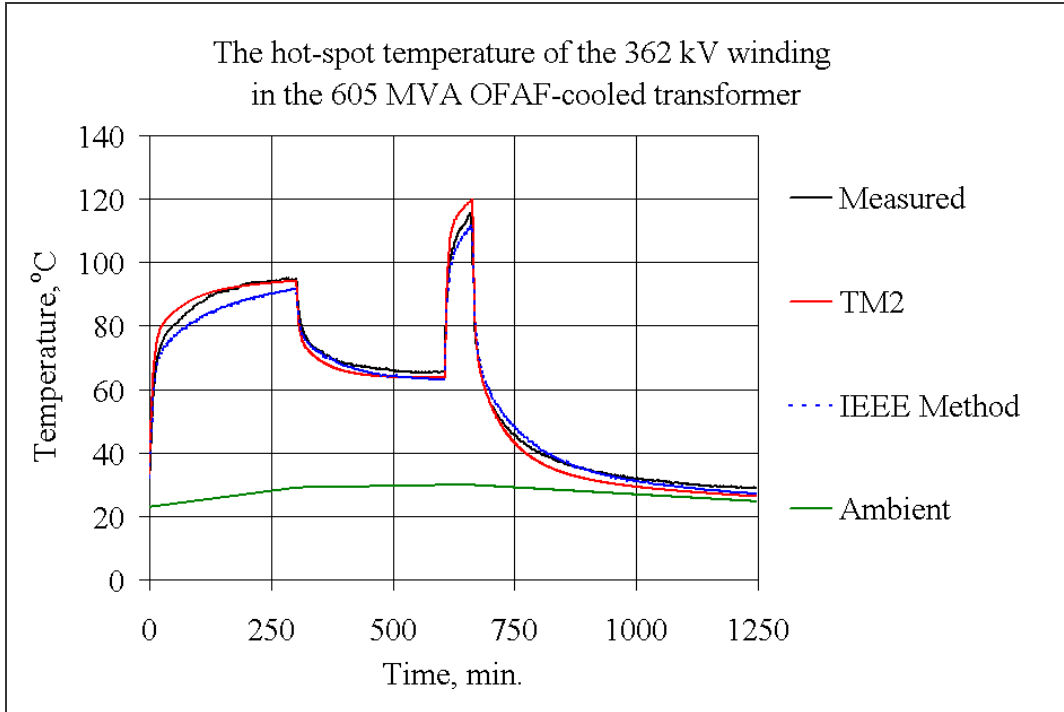
- the IEEE-Annex G method, [28]

Fig. 4.19. The hot-spot temperature of the 362 kV winding in the 605 MVA OFAF-cooled transformer

Fig. 4.19 compares the measured hot-spot temperature of the 362 kV winding in the 605 MVA OFAF-cooled transformer with the hot-spot temperatures obtained by the following calculation methods:

- "TM2" refers to the hot spot temperature model, equation (3.41), section 3.2.2
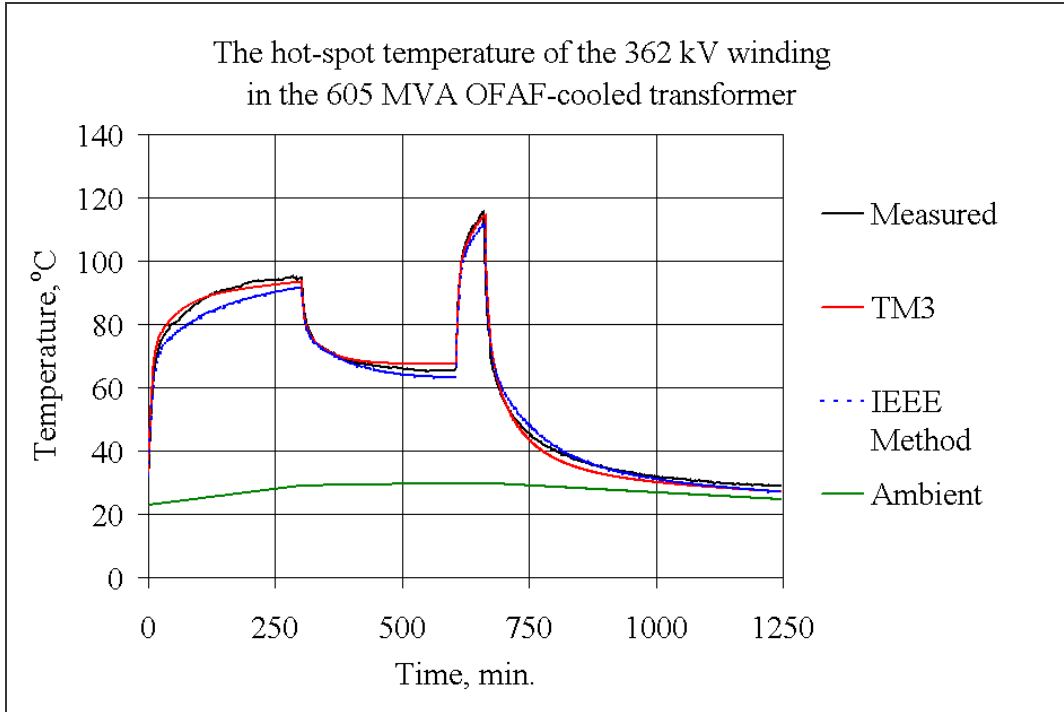
- the IEEE-Annex G method, [28]

75

Fig. 4.20. The hot-spot temperature of the 362 kV winding in the 605 MVA OFAF-cooled transformer

Fig. 4.20 shows the measured hot-spot temperature of the 362 kV winding in the 605 MVA OFAF-cooled transformer alongside the hot-spot temperatures obtained by the following calculation methods:

- "TM3" refers to the hot spot temperature model, equation (3.49), section 3.2.4
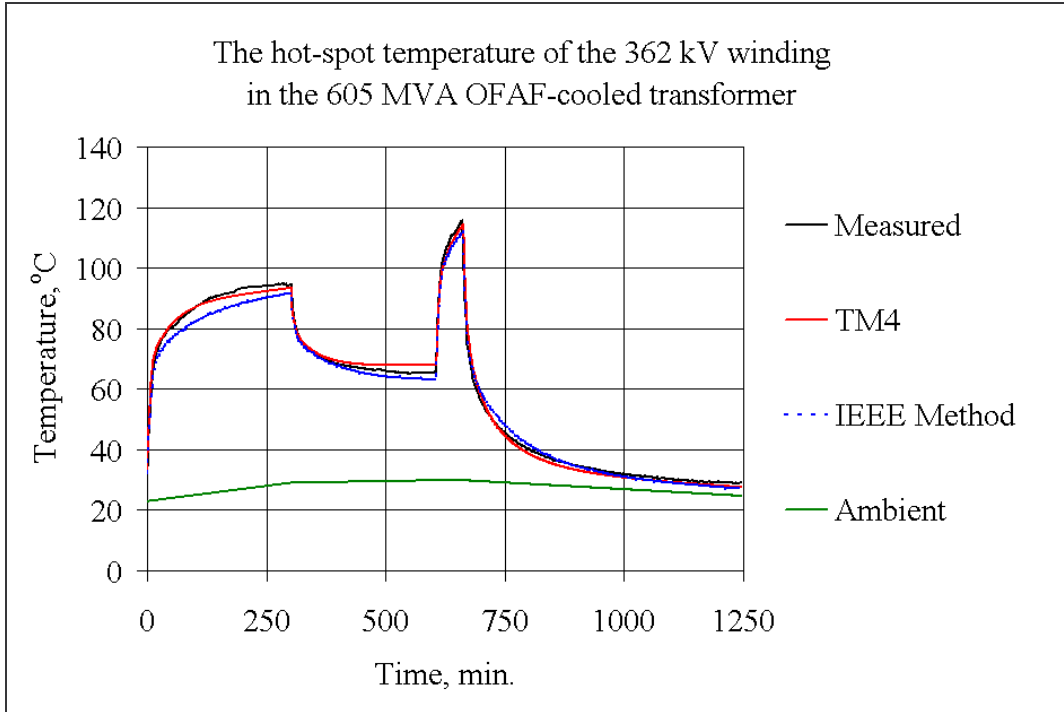
- the IEEE-Annex G method, [28]

Fig. 4.21. The hot-spot temperature of the 362 kV winding in the 605 MVA OFAF-cooled transformer

Fig. 4.21 compares the measured hot-spot temperature of the 362 kV winding in the 605 MVA OFAF-cooled transformer to the hot-spot temperatures obtained by the following calculation methods:

– "TM4" refers to the hot spot temperature model, equation (3.52), section 3.2.4

– the IEEE-Annex G method, [28]

Additionally, both the measured bottom- and top-oil temperatures, recorded during a varying current test, are compared with results obtained from the thermal models in Figs. 4.22 and 4.23 below.
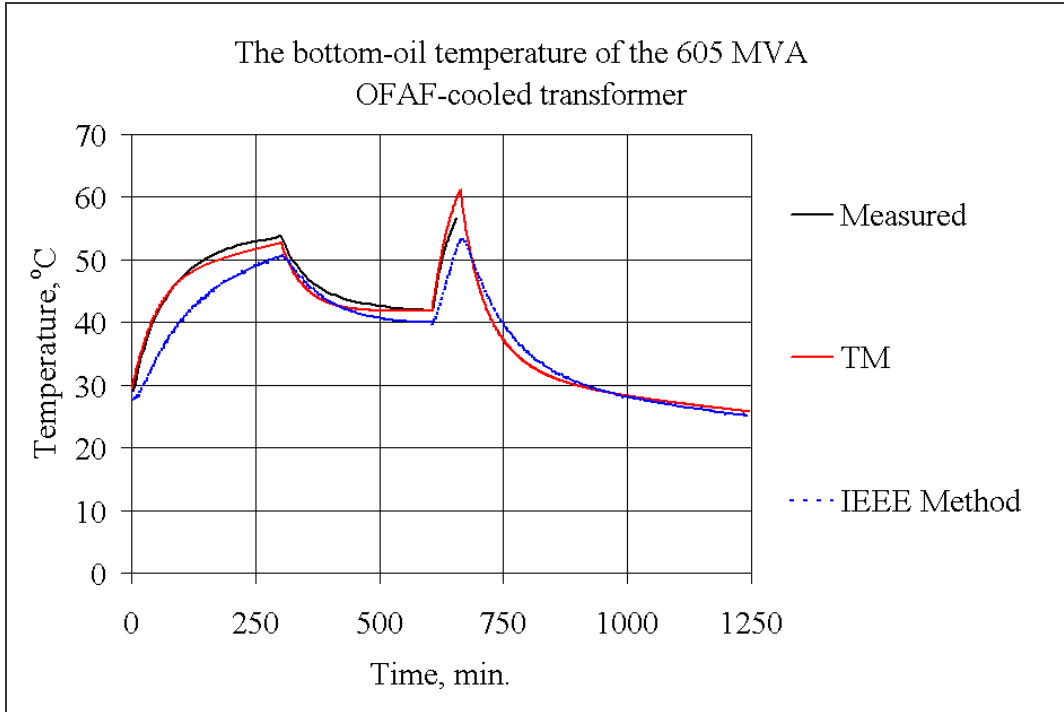
Fig. 4.22. The bottom-oil temperature of the 605 MVA OFAF-cooled transformer

Fig. 4.22 compares the measured bottom-oil temperature of the 605 MVA OFAF-cooled transformer with the bottom-oil temperatures obtained using the following calculation methods:

- "TM" refers to the bottom-oil temperature model, equation (3.43) in section 3.2.3
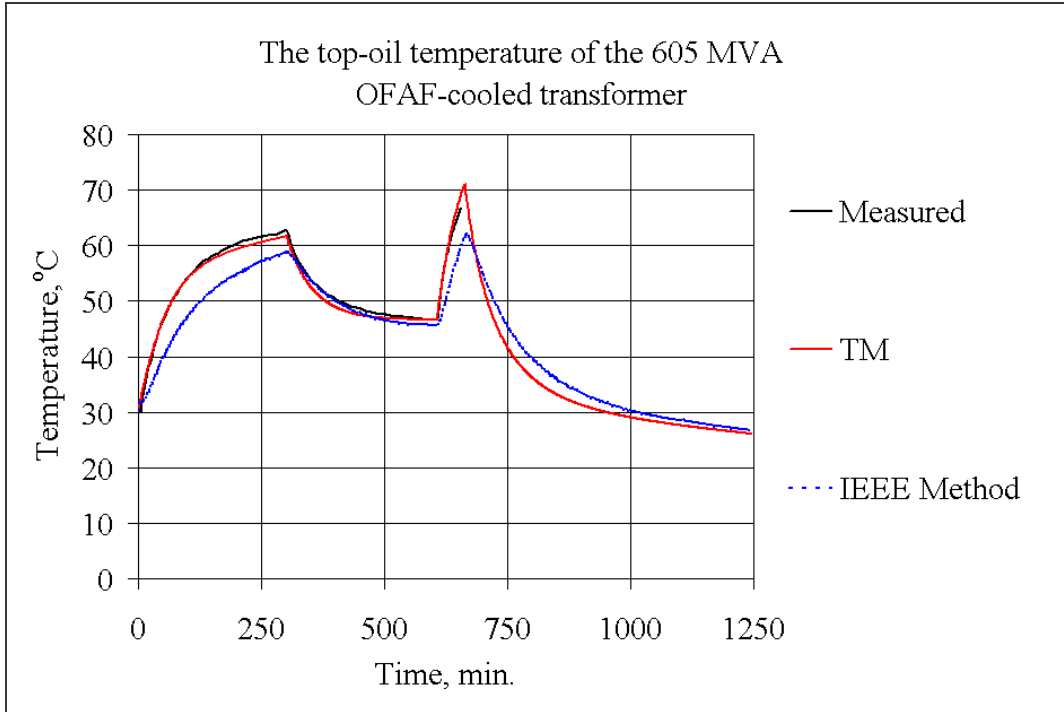
- the IEEE-Annex G method, [28]

Fig. 4.23. The top-oil temperature of the 605 MVA OFAF-cooled transformer

Fig. 4.23 shows the measured top-oil temperature of the 605 MVA OFAF-cooled transformer and the top-oil temperatures obtained by the following calculation methods:

- "TM" refers to the top-oil temperature model, equation (3.24) in section 3.2.1

- the IEEE-Annex G method, [28]

It should be pointed out that the winding chosen for the comparison is the hottest of the two main windings in the tested transformer unit. Also, the results are portrayed graphically, to enable a convenient visual assessment. The presented results are discussed further in section 4.4.

4.1.5 Three-phase 650-MVA ONAF-cooled transformer

The 650-MVA transformer was a GSU unit with the windings seen from the limb side: half of the LV-winding (i.e., 21 kV), the HV-winding (i.e., 415 kV), and the other half of the LV-winding (double-concentric). A sketch of the core window and winding arrangement of the transformer is given in Appendix H. The two LV-windings were helical windings with axial cooling ducts (no oil guiding rings). In addition, the HV-winding was equipped with axial cooling ducts. The top turns of the inner LV-shell were equipped with a total of eight fibre optic sensors. In addition to the normal heat run tests (ONAN and ONAF), the following test was made in the ONAF-cooling mode:

- constant load current: 1.20 p.u., duration: 15 h.

The measured hot-spot temperature results, which were recorded during a constant load current test, are compared with results obtained from the thermal models in Figs. 4.24, 4.25 and 4.26 below.
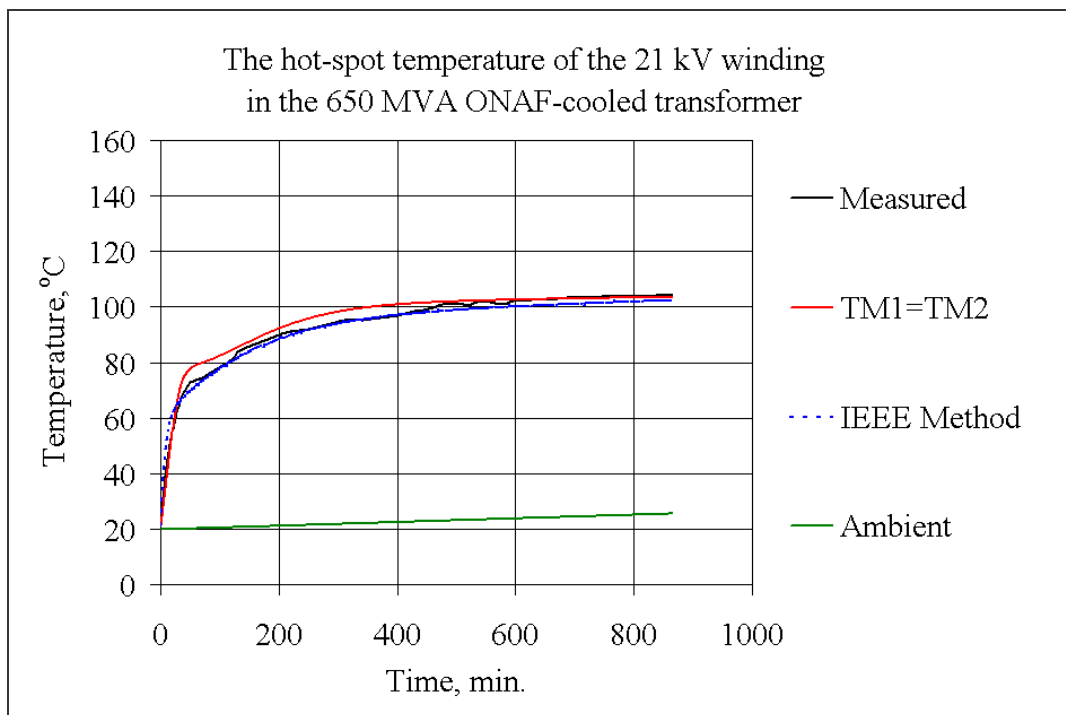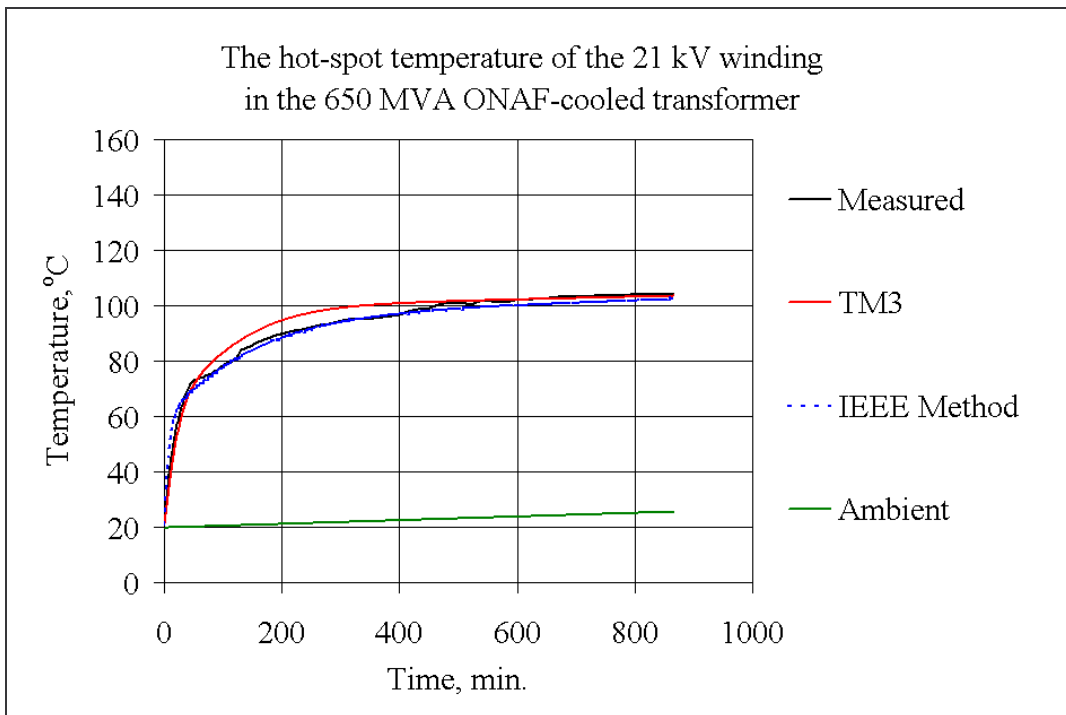

4.24. The hot-spot temperature of the 21 kV winding in the 650 MVA ONAF-cooled transformer

Fig. 4.24 shows the measured hot-spot temperature of the 21 kV winding in the 650 MVA ONAF-cooled transformer along with the hot-spot temperatures obtained by the following calculation methods:

- "TM1" refers to the hot spot temperature model, equation (3.38), section 3.2.2

- "TM2" refers to the hot spot temperature model, equation (3.41), section 3.2.2

- the IEEE-Annex G method, [28]

When the transformer is run from a cold start the thermal models TM1 and TM2 will yield the same results. Once the transformer is energised, the "cold start" exponents, which are given in Tables 3.4, 3.5 and 3.6, should be substituted for the transformer "on load" exponents at the first load change, Appendix B. Therefore, the temperature results obtained by these models can be represented with a single red line in Fig. 4.24.

4.25. The hot-spot temperature of the 21 kV winding in the 650 MVA ONAF-cooled transformer

Fig. 4.25 compares the measured hot-spot temperature of the 21 kV winding in the 650 MVA ONAF-cooled transformer to the hot-spot temperatures obtained by the following calculation methods:

- "TM3" refers to the hot spot temperature model, equation (3.49), section 3.2.4
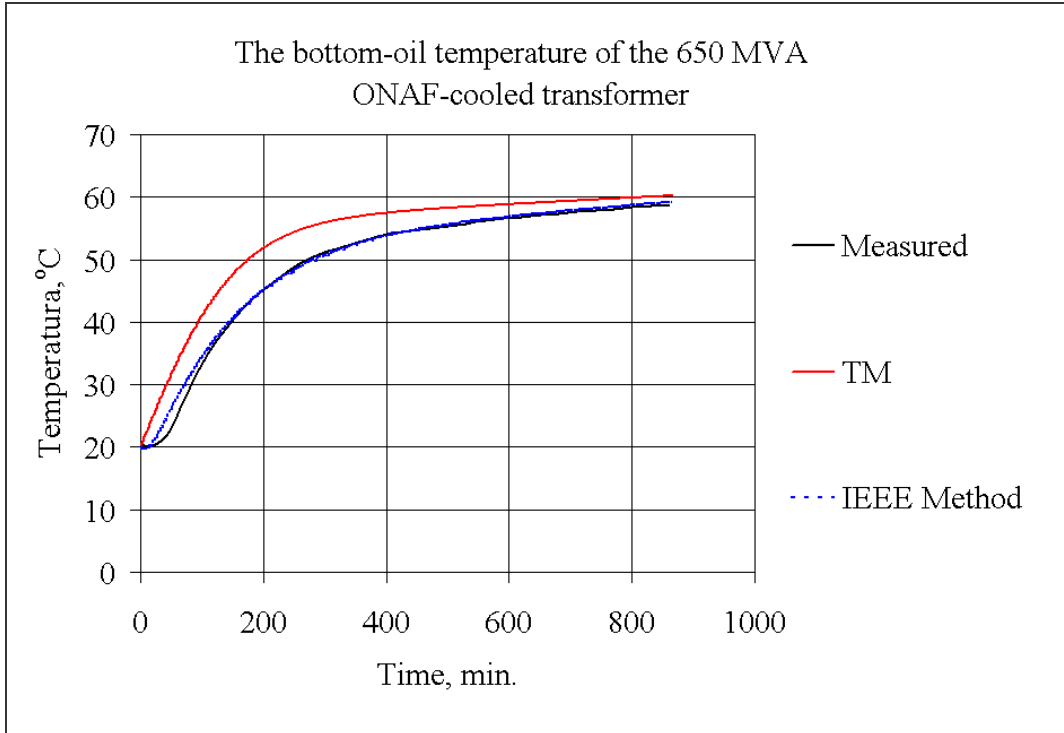
- the IEEE-Annex G method, [28]
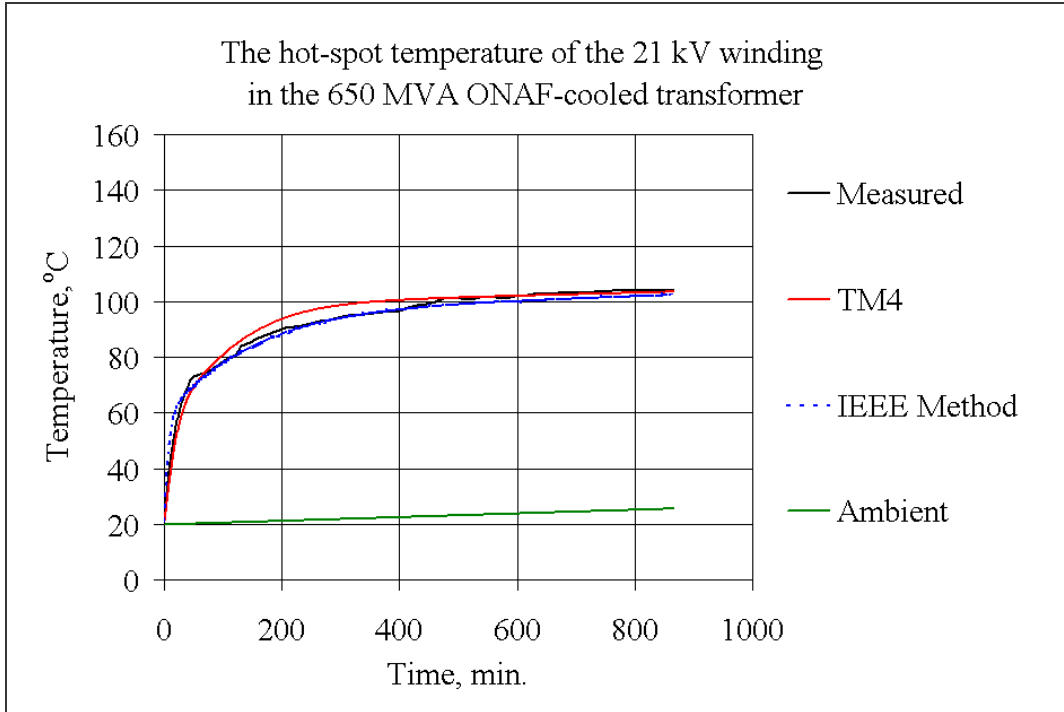
4.26. The hot-spot temperature of the 21 kV winding in the 650 MVA ONAF-cooled transformer

Fig. 4.26 compares the measured hot-spot temperature of the 21 kV winding in the 650 MVA ONAF-cooled transformer with the hot-spot temperatures obtained by the following calculation methods:

- – "TM4" refers to the hot spot temperature model, equation (3.52), section 3.2.4

- – the IEEE-Annex G method, [28]

Additionally, both the measured bottom- and top-oil temperatures, which have been recorded during a constant current test, are compared with results obtained from the thermal models in Figs. 4.27 and 4.28 below.

82

4.27. The bottom-oil temperature of the 650 MVA ONAF-cooled transformer

Fig. 4.27 shows the comparison between the measured bottom-oil temperature of the 650 MVA ONAF-cooled transformer and the bottom-oil temperatures obtained by the following calculation methods:

– "TM" refers to the bottom-oil temperature model, equation (3.43) in section 3.2.3

– the IEEE-Annex G method, [28]

4.28. The top-oil temperature of the 650 MVA ONAF-cooled transformer

Fig. 4.28 compares the measured top-oil temperature of the 650 MVA ONAF-cooled transformer with the top-oil temperatures obtained by the following calculation methods:

- "TM" refers to the top-oil temperature model, equation (3.24) in section 3.2.1
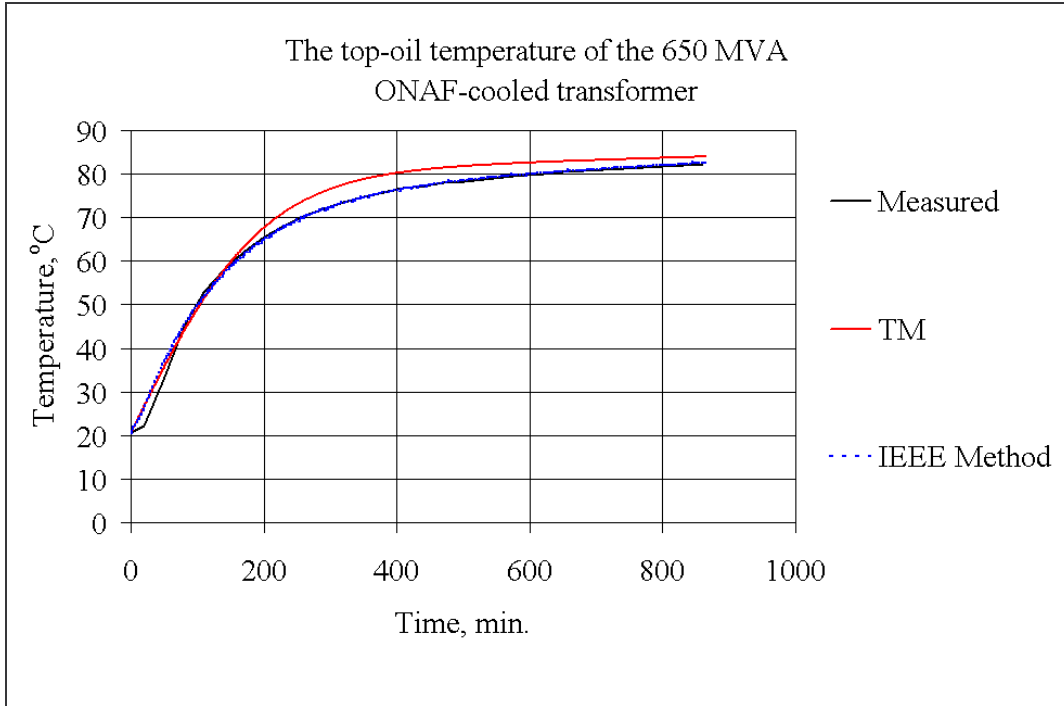
- the IEEE-Annex G method, [28]

It should be pointed out that the winding chosen for the comparison is the hottest of the two main windings in the presented transformer unit. These results are also shown graphically, which allows quick verification. Further discussion of the presented results is given in section 4.4.

4.2 Transformer without external cooling

A short description of the tested transformer, performed tests and position of the installed thermocouples is given below, [69]:

The rated voltages of the transformer are 20.5±2×2.5%/0.71 kV. The low voltage winding (0.71 kV winding) consists of eighteen Al-foil layers with an axial cooling duct between the ninth and tenth layers. The distance from the LV-foils to the yokes is 15 mm at both the top and bottom. At the top and bottom an 8 mm pressboard bond is added to the foils, i.e., the yoke distance from the insulated winding is 7 mm at both the top and bottom. The cooling duct is collapsed at the LV- bus bar because the LV- bus bar needs space. The width of the bars is 100 mm, which means that a total of about 150 mm of the duct is blocked on the side of the core. The high voltage winding (20.5 kV) consists of 15 layers, each layer comprising 66 conductors except one layer which has only 21 conductors to obtain the proper number of turns. The winding has two axial cooling ducts, the first one between the fifth and sixth layers and the second one between the tenth and eleventh layers. The distance from the HV conductor metal to the yoke is 25 mm at the top and bottom. An 18 mm pressboard bond is added as end insulation at the top and bottom, i.e., the yoke distance from the insulated winding is also, in this case, 7 mm at the top and bottom. The connection is Dy11 and the short-circuit impedance is 6%. The tank is corrugated with 250 mm cooling ribs; the centre distance is 40 mm. There are 15 ribs, N, on the short sides and 39 on the long sides, Fig. 30. The tank is hermetically sealed and filled with oil.

The transformer was equipped with a total of 28 thermocouples, Figs. 4.29 and 4.30, which were fitted in the transformer as follows:
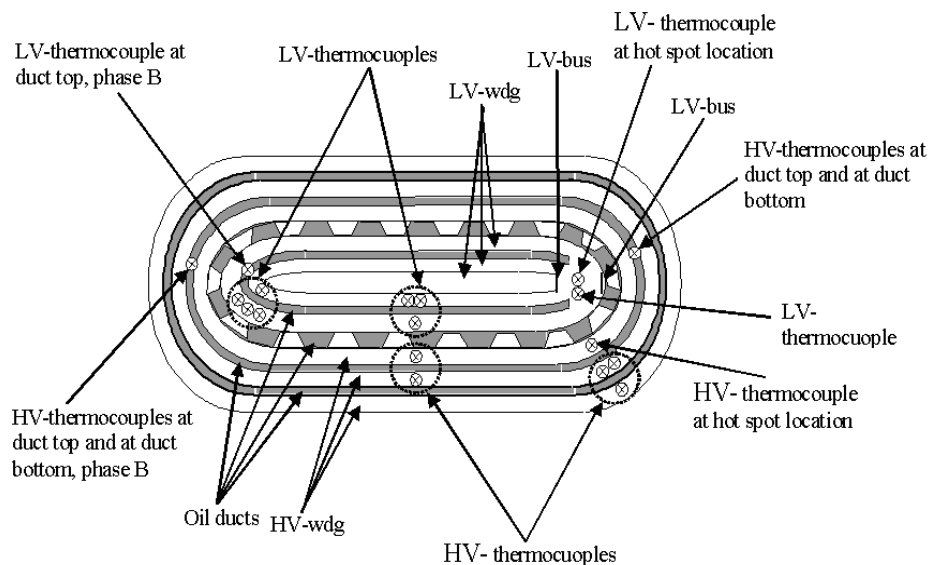

Fig. 4.29. Positions of thermocouples, top view, phase C
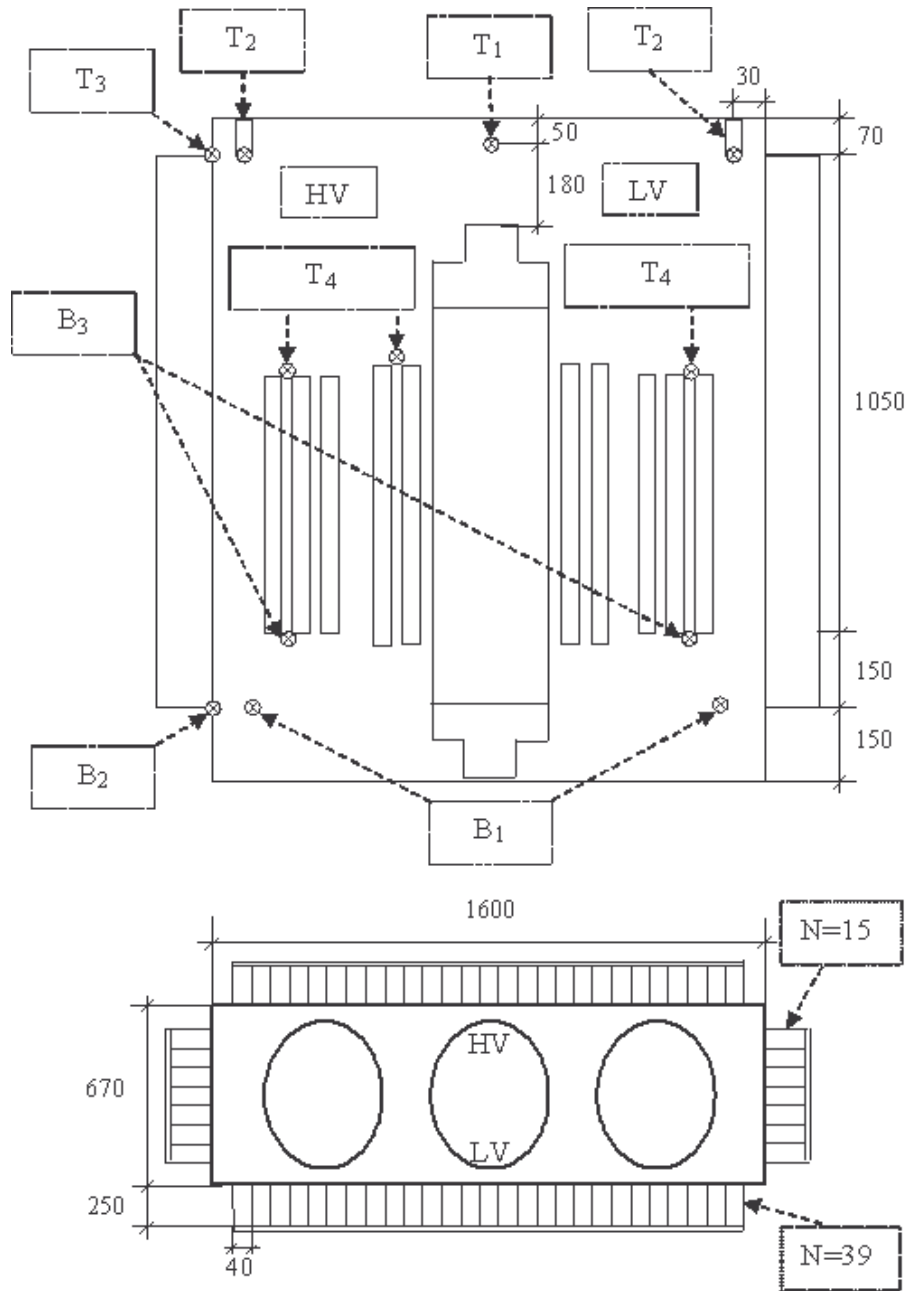
Fig. 4.30. Position of thermocouples in the tank, side and top view; dimensions are in mm

– 9 in the low voltage winding, where the thermocouples were inserted to a depth of about 5 mm between adjacent foils, Figs. 4.29. It was expected that the hottest spot temperature occurs at the location of the collapsed ducts. Therefore, two thermocouples were inserted there.

– 6 in the high voltage winding, where the thermocouples were inserted to a depth of about 5 mm from the edge of the conductor, between adjacent flat conductors, Fig. 4.29.

- 2 in the oil pockets at each end of the tank, T_2. The distance from both tank walls to the centre of the pocket pipe is about 30 mm, Fig. 4.30.

- 2 on the outside surface of the tank, at the top, T_3, and the bottom, B_2. They were attached to the centre line of the long sides of the tank wall, between two adjacent cooling ribs, right at the top and bottom levels of the cooling ribs, Fig. 4.30.

- 2 thermocouples 50 mm under the tank cover, T_1, were directly above the centre line of the active part, Fig. 4.30.

- 2 in the mixed bottom oil, B_1, located on the centre line between two adjacent phases, on a line along the outer edges of the winding block at the top level of the bottom yoke, Fig. 4.30. They were fixed to pressboard sheets functioning as phase insulation.

- 2 in both the duct inlet, B_3, and the duct outlet, T_4, for the high voltage winding of different phases and 1 in the duct outlet for the low voltage winding, T_4. The thermocouples measuring the duct oil were right in the centre of the duct, at the edge of the winding insulation. This means that their vertical positions were 8 mm from the LV-foil and 18 mm from the HV-conductor, at both the top and bottom, Figs. 4.29 and 4.30.

In addition to the normal delivery test, the following tests were made:

- Constant load current: 1.00 p.u., duration: 8.5 h
- Varying load current, Table 4.4.

Table 4.4. – The load steps of the 2500 kVA transformer

Time period (minutes)	Load factor
0.0 –300.0	1.0
300.0 –382.2	2.0
382.2–415	0.0

The measured hot-spot temperature results, which were recorded during a varying load current test, are compared with results obtained from the thermal models in Figs. 4.31, 4.32 and 4.33 below.
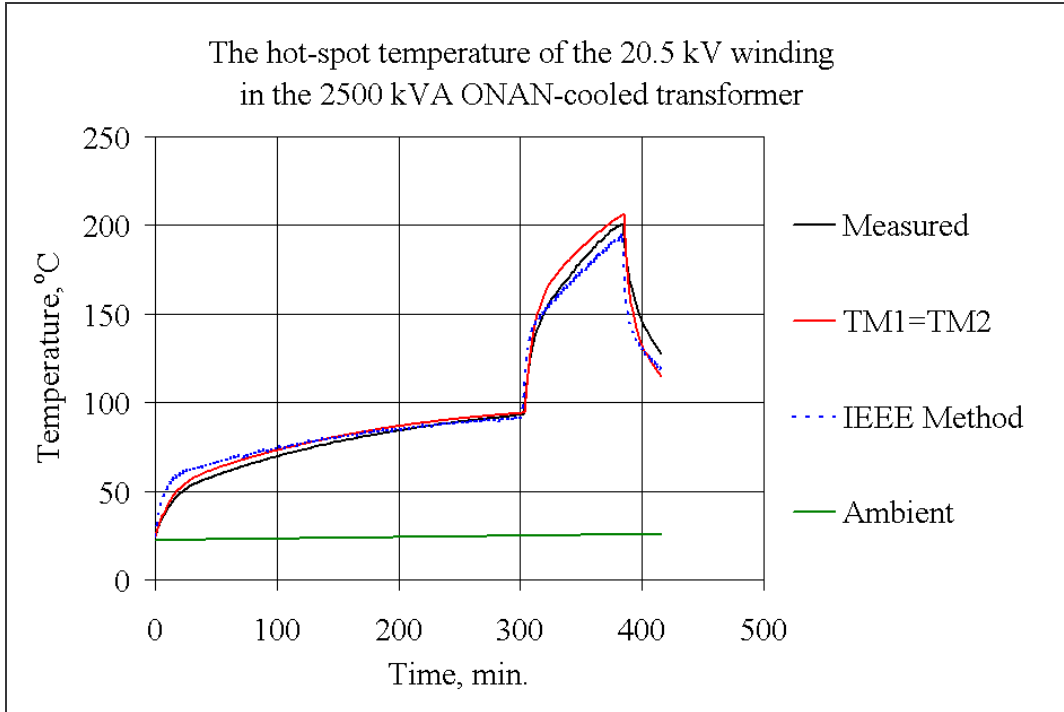
Fig. 4.31. The hot-spot temperature of the 20.5 kV winding in the 2500 kVA ONAN-cooled transformer

Fig. 4.31 compares the measured hot-spot temperature of the 20.5 kV winding in the 2500 kVA ONAN-cooled transformer with the hot-spot temperatures obtained using the following calculation methods:

- "TM1" refers to the hot spot temperature model, equation (3.38), section 3.2.2

- "TM2" refers to the hot spot temperature model, equation (3.41), section 3.2.2

- the IEEE-Annex G method, [28]

When the transformer is run from a cold start the thermal models TM1 and TM2 will yield the same results. Once the transformer is energised, the "cold start" exponents, which are given in Tables 3.4, 3.5 and 3.6, should be substituted for the transformer "on load" exponents at the first load change, Appendix B. Therefore, the temperature results obtained by these models can be represented with the single red line in Fig. 4.31.

88

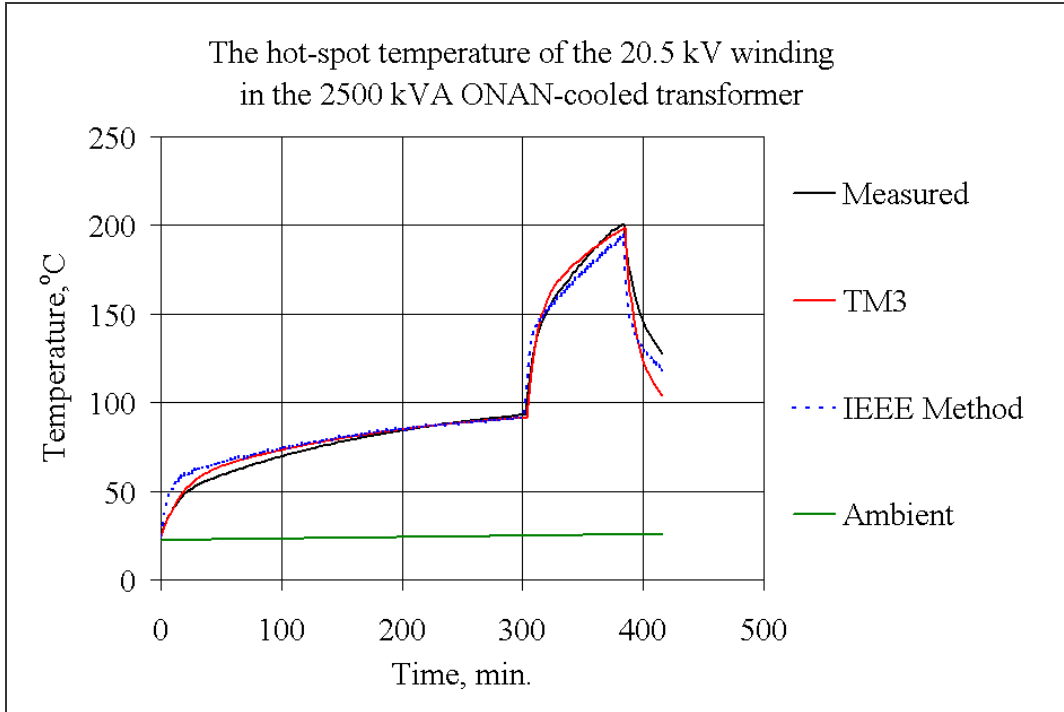Fig. 4.32. The hot-spot temperature of the 20.5 kV winding in the 2500 kVA ONAN-cooled transformer

Fig. 4.32 shows the measured hot-spot temperature of the 20.5 kV winding in the 2500 kVA ONAN-cooled transformer alongside the hot-spot temperatures obtained by the following calculation methods:

- "TM3" refers to the hot spot temperature model, equation (3.49), section 3.2.4

- the IEEE-Annex G method, [28]

Fig. 4.33. The hot-spot temperature response of the 20.5 kV winding in the 2500 kVA ONAN-cooled transformer

Fig. 4.33 compares the measured hot-spot temperature of the 20.5 kV winding in the 2500 kVA ONAN-cooled transformer to the hot-spot temperatures obtained by the following calculation methods:

- "TM4" refers to the hot spot temperature model, equation (3.52), section 3.2.4
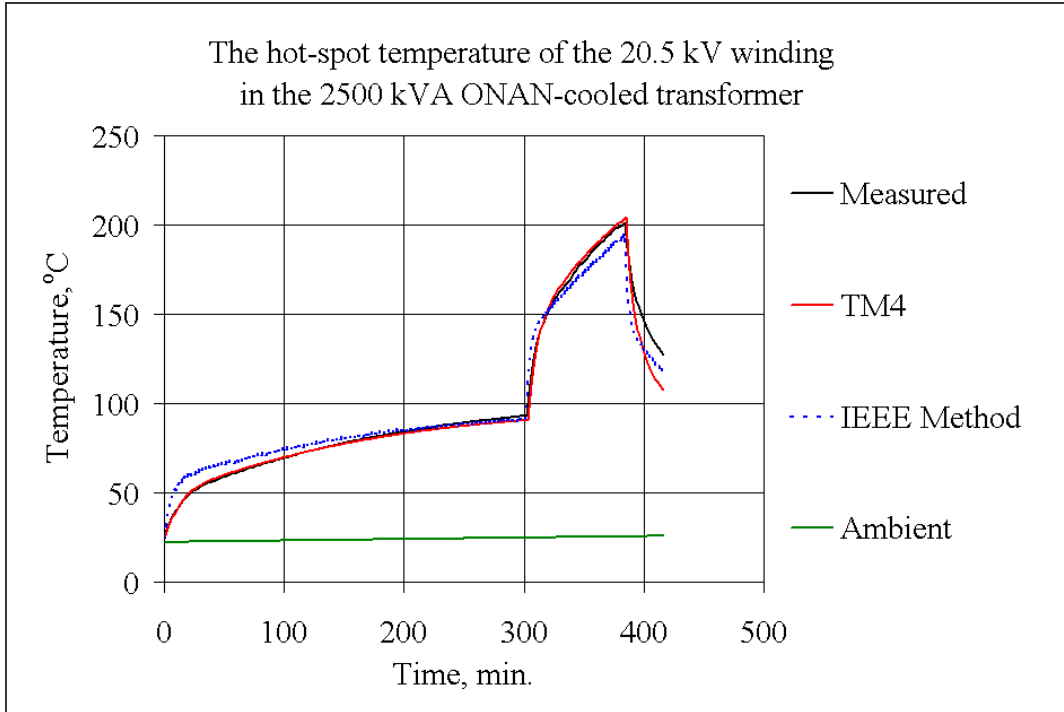
- the IEEE-Annex G method, [28]

Additionally, the measured bottom- and top-oil temperature results, which were recorded during a constant current test, are compared with results obtained from the thermal models in Figs. 4.34, and 4.35 below.
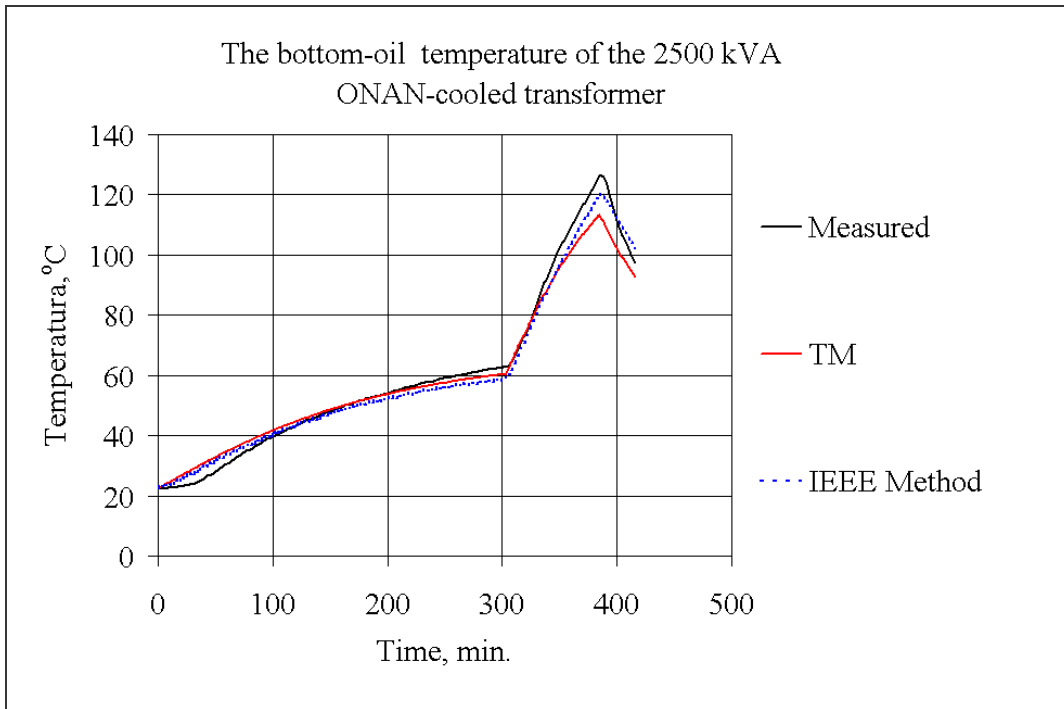
Fig. 4.34. The bottom-oil temperature of the 2500 kVA ONAN-cooled transformer

Fig. 4.34 compares the measured bottom-oil temperature of the 2500 kVA ONAN-cooled transformer with the bottom-oil temperatures calculated using the following methods:

- "TM" refers to the bottom-oil temperature model, equation (3.43) in section 3.2.3

- the IEEE-Annex G method, [28]
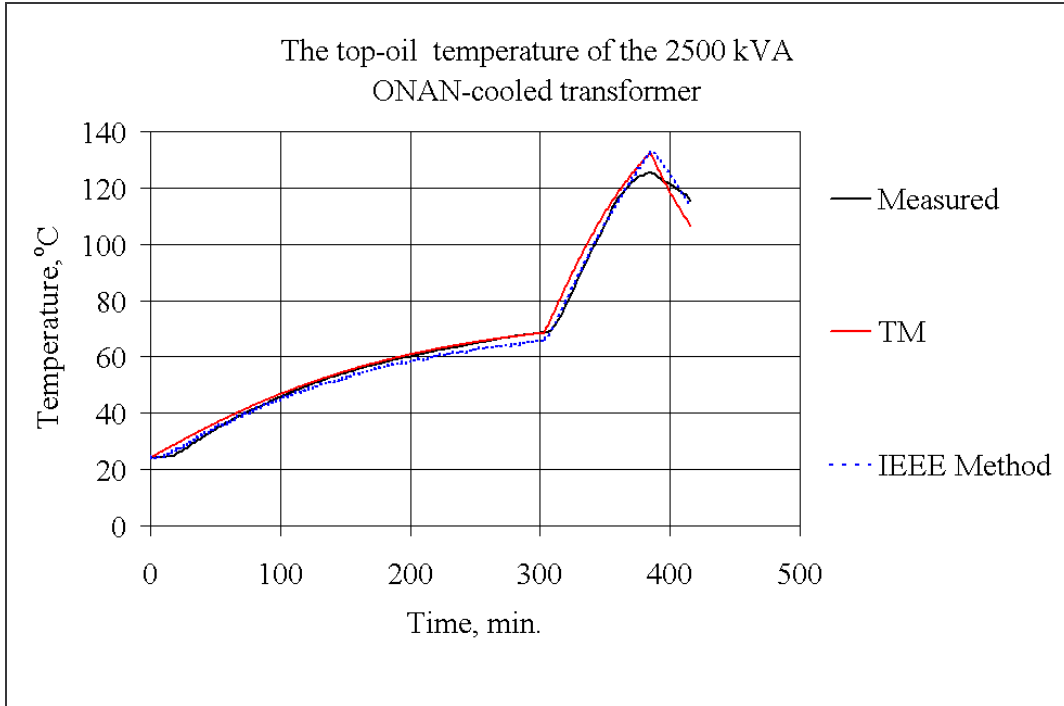
Fig. 4.35. The top-oil temperature of the 2500 kVA ONAN-cooled transformer

Fig. 4.35 shows the measured top-oil temperature of the 2500 kVA ONAN-cooled transformer with the top-oil temperatures obtained using the following calculation methods:

- – "TM" refers to the top-oil temperature model, equation (3.24) in section 3.2.1

- – the IEEE-Annex G method, [28]

It should be pointed out that the winding chosen for the comparison is the hottest of the two main windings in the transformer unit under consideration. These results are also shown in a graphical format to facilitate verification. The presented results are discussed further in section 4.4.

4.3 Real-time application

The real-time application of the thermal model and radiator thermal monitoring were used for assessing the operating conditions of a 40 MVA, OFAF cooled transformer unit in service, [70]. The rated voltages of the transformer were 115±9×1.67%/21 kV. The connection is YNyn0/d, and the short circuit impedance was 11.18%. The transformer data obtained during the delivery test are given in Appendix G, Table G.1.

The permanent on-line monitoring system (SCADA) was upgraded with nine PT-100 thermal sensors installed as follows, Fig. 4.36:

- – one, "1", on the outside surface of the oil outlet pipe of the tank, T_1,
- – one, "1", on the outside surface of the oil inlet pipe of the tank, T_1,
- – two, "2", in the transformer room at different heights. One was attached to the room wall at half height, T_4, with the other at the full height of the transformer, T_3,
- – three, "3", were attached to the cooler. The first on the outside surface of the oil outlet pipe, C_3, the second on the inlet pipe, C_4, and the third was inserted in the cooler pocket (at the oil inlet),
- – three, "3", in the cooler room; one at the air inlet, C_2, and another at the air outlet, C_1, of the cooler. The other sensor was attached to the room wall at the height of the cooler top surface, C_5.
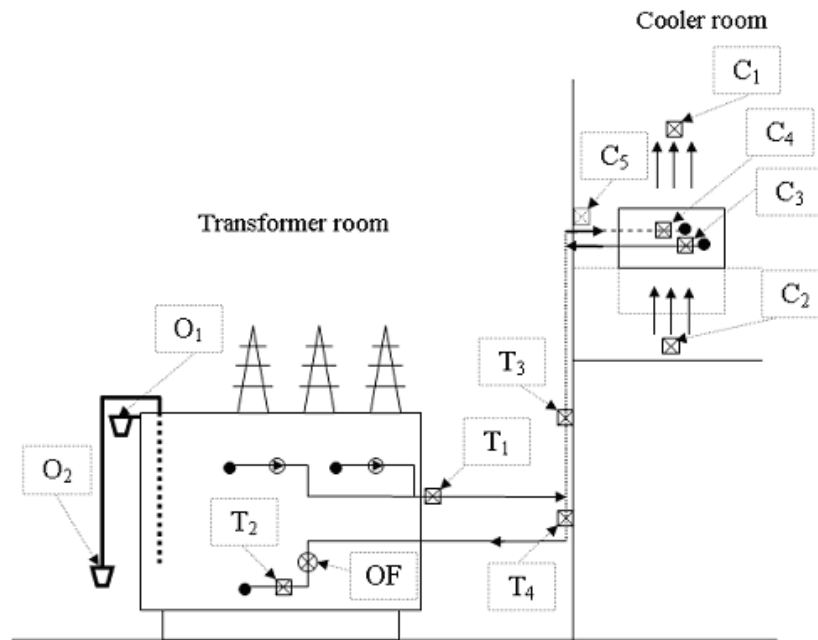

Fig. 4.36. PT-100 installation; on-line monitoring system Hydran 201i; oil sampling, O_2

In addition to the thermal sensor installation, an oil flow meter, OF, was installed in the tank inlet pipe, Fig. 4.36.

The transformer experienced high temperatures during a load pattern below the allowable rating for the unit, although a DGA analysis (which was used as a prevention tool in assessing transformer operational conditions) showed normal levels of gas concentration according to [16], [25] and [27]. However, the analysis indicated an increase in concentration of both carbon monoxide and carbon dioxide. This could have been caused by certain transformer operating problems. Generally, both carbon monoxide and carbon dioxide are developed as the result of thermal degradation of the oil-impregnated cellulose. Hydrocarbons are produced as the result of oil degradation caused by overheating, partial discharges and arcing at higher temperature values than carbons, [63].

In the case under consideration, the transformer overheating was caused by too high temperature settings for switching the cooler fan on (the tested transformer had the thermostat set at a top-oil temperature equal to 55ºC). Therefore, the first remedial action was taken by running the cooling fan continuously. The second remedial action (the final solution) was accomplished by reducing the temperature at which the cooler fan switches on:

- the top-oil temperature: start (35°C) / stop (27°C);
- the winding image: start (38°C) / stop (30°C)

Measured temperature results from after the transformer was treated were compared with results obtained by all the thermal calculation methods to verify the transformer thermal behaviour and this is shown in the figures below.

– Permanently switched-on fan

The measured hot-spot temperature results, which have been recorded since the fan setting was changed, are compared with results obtained from the thermal models in Figs. 4.37, 4.38, 4.39 and 4.40.

Fig. 4.37. The hot-spot temperature of the 115 kV winding in the 40 MVA OFAF-cooled transformer

Fig. 4.37 compares the measured hot-spot temperature of the 115 kV winding in the 40 MVA OFAF-cooled transformer with the hot-spot temperatures obtained by the following methods:

– "TM1" refers to the hot spot temperature model, equation (3.38), section 3.2.2

– the IEEE-Annex G method, [28]

The hot-spot temperature of the 115 kV winding
in the 40 MVA OFAF-cooled transformer

Fig. 4.38. The hot-spot temperature of the 115 kV winding in the 40 MVA OFAF-cooled transformer

Fig. 4.38 compares the measured hot-spot temperature of the 115 kV winding in the 40 MVA OFAF-cooled transformer to the hot-spot temperatures obtained by the following calculation methods:

- "TM2" refers to the hot spot temperature model, equation (3.41), section 3.2.2

- the IEEE-Annex G method, [28]
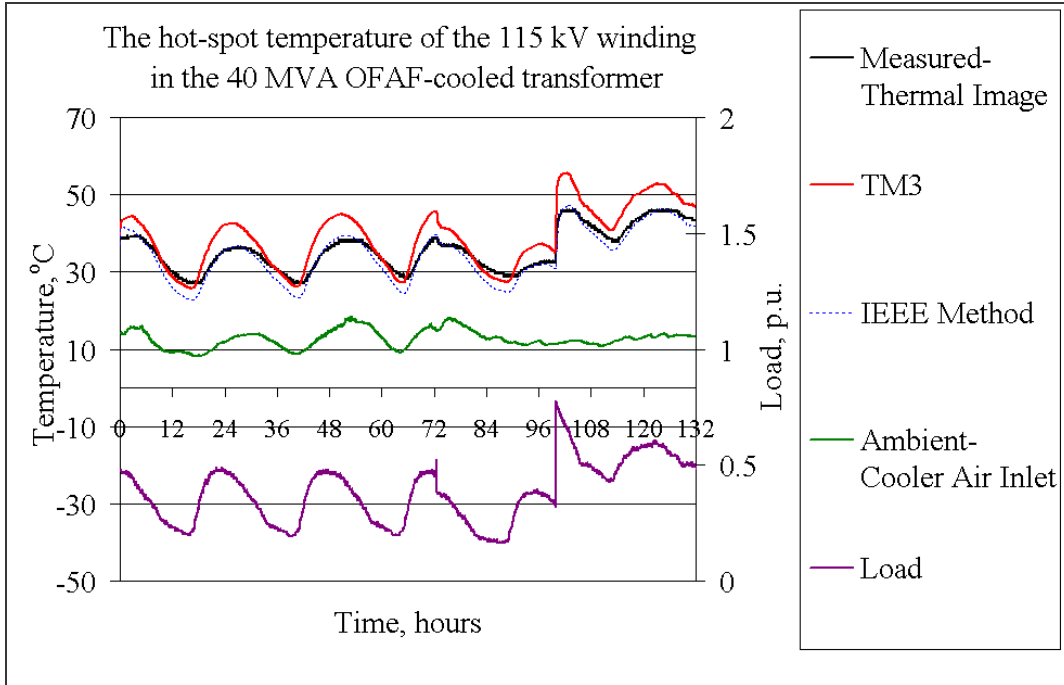
Fig. 4.39. The hot-spot temperature of the 115 kV winding in the 40 MVA OFAF-cooled transformer

Fig. 4.39 compares the measured hot-spot temperature of the 115 kV winding in the 40 MVA OFAF-cooled transformer to the hot-spot temperatures obtained by the following calculation methods:

- "TM3" refers to the hot spot temperature model, equation (3.49), section 3.2.4
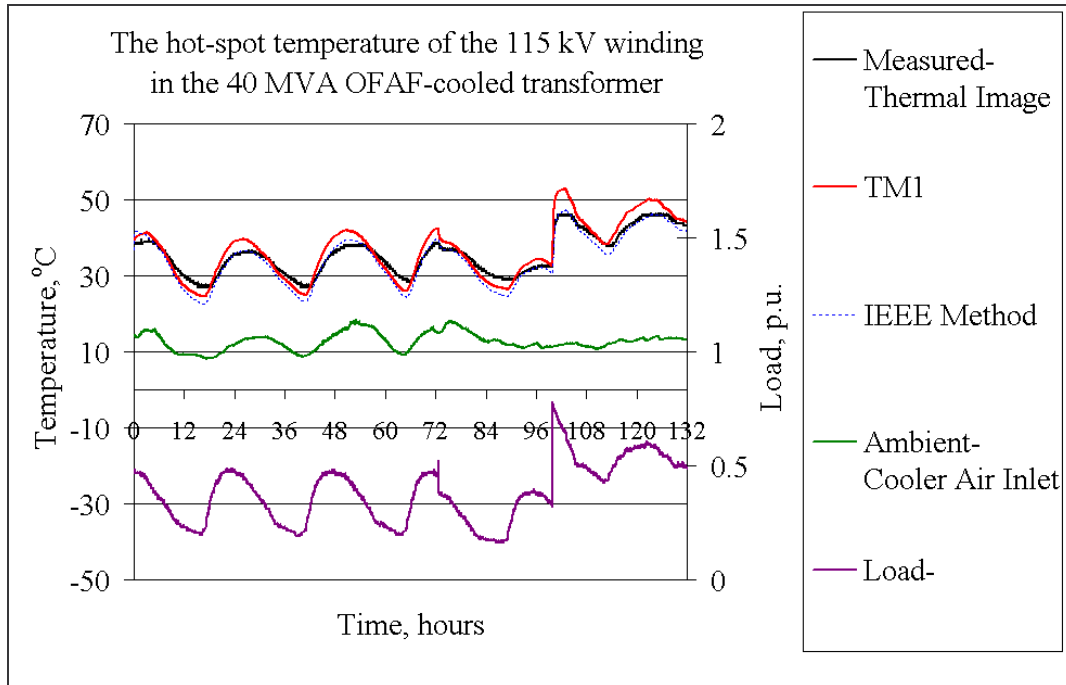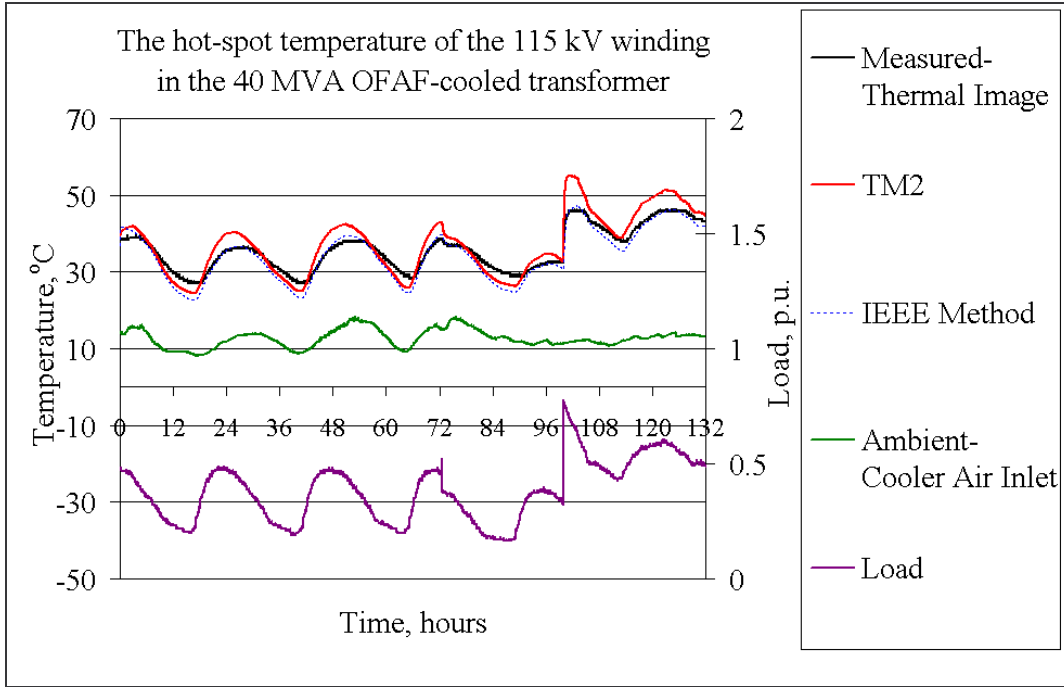
- the IEEE-Annex G method, [28]
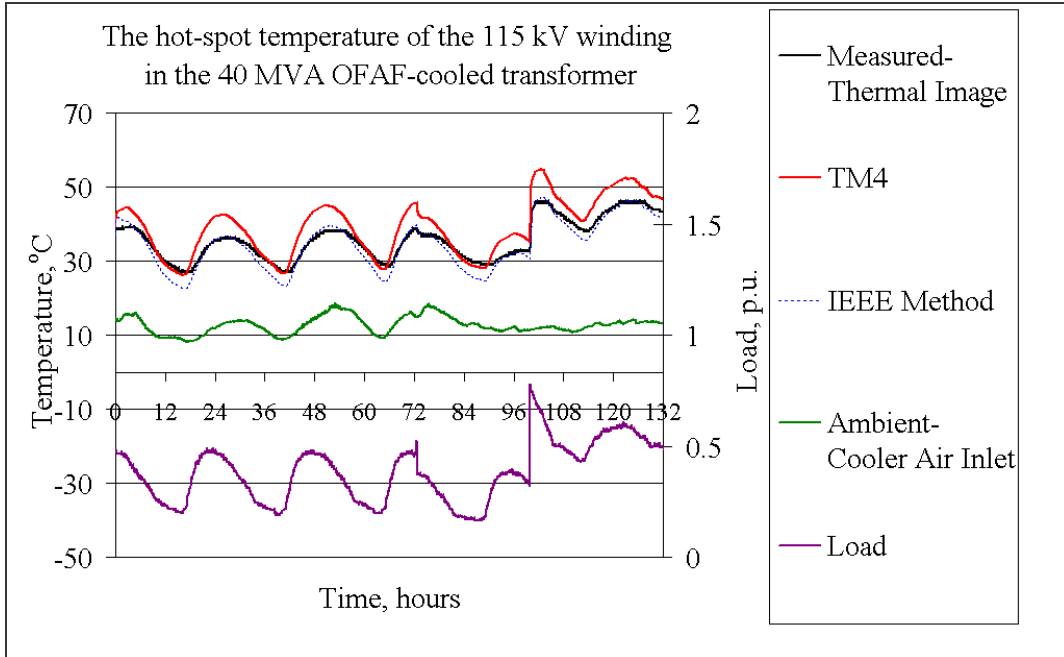
Fig. 4.40. The hot-spot temperature of the 115 kV winding in the 40 MVA OFAF-cooled transformer

Fig. 4.40 compares the measured hot-spot temperature of the 115 kV winding in the 40 MVA OFAF-cooled transformer with the hot-spot temperatures obtained by the following calculation methods:

- "TM4" refers to the hot spot temperature model, equation (3.52), section 3.2.4

- the IEEE-Annex G method, [28]

In addition, the measured bottom- and top-oil temperatures, which have been recorded since the fan setting was changed, are compared with results obtained from the thermal models in Figs. 4.41 and 4.42.
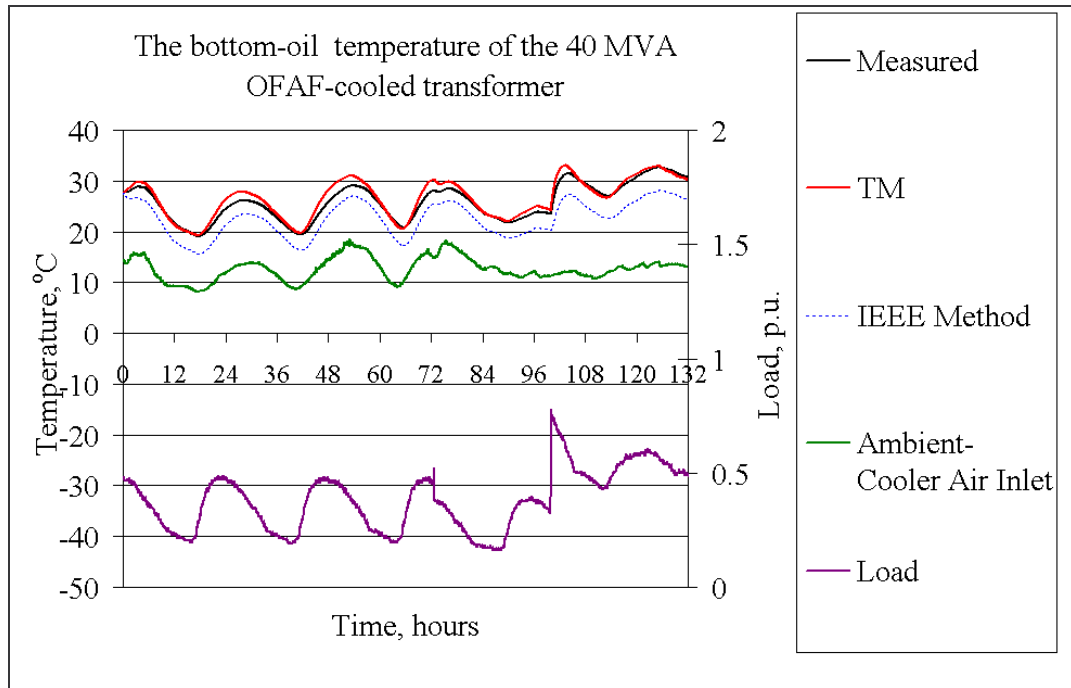
Fig. 4.41. The bottom-oil temperature of the 40 MVA OFAF-cooled transformer

Fig. 4.41 compares the measured bottom-oil temperature of the 40 MVA OFAF-cooled transformer to the bottom-oil temperatures obtained by the following calculation methods:

- "TM" refers to the bottom-oil temperature model, equation (3.43) in section 3.2.3

- the IEEE-Annex G method, [28]

99
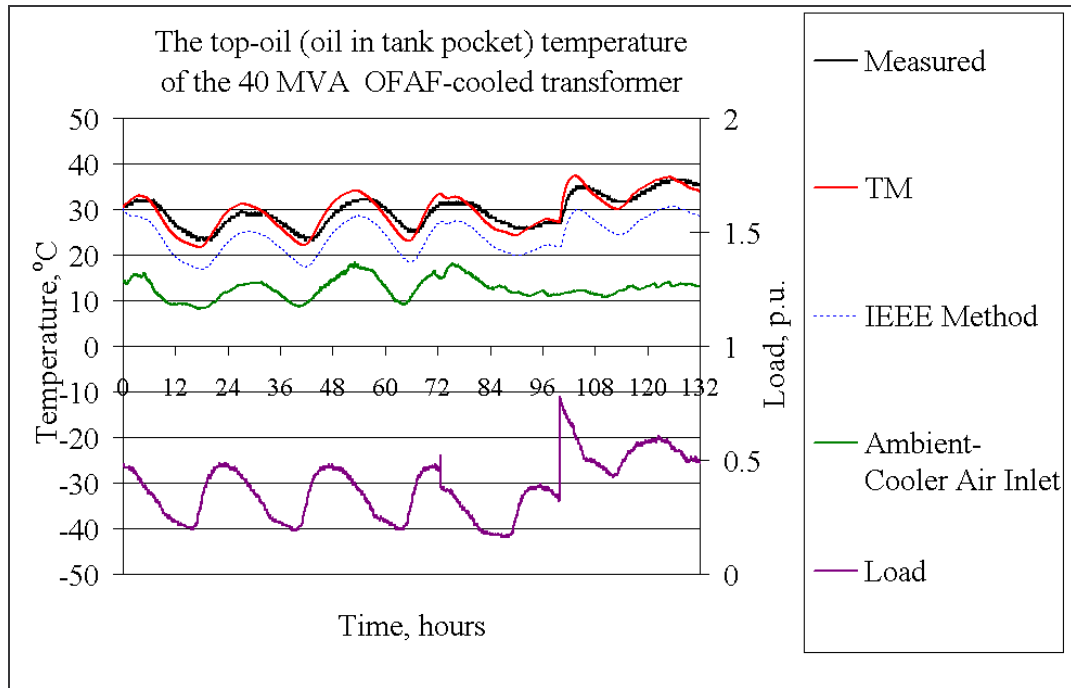
Fig. 4.42. The top-oil (oil in tank pocket) temperature of the 40 MVA OFAF-cooled transformer

Fig. 4.42 compares the measured top-oil temperature of the 40 MVA OFAF-cooled transformer to the top-oil temperatures obtained by the following calculation methods:

- "TM" refers to the top-oil temperature model, equation (3.24) in section 3.2.1

- the IEEE-Annex G method, [28]

The top-oil temperature rise over ambient as a per unit value, Fig. 4.43, was also compared with the calculated values, and indicates that the transformer has recovered.
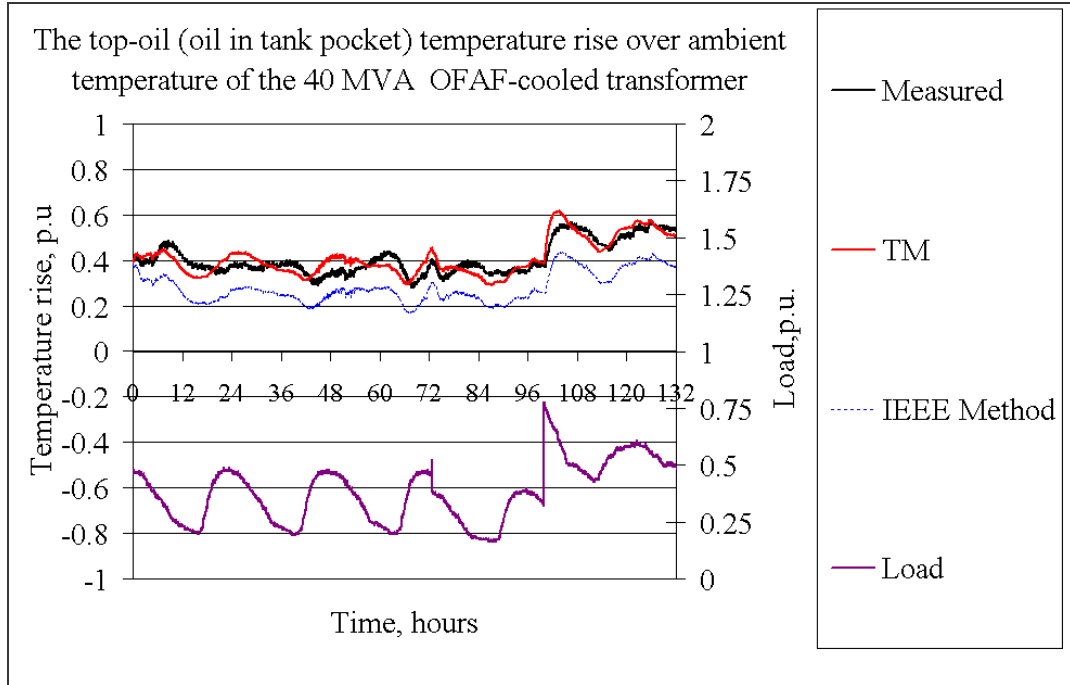
Fig. 4.43. The top-oil (oil in tank pocket) temperature rise over ambient temperature of the 40 MVA OFAF-cooled transformer

Fig. 4.43 compares the measured top-oil temperature rise over ambient temperature of the 40 MVA OFAF-cooled transformer with the top-oil temperature rises obtained by the following calculation methods:

- "TM" refers to the top-oil temperature model, equation (3.24) in section 3.2.1

- the IEEE-Annex G method, [28]

Furthermore, the measured oil flow curve and the air flow curves, which were obtained by the calculation method given in Appendix F for the different fan settings, are shown in Fig. 4.44.
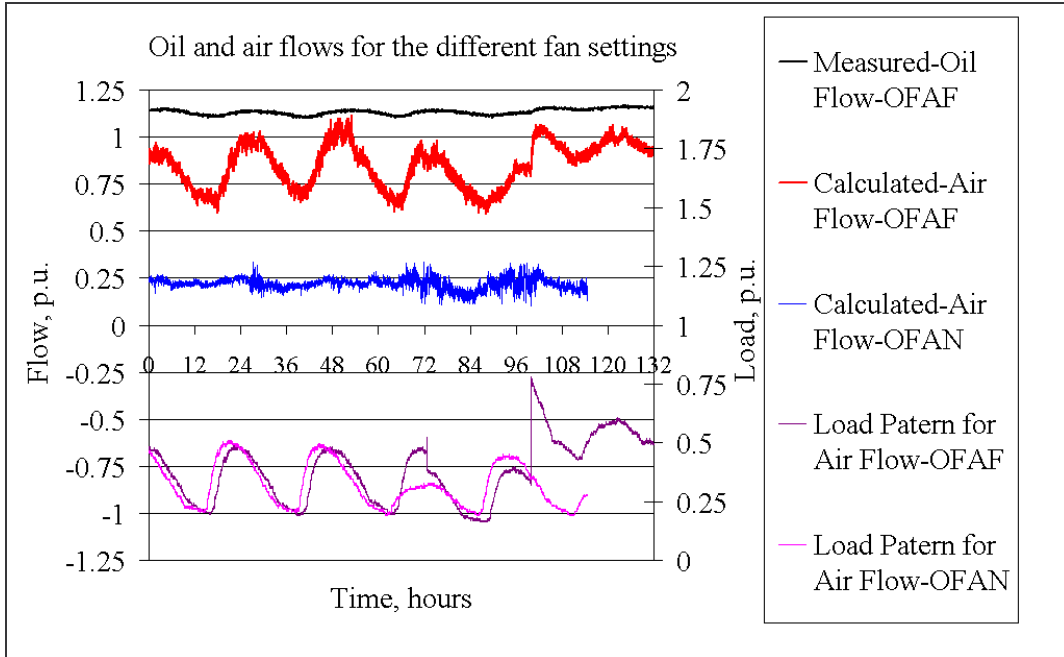
Fig. 4.44. Oil and air flows for the different fan settings

The comparison between the air flow curve for the OFAN cooling mode and the air flow curve for the OFAF cooling mode in Fig. 4.44 suggests how much the wrong fan setting can decrease the cooler efficiency for approximately the same load pattern. In this particular case, the air flow for the OFAF cooling mode is increased approximately 2.5 times compared to the air flow for the OFAN cooling mode. This, in turn, will cause a corresponding decrease of the air temperature gradients across the cooler, Appendix F, equation (F.1), which will further decrease the oil temperatures within the transformer as well as the hot-spot temperature.

The presented results are discussed further in section 4.4.

4.4 Discussion

The results plotted by the proposed thermal models are in good agreement with the measured values for both the load increase and load decrease in the transformers with external cooling. However, the uncertain result obtained with the TM model for the bottom-oil temperature during a 160% overload for the 400 MVA unit, Fig. 4.16, is most probably caused by restricted oil flow through the 120 kV winding, [48-49] and [62]. Namely, although the oil circulation through the low voltage winding was guided with rings, the winding radial spacers were less than 2 mm, creating an increased resistance to the oil flow. Therefore, the cooling was restricted and the oil temperatures rose at a slower rate than would normally be expected for this transformer type. It should be pointed out that the oil flow through the high voltage winding was unrestricted and for that reason the top-oil temperature was less affected. This mismatch also directly affects the hot-spot temperature results obtained by models TM3 and TM4, shown in Figs. 4.14 and 4.15, respectively. It was also observed that the bottom-oil temperature delay was more pronounced for a cool start of the 80 MVA, ONAN-cooled and 650 MVA, ONAF cooled units, due to the specific cooling mode in the first case and the transformer winding design in the second. The delay was not taken into account in the suggested thermal model, TM, in order to keep the modelling as simple as possible (modelling of the delay can be achieved by adding a certain number of RC elements in both the top-oil and the bottom-oil circuits of the model). Therefore, the thermal model, TM, yields the more conservative results in Figs. 4.4, 4.5, 4.27 and 4.28. It is also necessary to point out that most of the tested units (i.e., 80 MVA ONAN, 250 MVA ONAF, 400 MVA ONAF, and the 650 MVA ONAF cooled unit) were run from a cold start, Appendix B.

It should be noted that the IEEE-Annex G method also generally yields results that match well with the measured results.

The suggested thermal models and the IEEE-Annex G method compare well with the measurement results for the transformer without external cooling, provided proper values for oil temperature rises are used. The oil temperatures used to obtain the calculated curves in Figs. (4.31 - 4.35) are as follows:

- Top-oil temperature is equal to the oil temperature in the oil pockets.
- Bottom oil temperature is equal to the bottom oil temperature inside the tank, under the windings.

If the liquid temperature were strictly defined according to IEEE, [29], then both calculation methods would yield certain deviations from the measured values, [69].

The results plotted by all thermal models for the real time application agree with the measured values with good accuracy, proving that the transformer operating conditions have fully recovered. It was also observed that the thermal models TM1, TM2, TM3 and TM4 yield higher hot-spot temperature values when compared to the values obtained by both the IEEE Annex-G method and the thermal image device. On the other hand, the thermal image device is based on IEC 354, [22], with OFAF cooling mode settings and at the measured top-oil temperature shown in Fig. 4.42. Therefore, it can be

concluded that the hot-spot temperature calculated by the TM1, TM2, TM3 and TM4 models are generally more accurate, especially after a sudden load change.

A similar transformer operational problem would be avoided if the transformer were to be operated continuously in the cooling mode for which it is designed. However, if there is an economic need to operate a transformer in alternative cooling modes, e.g., to decrease the operational cost for auxiliary power, the switch-on temperature should be set at lower values than the original top-oil temperature by taking into account both the transformer rating change and seasonal changes in ambient temperature. Furthermore, to define the proper setting of the fan controls and the calibration of the thermal image device, additional heat run tests should be made for all intended cooling modes (e.g., OFAN, ONAF, or ONAN). Based on the obtained data, the transformer could be safely operated when it is switched from one cooling mode to the other. The heat exchanger type (e.g., radiator or cooler) used during tests should also be clarified.

In addition, the windings chosen for comparison were the hottest of the two main windings in the presented transformer units. The results were all depicted graphically, to aid visual verification.

5 Conclusions

Power transformers are among the most valuable and important assets in electrical power systems. Insulation system ageing reduces both the mechanical and dielectric-withstand strength of the transformer. An ageing transformer is subject to faults that result in high radial and compressive forces. In an aged transformer failure, the conductor insulation has typically deteriorated to the point where it cannot longer sustain the mechanical stresses caused by a fault. The turn to turn insulation then suffers a dielectric failure, or a fault causes a loosening of winding clamping pressure, which reduces the transformer's ability to withstand future short circuit forces. The ageing of the used oil/paper insulation primarily depends on the hot-spot temperature of the solid insulation system. Hence it is the dominant factor in limiting the lifetime of the transformer.

There are two basic thermal models (IEC and IEEE) that have been used by the industry. By the means of such models only the steady state hot-spot temperature can be estimated and used with good accuracy for determining the ageing of the oil/paper insulation. In addition, the IEEE Loading Guide-Annex G offers a more accurate but more complicated thermal calculation method. During the last 20 years fibre optic probes have been used by many authors in order to obtain as accurate values for transformer temperatures as possible. By analysing the measured results from a range of power transformers it was noticed that the hot-spot temperature rise over top-oil temperature at load changes is a function depending on time as well as the transformer loading (the "overshoot time dependent function"). This explains why it takes some time before the oil circulation has adapted its speed to correspond to the increased load level. The hot-spot temperature increases rapidly with a time constant equal to the time constant of the windings. During transient states this results in winding hottest spot temperatures higher than those predicted by the present loading guide for oil-immersed power transformers.

A thermal investigation performed on a distribution transformer with external cooling showed similar results. Therefore a comprehensive test program was made on a distribution transformer without external cooling. The test showed that the hot-spot temperature rise over top-oil temperature for the oil temperature measured in the oil pocket due to a change in load is an exponential function with a time constant equal to the winding time constant. It was also observed that the top-oil time constant is longer than the time constant obtained for transformers with both external cooling and guided horizontal oil flow through the windings, whereas it is similar to the time constant obtained for the transformers with both external cooling and no oil guiding rings. The time constant values used in the comparison were estimated by exponential curve fitting.

This research work has been an attempt to develop generalised models that are able to explain the physical background of the previous findings. The main results of this doctoral work can be summarised as follows:

- The definition for both the transformer oil-air and winding-oil nonlinear thermal resistances at the top and bottom level is given as a unique solution.

Additionally, the transformer top-winding to bottom-oil nonlinear resistance is defined.

− Four different general hot-spot temperature thermal models for more accurate temperature calculations during transient states are developed, i.e., TM1, TM2, TM3 and TM4. Models TM1 and TM2 are based on data received in a normal heat run test, i.e., the top oil temperature in the tank of the transformer and the average winding-to-average oil temperature gradient, whereas the TM3 and TM4 models need, as additional input data, the bottom-oil temperature.

− General dynamic thermal models for both the top-oil and bottom-oil are also determined, where the effects of ambient temperature dynamics on both the top-oil and bottom-oil temperature are taken into account.

− Oil viscosity changes and loss variation with temperature are taken into account in the thermal models. The influence of all other oil parameters is also considered.

− Additionally, the changes in the transformer time constants with oil viscosity are accounted for.

− The transformer top-oil time constant equation is presented, where the equivalent thermal capacitance of the transformer oil for the transformer design with external cooling and winding-oil circulation in the zigzag pattern is suggested as a new solution based on the uneven distribution of the transformer losses. It is suggested that for different transformer designs, i.e., transformers without either external cooling or guided horizontal oil flow through the windings, the other equation for the equivalent thermal capacitance of the transformer oil should be applied.

− The difference between transformer cooling modes is taken into account by the modified "top-oil time constant" formula and a properly estimated value for the empirical constant n.

The thermal models were validated using experimental (fibre optic test) results obtained at varying load current on different transformer units. All the models were successfully used to properly assess the operating conditions of a 40 MVA, OFAF transformer unit in service. Their real-time application provides an accurate picture of the operating condition of the transformer, which allows the operator to detect early signs of faults and correct them. A considerable advantage of the suggested thermal models, especially the models based on the top-oil temperature, TM1 and TM2, is that they are tied only to measured parameters that are readily available, i.e., the top oil in the tank of the transformer and the average winding-to-average oil gradient. Thus, the intended scope of this research work has been fully achieved.

The thermal models are fully dependent on accurately defined steady-state temperature rises. Therefore, it will be important to develop a steady-state calculation method, especially because most installed transformers are not heat-run tested. However, further research and development is needed to improve the existing monitoring systems and introduce new solutions that include the transformer thermal models and their real-time application. Utilising thermal models allows both transformer manufactures and users to run different loading and ambient scenarios and, by analysing the results, improve the transformer design (costs, size and load carrying capacity).

References

[1]   (Alegi, 1990) Alegi, G.L., and Black W.Z., "Real-time thermal model for an oil-immersed, forced-air cooled transformer", IEEE Transactions on Power Delivery, Vol. 5, Iss. 2, April 1990, pp.991-999.

[2]   (Aubin, 1990) J. Aubin, R. Bergeron, and R. Morin, "Distribution Transformer Overloading Capability Under Cold-Load Pickup Conditions", IEEE Transactions on Power Delivery, Vol. 5, Iss. 4, October 1990, pp. 1883-1891.

[3]   (Aubin, 1992) J. Aubin, and Y. Langhame, "Effect of oil viscosity on transformer loading capability at low ambient temperatures", IEEE Transactions on Power Delivery, Vol.7, Iss.2, April 1992, pp.516-524.

[4]   (Betta, 2000) Betta, G., Pietrosanto A., and Scaglione A., "An enhanced fiber optic temperature sensor system for power transformer monitoring", Instrumentation and Measurement Technology Conference, 2000. IMTC 2000. Proceedings of the 17th IEEE ,Vol.1 , 1-4 May 2000, pp.153-158.

[5]   (Blake, 1969) Blake H. John, and Kelly J. Edward, "Oil-Immersed Power Transformer Overload Calculation by Computer", IEEE Power Transactions on Power Apparatus and Systems, Vol. Pas-88, August 1969, pp. 1205

[6]   (Blume, 1951) Blume L. F., Boyajian A., Camilli G., Lennox T. C., Minneci S., and Montsinger V. M., "Transformer Engineering – 1st edition", John Wiley & Sons, Inc., New York, 1938.

[7]   (Blume, 1938) Blume L. F., Boyajian A., Camilli G., Lennox T. C., Minneci S., and Montsinger V. M., "Transformer Engineering – 2nd edition", John Wiley & Sons, Inc., New York, 1951.

[8]   (Carballeira, 1991) Carballeira, M., " HPLC contribution to transformer survey during service or heat run tests", Assessment of Degradation Within Transformer Insulation Systems, IEE Colloquium on , 6 Dec 1991, pp.5/1 - 5/4

[9]   (Chu, 1999) Chu D., Lux, A., " On-line monitoring of power transformers and components: a review of key parameters", Electrical Insulation Conference and Electrical Manufacturing & Coil Winding Conference, 1999. Proceedings , 26-28 October 1999, pp. 669 - 675

[10]   (Declercq, 1999) Declercq J., and Van der Veken W., " Accurate hot spot modeling in a power transformer leading to improved design and performance", Transmission and Distribution Conference, 1999 IEEE ,Vol. 2 , 11-16 April 1999, pp. 920-924.

[11]   (Doherty, 1924) Doherty R.E., and Carter E.S., "Effect of Altitude on Temperature rise", A.I.E.E. Trans., Vol. 43 , June 1924, pp.

[12] (Eckholz, 2004) Eckholz K., Knorr W., and Schäfer M.,"New Developments in Transformer Cooling Calculations", Cigre, Rep. 12-09, International Conference on Large High Voltage Electric Systems, 2004 Session, 29th August-6th September.

[13] (Electra, 1990) "Direct Measurements of the Hot-Spot Temperature of Transformers", CIGRÉ WG 12–09, vol. 129, 1990.

[14] (Electra, 1990) "A survey of facts and opinions on the maximum safe operating temperature of power transformers under emergency conditions", CIGRÉ WG 12–09, vol. 129, 1990.

[15] (Electra, 1990) "Heat-Run Test procedure for power transformers", CIGRÉ WG 12–09, vol. 129, 1990.

[16] (Emsley, 1994)Emsley A. M., and Stevens G. C., "Review of chemical indicators of degradation of cellulosic electrical paper insulation in oil-filled transformers," IEEE Proc.-Sci. Technol., Vol. 141, No. 5, September 1994, pp.324-334.

[17] (Feng, 2002) Feng J.Q., Sun P., Tang W.H., Buse D.P., Wu Q.H., Richardson Z., and Fitch J., " Implementation of a power transformer temperature monitoring system", International Conference on Power System Technology, 2002. Proceedings PowerCon 2002.,Vol. 3 , 13-17 Oct. 2002, pp.1980 - 1983

[18] (Grubb, 1981) Grubb R.L., Hudis M., and Traut A. R.,"A Transformer Thermal Duct Study of Various Insulating Fluids", Power Apparatus and Systems, IEEE Transactions on ,Vol. PAS-100 , No. 2 , February 1981, pp. 466 - 473.

[19] (Harris, 1997) Harris D., and Saravolac M.P., "Condition monitoring in power transformers", Condition Monitoring of Large Machines and Power Transformers (Digest No: 1997/086), IEE Colloquium on , 19 June 1997 , pp. 7/1 - 7/3

[20] (Harrison, 1995) Harrison, D. ,"Loading capabilities of large power transformers", Power Engineering Journal [see also Power Engineer] ,Vol. 9 , Issue: 5 , Oct. 1995, pp. 225-230

[21] (Heathcote, 2003) Martin J. Heathcote, "J&P Tranformer Book," 12th ed. Elsevier Science Publishers, 2003, pp. 945.

[22] (IEC, 1991) "IEC 354-1991 Loading Guide for Oil-immersed Power Transformers"

[23] (IEC , 1993) "IEC 72-1 Power Transformers; Part 1: General",1993-03 second edition

[24] (IEC , 1994) "IEC 72-2 Power Transformers; Part 2: Temperature rise",1994-04 second edition

[25] (IEC, 1999) "Guide to the interpretation of dissolved and free gases analysis", IEC 60599; 1999-03 second edition

[26] (IEEE PES Transformers Committee, 1994) IEEE PES Transformers Committee, Working Group Report, Insulation Life Subcommittee, Working Group on High Temperature Insulation for Liquid-Immersed Power Transformers, "Background Information on High Temperature Insulation for Liquid-Immersed Power Transformers", IEEE Transactions on Power Delivery, Vol. 9, No. 4, Oct. 1994, pp.1892-1906

[27] (IEEE, 1991) "IEEE Std C57.104-1991 IEEE guide for the interpretation of gases generated in oil-immersed transformers"

[28] (IEEE, 1995) "IEEE Std C57.91-1995 IEEE guide for loading mineral-oil-immersed transformers"

[29] (IEEE, 1999) "IEEE Standard Test Code for Liquid-Immersed Distribution, Power, and Regulating Transformers", IEEE Std C57.12.90 – 1999.

[30] (IEEE, 2000) "IEEE Std 1538-2000 IEEE Guide for Determination of Maximum Winding Temperature Rise in Liquid-Filled Transformers"

[31] (IEEE, 2001) "IEEE Std C57.119-2001 IEEE recommended practice for performing temperature rise tests on oil-immersed power transformers at loads beyond nameplate ratings"

[32] (IEEE, 2002) "IEEE Std C57.91-1995/Cor 1-2002 "

[33] (Incropera, 1996) Incropera F. P., and DeWitt D. P., "Fundamentals of Heat and Mass Transfer", 4th ed., John Wiley & Sons, 1996, pp. 886.

[34] (Karsai, 1987) Karsai K., Kerenyi D., and Kiss L.,"Large Power Transformers," Elsevier Science Publishers, 1987, pp 607.

[35] (King, 1932) King W.J., "The basic Laws and Data of Heat Transmission", Mechanical Engineering, March-August, 1932, pp.191

[36] (Lachman, 2003) Lachman M.F., Griffin P.J., Walter W., and Wilson A.," Real-time dynamic loading and thermal diagnostic of power transformers", IEEE Transactions on Power Delivery ,Vol. 18 , Issue: 1 , Jan 2003, pp.142-148

[37] (Lampe, 1984) Lampe W., Pettersson L., Ovren C., and Wahlström B., "Hot-Spot Measurements in Power Transformers", Cigre, Rep. 12-02, International Conference on Large High Voltage Electric Systems, 1984 Session, 29th August-6th September.

[38] (Leibfried, 1998) Leibfried T.," Online monitors keep transformers in service" Computer Applications in Power, IEEE ,Vol.11 , Issue: 3 , July 1998 , pp.36 - 42

[39] (Lesieutre , 1997) Lesieutre B.C., Hagman W.H., Kirtley J.L.Jr., "An improved transformer top oil temperature model for use in an on-line monitoring and diagnostic system", IEEE Transactions on Power Delivery, Volume: 12 , Issue: 1 , January 1997, pp. 249 - 256

[40] (Montsinger, 1916) Montsinger V. M., "Effect of Barometric Pressure on Temperature Rise of Self-Cooled Stationary Induction Apparatus", A.I.E.E. Trans., 1916

[41] (Montsinger, 1917) Montsinger V. M., "Cooling of Transformer windings After Shut-Down", A.I.E.E. Trans., 1917, Vol.36, p. 711.

[42] (Montsinger, 1924) Montsinger V. M., and W.H. Cooney, "Temperature Rise of Stationary Electrical apparaturs as Influenced by Radiation, Convection, and Altitude", A.I.E.E. Trans., Vol.43, 1924, p. 803

[43] (Montsinger, 1930) Montsinger V. M., and Wetherill L., "Effect of Color of Tank on the   on Temperature Self-Cooled Transformers under Service Conditions", A.I.E.E. Trans., 1930, Vol.49, p. 41.

[44] (Montsinger, 1930) Montsinger V. M., "Loading Transformer by Temperature", A.I.E.E. Trans., Vol.49, 1930, p. 776

[45] (Montsinger, 1934) Montsinger V. M., and W.M. Dann, "Overloading of Power transformers", Electrical Engineering, October, 1934.

[46] (Montsinger, 1942) Montsinger V. M., and Ketchum M.P., "Emergency Overloading of Air-Cooled Transformers by Hot-Spot Temperature", Supplemental Issue Elec. Eng, Decembar 1942

[47] (Nordman, 1990) Nordman H., Hironniemi E., and Pesonen A.J., "Determination of hot-spot temperature rise at rated load and at overload", CIGRE Paper 12-103, 1990.

[48] (Nordman, 2003) Nordman H., and Lahtinen M., "Thermal overload tests on a 400-MVA power transformer with a special 2.5-p.u. Short time loading capability", IEEE Transactions on Power Delivery, Vol. 18 , Iss. 1 , Jan 2003, pp.107 - 112

[49] (Nordman, 2003) Nordman H., Rafsback N., and Susa, D., "Temperature responses to step changes in the load current of power transformers", IEEE Transactions on Power Delivery, Vol. 18 , Iss. 4 , Oct. 2003, pp.1110 - 1117

[50] (teNyenhuis, 2002) teNyenhuis E.G., Girgis R.S., Mechler G.F., and Gang Zhou, "Calculation of core hot-spot temperature in power and distribution transformers", IEEE Transactions on   Power Delivery, Vol. 17 , Iss. 4 , Oct. 2002, pp. 991-995

[51] (Oommen, 2001) Oommen T.V., and Lindgren S.R., "Bubble evolution from transformer overload", Transmission and Distribution Conference and Exposition, 2001 IEEE/PES ,Vol. 1 , 28 Oct.-2 Nov. 2001, pp.137-142

[52] (Pierce, 1992) Pierce L.W., "An investigation of the thermal performance of an oil filled transformer winding", IEEE Transactions on Power Delivery, Vol. 7 , Iss. 3 , July 1992, pp.1347-1358

[53] (Pierce, 1994) Pierce, L.W., "Predicting liquid filled transformer loading capability", IEEE Transactions on Industry Applications, Vol. 30 , Iss.1, Jan.-Feb. 1994, pp.170-178

[54] (Pierce, 1999) Pierce L.W., and Holifield T., "A thermal model for optimized distribution and small power transformer design", Transmission and Distribution Conference, 1999 IEEE ,Vol. 2 , 11-16 April 1999 , pp. 925 - 929.

[55] (Pradhan, 2003) Pradhan M.K., and Ramu T.S.,"Prediction of hottest spot temperature (HST) in power and station transformers", IEEE Transactions on Power Delivery, Vol. 18 , Iss. 4, October 2003, pp.1275 - 1283

[56] (Radakovic, 1997) Radakovic Z, Kalic Dj., "Results of a novel algorithm for the calculation of the characteristic temperatures in power oil transformers", Electrical Engineering 80, 1997, pp. 205–214

[57] (Radakovic, 2003) Radakovic Z.,Feser K.,"A new method for the calculation of the hot-spot temperature in power transformers with ONAN cooling", IEEE Transactions on Power Delivery, Vol. 18 , Iss. 4, October 2003, pp.1284-1292

[58] (Radakovic, 2003) Radakovic Z., "Numerical determination of characteristic temperatures in directly loaded power oil transformer", European Transaction on Electrical Power (ETEP), vol.13, no.1, 2003, pp.47-54.

[59] (Rice, 1923) Rice W. Chester," Free and Forced Convection of Heat in Gases and Liquides-II", Physical Review, Vol. 21, April, 1923and A.I.E.E. Trans., 1923, p. 1288

[60] (Rice, 1931) Rice W. Chester," Free and Forced Convection of Heat in Gases and Liquides-II", A.I.E.E. Trans., February 1924, pp. 131

[61] (Ryder, 2002) Ryder S.A., "A simple method for calculating winding temperature gradient in power transformers", IEEE Transactions on Power Delivery, Vol. 17 , Iss. 4, October 2002, pp. 977 – 982

[62] (Räfsbäck, 2001) Räfsbäck N. T., "Short-time emergency overloading of power transformers, Bachelor thesis", Power transformer company, ABB, Vaasa, 2001

[63] (Saha, 2003) Saha T. K., "Review of Modern Diagnostic Techniques for Assessing Insulation Condition in Aged Transformers", IEEE Trans. on Dielectrics and Electrical Insulation, Vol. 10, No. 5, October 2003, pp.903-917.

[64] (Saravolac, 1994) Saravolac, M.P., "The use of optic fibres for temperature monitoring in power transformers", Condition Monitoring and Remanent Life Assessment in Power Transformers, IEE Colloquium on , 1994, pp.7/1 - 7/3

[65] (Schaefer, 2000) Schäefer M., Kutzner R. and Feser, K., " Condition monitoring system for power transformers", International Conference on Power System Technology, 2000. Proceedings. PowerCon 2000., Vol.: 3 , 4-7 Dec. 2000, pp. 1701 - 1705

[66] (Simonson, 1995) Simonson E.A., and Lapworth J.A.," Thermal capability assessment for transformers", Second International Conference on the Reliability of Transmission and Distribution Equipment 1995., 29-31 Mar 1995, pp.103 - 108

[67] (Susa, 2002) Susa D., Lehtonen M., and Nordman H., "Transformer Temperature Calculation During Transient States", Modern Electric Power Systems MEPS'02 , Wroclaw University of Technology, Wroclaw, Poland, September 11-13, 2002, 6 p.

[68] (Susa, 2002) Susa D. and Lehtonen M., "New aspects on the dynamic loading of power transformers", Fifth Nordic Distribution and Asset Management Conference, NORDAC 2002, Copenhagen, Denmark, November 7-8 2002, 9 p.

[69] (Susa, 2004) Susa D., Lehtonen M., and Nordman H., "Dynamic Thermal Modelling of Distribution Transformers", The paper has been approved for publication in the Transactions on Power Delivery

[70] (Susa, 2004) Susa D., Palola J., Lehtonen M., and Hyvarinen M., " Temperature Rises in an OFAF Transformer at OFAN Cooling Mode in Service", The paper has been approved for publication in the Transactions on Power Delivery on 31st December, 2004.

[71] (Susa, 2005) Susa D., Lehtonen M., and Nordman H.," Dynamic Thermal Modelling of Power Transformers", IEEE Transactions on Power Delivery, Vol. 20, Iss. 1, January 2005, pp. 197 – 204

[72] (Swift, 2001) Swift G., Molinski T.S., Bray R., and Menzies, R., "A fundamental approach to transformer thermal modelling-II. Field verification", IEEE Transactions on Power Delivery, Vol. 16, Iss. 2, April 2001, pp. 176 - 180

[73] (Swift, 2001) Swift G., Molinski T.S., and Lehn W., "A fundamental approach to transformer thermal modelling- I. Theory and equivalent circuit", IEEE Transactions on Power Delivery, Vol. 16, Iss. 2, April 2001, pp. 171 - 175

[74] (Swift, 2001) Swift G.W., Zocholl E.S., Bajpai M., Burger J.F., Castro C.H., Chano S.R., Cobelo F. de Sa P., Fennell E.C., Gilbert J.G., Grier S.E., Haas R.W., Hartmann W.G., Hedding R.A., Kerrigan P., Mazumdar S., Miller D.H., Mysore P.G., Nagpal M., Rebbapragada R.V., Thaden M.V., Uchiyama J.T., Usman S.M., Wardlow J.D., and Yalla M., "Adaptive transformer thermal overload protection", IEEE Transactions on Power Delivery, Vol. 16, Iss. 4, October 2001, pp. 516 - 521

[75] (Tang, 2002) Tang W.H., Wu Q.H., and Richardson Z.J., " Equivalent heat circuit based power transformer thermal model", Electric Power Applications, IEE Proceedings, Vol. 149, Iss. 2, March 2002, pp. 87 - 92

[76] (Tang, 2004) Tang W.H., Wu Q.H., and Richardson Z.J., "A simplified transformer thermal model based on thermal-electric analogy", IEEE Transactions on Power Delivery, Vol. 19, Iss. 3 , July 2004, pp. 1112 - 1119

[77] (Tenbohlen, 2001) Tenbohlen S., Stirl T., and Stach M., " Assessment of overload capacity of power transformers by on-line monitoring systems", Power Engineering Society Winter Meeting, 2001-IEEE , Vol. 1, 28 Jan.-1 Feb. 2001, pp.329 - 334

[78] (Thaden, 1995) Thaden M.V., Mehta S.P., Tuli S.C., and Grubb R.L., "Temperature rise tests on a forced-oil-air cooled (FOA) (OFAF) core-form transformer, including loading beyond nameplate", IEEE Transactions on Power Delivery, Vol. 10, Iss. 2, April 1995, pp. 913 – 923

[79] (Tylavsky, 2000) Tylavsky D.J., Qing He, Jennie Si, McCulla G.A., Hunt J.R., "Transformer top-oil temperature modeling and simulation", IEEE Transactions on Industry Applications,Vol.36, Iss.5, Sept.-Oct.2000, pp. 1219 - 1225

[80] (Van der Veken, 2001) Van der Veken W., Declercq J., Baelmans M., and Van Mileghem S., "New perspectives to overloading with accurate modeling of thermal transients in oil-immersed power transformers", Transmission and Distribution Conference and Exposition, 2001 IEEE/PES ,Vol. 1 , 28 Oct.-2 Nov. 2001, pp. 147 - 152

[81] (Weekes, 2004) Weekes T., Molinski T., Xin Li, and Swift G., "Risk assessment using transformer loss of life data", Electrical Insulation Magazine, IEEE ,Vol. 20, Iss. 2, March-April 2004, pp. 27 - 31

[82] (Weekes, 2004) Weekes T., Molinski T., and Swift, G., "Transient transformer overload ratings and protection", Electrical Insulation Magazine, IEEE ,Vol. 20, Iss. 2, March-April 2004, pp.32 - 35

Appendix A – Description of the different insulation oils

The transformer insulation oils are characterised by the following parameters:

- μ is the oil viscosity
- c_{oil} is the specific heat of the oil
- ρ_{oil} is the density of the oil
- k is the thermal conductivity of the oil
- β is the coefficient of thermal expansion of the oil

The temperature dependence of these parameters, [18] and [52], is given as follows:

$$\mu = A_1 \times e^{\left[\frac{A_2}{\theta_{oil}+273}\right]} \tag{A.1}$$

$$c_{oil} = A_3 + A_4\theta_{oil} \tag{A.2}$$

$$\rho_{oil} = A_5 + A_6\theta_{oil} \tag{A.3}$$

$$k = A_7 + A_8\theta_{oil} \tag{A.4}$$

$$\beta = A_9 \tag{A.5}$$

The nine constants for the two basic transformer insulation oils are listed in Table A.1 below:

Table A.1. Insulation oil constants, [18], [52]

Oil /Constant	Transformer oil	Silicone
A_1	0.13573×10^{-5}	0.12127×10^{-3}
A_2	2797.3	1782.3
A_3	1960	1424
A_4	4.005	2.513
A_5	887	989
A_6	-0.659	-0.870
A_7	0.124	0.138
A_8	-1.525×10^{-4}	-9.621×10^{-5}
A_9	8.6×10^{-4}	9.5×10^{-4}

It is generally valid for all transformer insulation oils that the variation of the oil viscosity with temperature is much higher than the variation of other oil parameters. Thus, all oil physical parameters except the viscosity in (3.9) can be replaced by a constant. However, if it is necessary to consider the influence of all oil parameters the following changes should be made:

– Equation (3.10) for the heat transfer coefficient will be changed as follows:

$$h = C_1 \times \left(\Delta\theta_{oil} \times \frac{\rho^2 \times \beta \times c_{oil} \times k^{(1-n)/n}}{\mu} \right)^n \tag{A.6}$$

where C_1 is assumed to be a constant, and is now expressed as:

$$C_1 = C \times \left(g \times L^{(3n-1)/n} \right)^n \tag{A.7}$$

and the variation with temperature of all oil parameters is given above in (A.1) – (A.5).

– Finally, the viscosity, μ, should be substituted with the following fraction:

$$\frac{\mu}{\rho^2 \times \beta \times c_{oil} \times k^{(1-n)/n}} \tag{A.8}$$

in the equations for the top-oil, hot-spot, bottom-winding and bottom-oil temperatures (3.24), (3.38), (3.41), (3.42) and (3.43) respectively.

Appendix   B – Transformer cold start

"Transformer cold start" refers to the operating condition where the transformer oil is initially still, as there is no prior oil circulation when a transformer is energised. Observations made during various thermal tests on transformers with external cooling, [48-49] and [62], show that the hot-spot to top-oil, top-oil to air and bottom-oil to air temperature gradients are directly affected by this condition, i.e., the gradients obtained during this particular state will reach higher values than those obtained when the oil circulation within the transformer is established. Further, the lack of moving oil will artificially create an effect similar to a condition with high oil viscosity that would, for example, occur in subzero ambient temperatures. Therefore, special exponents for a cold start are suggested in order to take account of this phenomenon, Tables 3.4, 3.5 and 3.6.

On the other hand, it is observed that the hot-spot to bottom-oil gradient does not differ from the state where oil circulation has been established. This can be explained by the location of the gradients in relation to the windings, which are the primary source of heat in the transformer. For example, when the position of the hot-spot to bottom-oil gradient is considered, it is obvious that heat will be transferred to the oil along almost the entire distance between the gradients, i.e., the oil will be heated up at each point without any delay, whereas the hot-spot to top-oil gradient is directly heated only at the point at the top of the transformer winding.

This phenomenon can be observed, with appropriate placement of temperature sensors, in a transformer work shop where temperature rise tests, i.e., heat run tests, are made according to IEC 76-2, [24]. In addition, this behaviour can be expected when new transformer units are installed and energised for the first time, or a used transformer is brought back into service after being treated. Once the transformer is energised, the "cold start" exponents, which are given in Tables 3.4, 3.5 and 3.6, should be substituted for the transformer "on load" exponents at the first load change.

Appendix   C – Insulation effect

Although unlikely, the correlation (3.27) may not hold for a specific transformer design where the transformer winding insulation layer is very thick. This effect, if significant, can be taken into account by adding the temperature gradient developed over the solid winding insulation as follows:

$$\theta_{ws} = \theta_{hs} + \Delta\theta_{ws-hs} \tag{C.1}$$

where:

θ_{ws} is the hottest temperature of the winding conductor surface, i.e., the temperature located at the inner surface of the insulation wrapped around the winding conductor,
θ_{hs} is the hot spot temperature located at the outer surface of the insulation wrapped around the winding conductor, as defined by the following equations in the text: 3.38, 3.41, 3.49 and 3.52,
$\Delta\theta_{ws-hs}$ is the temperature gradient between the inner and outer surface of the insulation wrapped around the winding conductor, for which an equation is given below.

Assuming that under transient conditions the temperature gradient, $\Delta\theta_{ws-hs}$, varies instantaneously with transformer loading and that the insulation properties do not vary with temperature, the following equation, consistent with the modelling performed in this thesis, is given:

$$\Delta\theta_{ws-hs} = K^2 \times P_{wdn,pu}(\theta_{ws}) \times \Delta\theta_{ws-hs,rated} \tag{C.2}$$

where:

K is the load factor (per unit value), [22],
$\Delta\theta_{ws-hs,\ rated}$ is the rated temperature gradient between the inner and outer surface of the insulation wrapped around the winding conductor, (K),
$P_{wdn,pu}(\theta_{ws})$ is the dependence of the load losses on temperature, (C.2).

The temperature dependence of the winding losses, $P_{wdn,pu}(\theta_{ws})$, is included as follows:

$$P_{wdn,pu}(\theta_{ws}) = P_{dc,pu} \times \left(\frac{\theta_{ws} + \theta_k}{\theta_{ws,rated} + \theta_k}\right) + P_{eddy,pu} \times \left(\frac{\theta_{ws,rated} + \theta_k}{\theta_{ws} + \theta_k}\right) \tag{C.3}$$

where:

$P_{dc,pu}$ is the DC losses per unit value,
$P_{eddy,pu}$ is the eddy losses per unit value,
θ_k is the temperature factor for the loss correction, equal to 225 for aluminium and 235 for copper.

However, it should be pointed out that equations (C.1) and (C.2) can be only applied if the transformer manufacturer provides the rated temperature gradient between the inner and outer surface of the insulation wrapped around the winding conductor, $\Delta\theta_{ws\text{-}hs,rated}$. In principle, the temperature gradient can be obtained as follows:

1. By installing fibre optic sensors on the inner and outer surface of the insulation wrapped around the winding conductor. This information is not included in data obtained from the normal heat run test. Therefore, it will demand an additional cost and a special agreement between the transformer manufacturer and customer.

2. By calculation techniques based on the specifics of the transformer design. These data should be specially ordered from the transformer manufacturer.

Appendix   D - Winding time constant

The winding time constant, [34], is as follows:

$$\tau_{wdn} = 2.75 \times \frac{\Delta\theta_{hs,\,rated}}{(1 + P_e) \times s^2} \quad \text{for Cu} \tag{D.1}$$

$$\tau_{wdn} = 1.15 \times \frac{\Delta\theta_{hs,rated}}{(1 + P_e) \times s^2} \quad \text{for Al} \tag{D.2}$$

where:

τ_{wdn} is the winding time constant in minutes at the rated load,
$\Delta\theta_{hs}$ is the winding hot-spot to the top-oil temperature gradient at the rated load,
P_e are the relative winding eddy losses, per unit of DC loss, corrected for the hot-spot temperature,
s is the current density in A/mm^2 at rated load.

When the winding time constant is calculated for the modelling presented in section 3.2.4, the winding hot-spot to top-oil gradient should be substituted with the winding hot-spot to bottom-oil gradient, $\Delta\theta_{hs\text{-}boil}$.

Appendix   E - Top-oil time constant

The top-oil time constant at the considered load is given by the following:

$$\tau_{oil,\,rated} = \frac{C_{th-oil} \times \Delta\theta_{oil,\,rated}}{q_{tot,\,rated}} \times 60 \tag{E.1}$$

where:

$\tau_{oil,rated}$ - is the rated top-oil time constant in minutes,
$\Delta\theta_{oil,rated}$ - is the rated top-oil temperature rise over ambient temperature in Kelvins, (K),
$q_{tot,rated}$ − are the total supplied losses (total losses) in watts (W), at rated load,
$C_{th\text{-}oil}$ − is the equivalent thermal capacitance of the transformer oil, (Wh/°C).

The equivalent thermal capacitance of the transformer oil is given by the following equations:

$$C_{th-oil} = 0.48 \times m_{oil} \tag{E.2}$$

where:

m_{oil}- is the weight of the oil in kilograms, (kg).

Equation (E.2) is an empirical formula based on the modelling that has already been performed and validated in the author's previous work, [71]. This equation is based on observations from heat run tests and implicitly takes into account the effect of the metallic parts as well. It is suggested to be used when the mass of the transformer fluid is the only known information.

Appendix   F- Air flow

The air flow (the air volume) passing through the cooler in a unit of time is calculated by the following equation, [34]:

$$\Psi_{air} = \frac{P_{TH}}{c_{air} \times \rho_{air} \times \Delta\theta_{cooler-air-gradient}} \qquad\qquad (F.1)$$

where:

Ψ_{air} is the air flow (the air volume), (m^3/s),
P_{TH} is the thermal power to be dissipated (E.2), (W),
c_{air} is the specific heat of the air, (Ws/(kg °C)),
ρ_{air} is the density of the air, kg/m^3,
$\Delta\theta_{cooler-air-gradient}$ is the measured temperature gradient between cooler air outlet and inlet, (K).

The thermal power (the amount of heat taken by the oil from the transformer active parts and transferred to the cooler) to be dissipated to the atmosphere in a unit of time is calculated as follows, [34]:

$$P_{TH} = c_{oil} \times \rho_{oil} \times \Psi_{oil} \times \Delta\theta_{cooler-oil-gradient} \qquad\qquad (F.2)$$

where:

Ψ_{oil} is the oil flow (the oil volume), (m^3/s),
c_{oil} is the specific heat of the oil, (Ws/(kg °C)),
ρ_{oil} is the density of the oil, (kg/m^3),
$\Delta\theta_{cooler-oil-gradient}$ is the measured temperature gradient between the cooler oil outlet and inlet, (K).

The power, P_{TH}, is equal to the difference between the total heat produced by the transformer losses and the amount of heat that is dissipated by the tank through radiation from the tank's external surfaces. The latter is insignificant compared to the amount of heat dissipated by the cooler for the large sizes of transformers, [21]. Of course, this balance can be easily disturbed by changing the transformer cooling mode. Therefore, the unit presented in section 4.3, due to lack of cooler air circulation, dissipated a higher proportion of heat from the tank surface through radiation.

Appendix   G - Input data

The input data for both the thermal model and the IEEE-Annex G calculation method are given in Tables G.1 and G.2 below, where LV and HV refer to the low voltage winding and the high voltage winding, respectively.

Table G.1. Input data for the thermal models

Quantity	Transformer/Winding							
	2.5		40		80		250	
	LV	HV	LV	HV	LV	HV	LV	HV
kVA base	2500		40 000		80 000		250 000	
*Temp. base	75ºC		75ºC		75ºC		75ºC	
$*P_w$, (W)	16028		145907		166434		411780	
$*P_E$, (W)	1170		14462		17340		29469	
$*P_S$, (W)	1041				24796		43391	
$*P_o$, (W)	"short circuit"		24018		"short circuit"		"short circuit"	
$*s$, (A/mm^2)	1.588	1.462	-		2.33		2.55	2.21
$*\Delta\theta_{W/A,R}$, (K)	64.7	60.5	54.4	41.7	42.6	44.2	41.7	39.7
$\Delta\theta_{H/A,R}$, (K)	72.5	68.3	62.8	58.6	55.2	59.8	58.6	50.8
$*\Delta\theta_{hs,rated}$, (K)	24.5	21.8	21.7	20.3	21	25.6	20.3	12.5
$*\Delta\theta_{TO,R}$, (K)	48		41.1		34.2		38.3	
$*\Delta\theta_{BO,R}$, (K)	40.35		34.4		19.7		16	
E_{HS}	0.7	0.71	0		0.5	0.8	0.4	0
H_{HS}	1		1		1		1	
$*H$	1.19	1.33	1.3		1.35	1.49	1.4	1
τ_{wdn}, (min.)	7.5	7.8	7		8	7	6	7
M_{CC}, (kg)	2829		36600		66690		153606	
$*m_{fe}$, (kg)	2066		-		51010		99389	
$*m_{wdn}$, (kg)	556		-		11322		29181	
$*m_{mp}=M_{TANK}$, (kg)	1030		7000		19833		44096	
$*m_{oil}=M_{FLUID}$, (kg)	1090		14000		34800		73887	
$*\theta_{HS}$, (°C)	24.4		35.6		23		38.3	
$*\theta_W$, (°C)	24.35		32		22.5		33.2	
$*\theta_{TO}$, (°C)	24.35		28.4		22.3		38.3	
θ_{TDO}, (°C)	23.7		28.4		22.3		38.3	
$*\theta_{BO}$, (°C)	22.4		25.8		19		28.1	

*Input data necessary for the suggested thermal model.

123

Table G.2. Input data for the thermal models

Quantity	Transformer/Winding				
	400		605		650
	LV	HV	LV	HV	LV
kVA base	400 000		605 000		780000
*Temp. base	75°C		85°C		75°C
*P_w, (W)	637100		929800		1307900
*P_E, (W)	59778		285000		114100
*P_S, (W)	65772		71000		194400
*P_o, (W)	"short circuit"		"short circuit"		"short circuit"
*s, (A/mm^2)	2.86	2.36	2.057	3.69	2.3
*$\Delta\theta_{W/A,R}$, (K)	47	46.9	44.7	56.5	58.6
$\Delta\theta_{H/A,R}$, (K)	58.3	56.6	56.9	65.3	78.4
*$\Delta\theta_{hs,rated}$, (K)	20.28	18.6	23.5	31.9	19.5
*$\Delta\theta_{TO,R}$, (K)	38.0		33.4		58.9
*$\Delta\theta_{BO,R}$, (K)	11.6		24.6		35.1
E_{HS}	0.15	0.2	0.71	0.23	1.1
H_{HS}	0.987	0.973	1	0.981	1
*H	1.3	1.2	1.5	1.16	1.68
τ_{wdn}, (min.)	5.3	8.2	10	5.5	6
M_{CC}, (kg)	205769		195152		272424
*m_{fe}, (kg)	132023		139448		160272
*m_{wdn}, (kg)	45563		48900		96178
*$m_{mp}=M_{TANK}$, (kg)	67 252		50153		52959
*$m_{oil}=M_{FLUID}$, (kg)	96018		79746		86809
*θ_{HS}, (°C)	34.6	31.6	32.9	32	21
*θ_W, (°C)	28.3		29.6		20.5
*θ_{TO}, (°C)	30.9		30.1		20.5
θ_{TDO}, (°C)	30.9		30.1		20.5
*θ_{BO}, (°C)	25.7		29.1		20

*Input data necessary for the suggested thermal model.

# Appendix   H – Transformer Sketches

The core window and winding arrangement drawings of the investigated transformers are given below.

1. Sketch of the single-phase 80 MVA ONAN – cooled transformer, Fig. H.1.
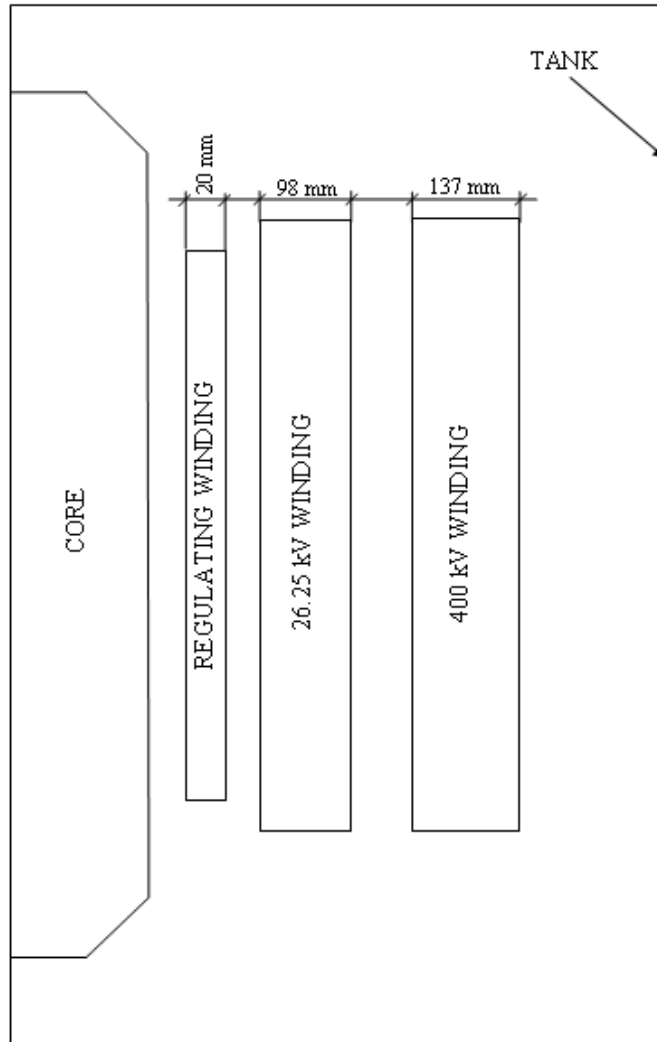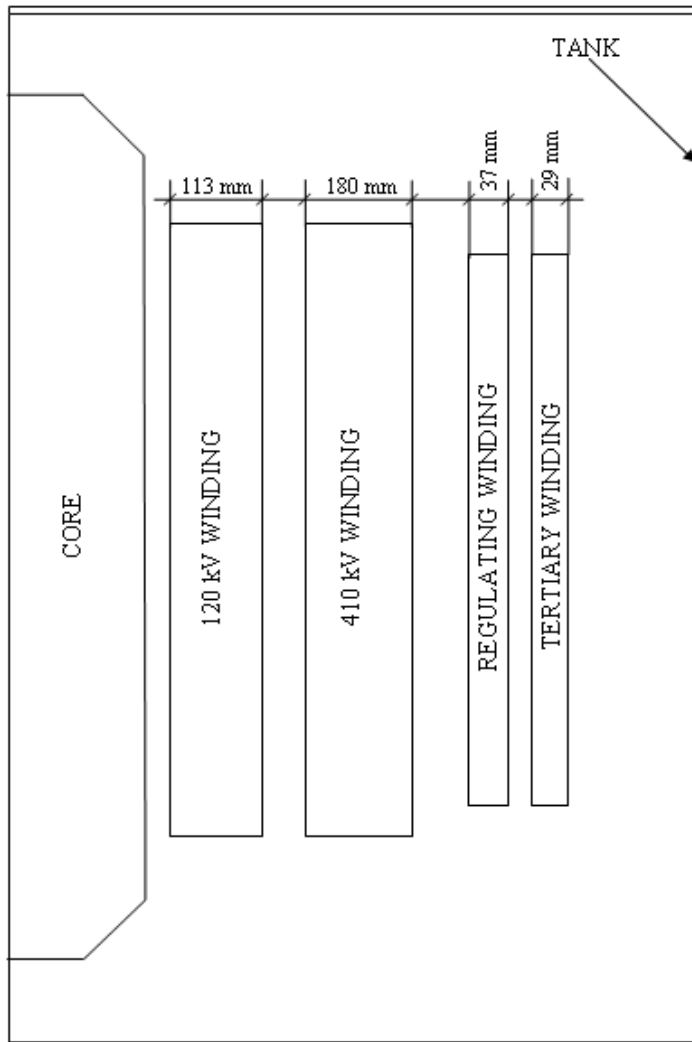

H.1. Sketch of the core window and winding arrangement of the single-phase 80 MVA ONAN – cooled transformer

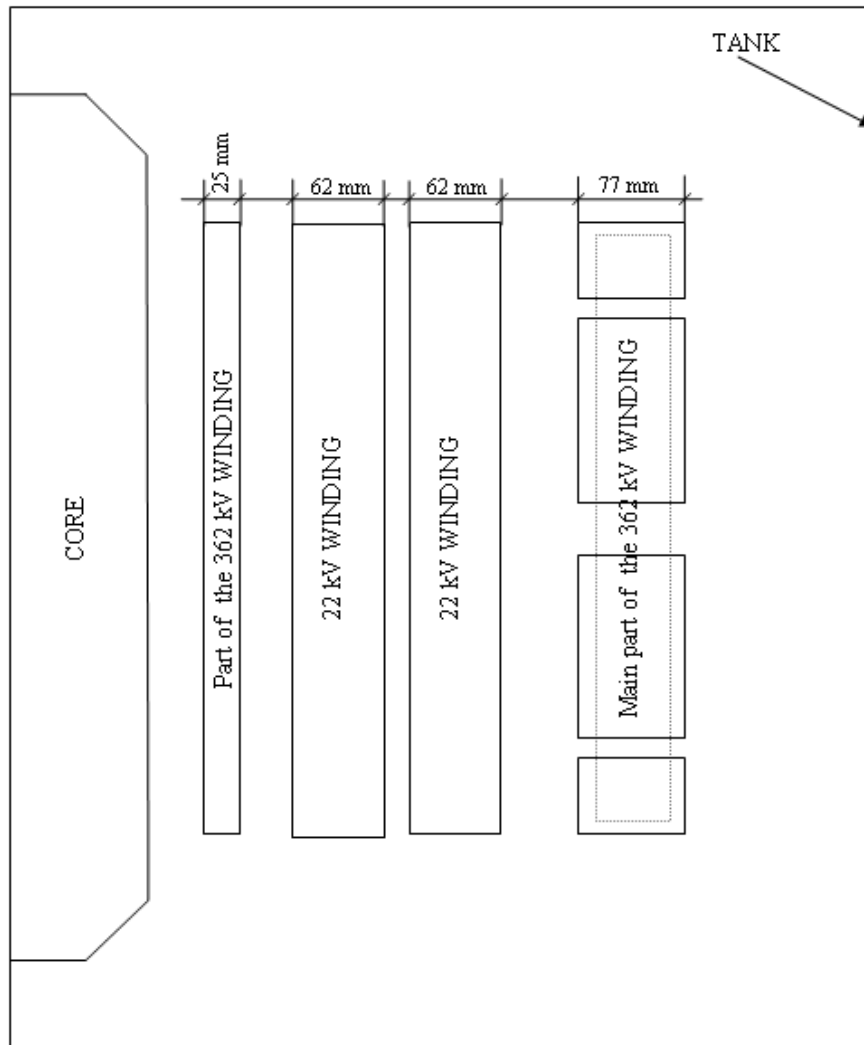2. Sketch of the three-phase 250/250/75 MVA ONAF – cooled transformer, Fig. H.2.
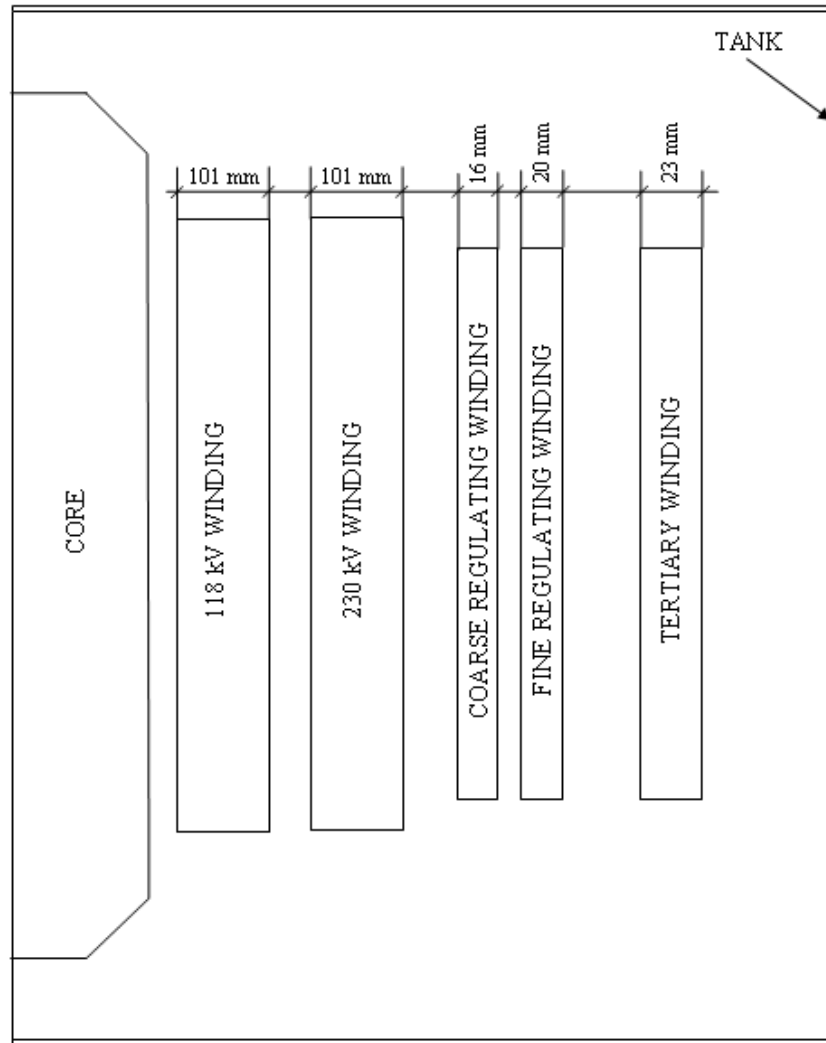
H.2. Sketch of the core window and winding arrangement of the three-phase 250/250/75 MVA ONAF – cooled transformer

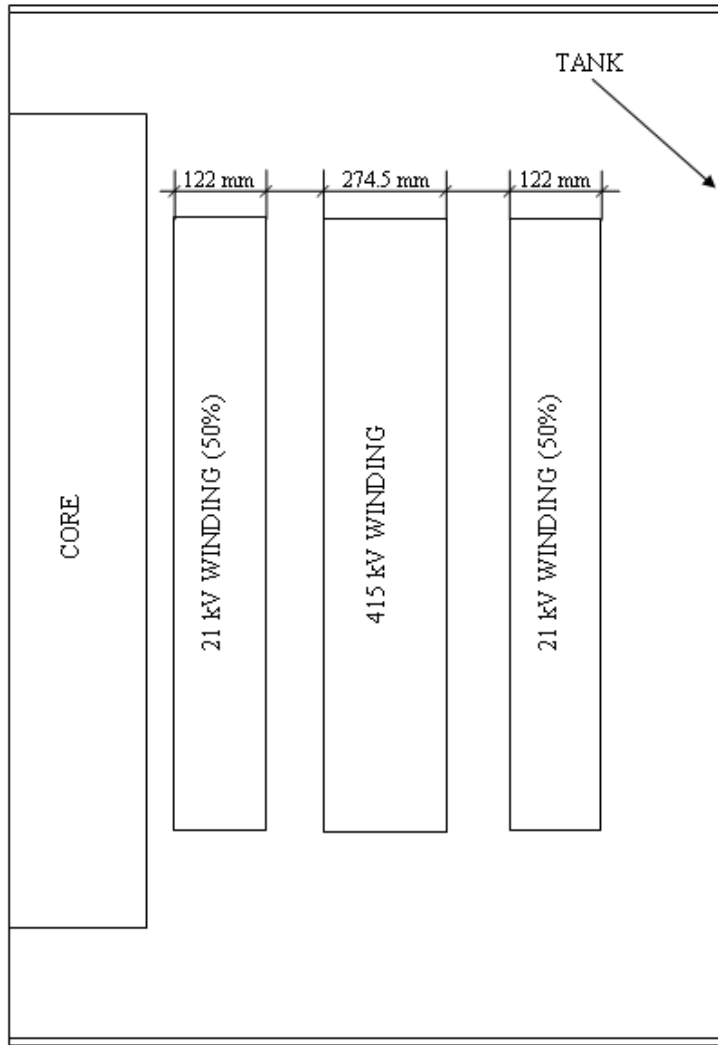3. Sketch of the three-phase 400/400/125 MVA ONAF – cooled transformer, Fig. H.3.

H.3. Sketch of the core window and winding arrangement of the three-phase 400/400/125 MVA ONAF – cooled transformer

4. Sketch of the three-phase 605 MVA OFAF – cooled transformer, Fig. H.4.

H.4. Sketch of the core window and winding arrangement of the three-605 MVA OFAF – cooled transformer

5. Sketch of the three-phase 650 MVA ONAF – cooled transformer, Fig. H.5.

H.5. Sketch of the core window and winding arrangement of the three-650 MVA ONAF – cooled transformer